

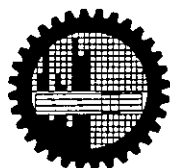
**ELECTROCHEMICAL PREPARATION OF COMPOSITE
ELECTRODES BASED ON ORGANIC/ORGANIC AND
ORGANIC/INORGANIC HYBRID STRUCTURE**

BY



MOSHARREFA AKTER

SUBMITTED IN PARTIAL FULFILMENT OF THE
REQUIREMENT FOR THE DEGREE OF
M.PHIL IN CHEMISTRY



DEPARTMENT OF CHEMISTRY
BANGLADESH UNIVERSITY OF ENGINEERING AND
TECHNOLOGY (BUET)
DHAKA-1000, BANGLADESH
MARCH, 2004



#99115#

DECLARATION

This thesis work has been done by the candidate herself and does not contain any material extracted from elsewhere or from a work published by anybody else. The work for this thesis has not been presented elsewhere by the author for any degree or diploma.

Mosharrefa Akter

**Mosharrefa Akter
(Candidate)**

M. Phil Student

Roll No. 100103201F

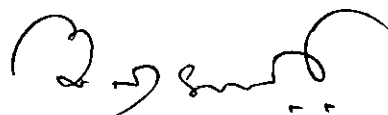
Department of Chemistry

BUET, Dhaka

Bangladesh

CERTIFICATE

This is to certify that the research work embodying in this thesis has been carried out under my supervision. The work presented herein is original. This thesis has not been submitted elsewhere for the award of any other degree or diploma in any University or institution.



*Dr. Al-Nakib Chowdhury
(Supervisor)
Associate Professor
Department of Chemistry
BUET, Dhaka
Bangladesh*

Dedicated

TO

MY SISTERS & BROTHERS WHO
ENCOURAGE AND INSPIRE ME
ALWAYS TO MY EDUCATION

ACKNOWLEDGEMENT

I am extremely grateful to my esteemed teacher Dr. AL-Nakib Chowdhury, Associate Professor, Department of Chemistry, Bangladesh University of Engineering & Technology (BUET), Dhaka, Bangladesh, for his thoughtful suggestions, invaluable guidance, untiring efforts, sympathy, constant encouragement and inspiration at all stages of my M. Phil. research work.

I am very thankful to Mr. Nurul Islam, Assistant Professor, Department of Chemistry, BUET, for his constant co-operation. I am also thankful to Prof. Dr. Abdur Rashid, Head of the Department Chemistry, BUET, Prof. Dr. Rafique Ullah, Prof. Dr. Wahab Khan, Prof. Dr. Enamul Huq, Department of Chemistry, BUET, Prof Md. Qamrul Ehsan, Dr. Md. Mufazzal Hossain and Dr. Md. Abdul Jabber, Assistant Prof. Department of Chemistry, Dhaka University, Dhaka, MD. Yusuf Khan Department of Metal & Metallurgy Engineering, BUET for their kind help and co-operation in different stages of my research work. I am also grateful to other teachers and staff of Chemistry Department, BUET, Dhaka.

I am grateful to the authority of BUET for providing me the opportunity of conducting the research.

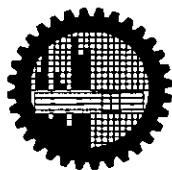
I would like to offer thanks to my friends. Tahmina Haque, Mamun-Ur-Rashid, Md. Saiful Islam, Md. Abdul Kalam Mollik, Syeda Rezina Jesmeen, Tanvir Sultana, Rima, Keka, Aporna, Julia Chowdhury, Topy Saha, Shimul, Suariaya Hossain, Shukla, Kanon and to all friends who shared with me to solve all the problems confronted in the whole thesis period. Special thanks to Md. Mamun Or Rashid of Chemistry Department, BUET for his assistance in composing of the thesis.

I would like to express my deep gratitude to my beloved parents, brothers and sisters for their sacrifice and continuous encouragement throughout the research work.

Above all, all thanks are due to almighty Allah for making things and situations congenial and favorable for me for the task undertaken.

MOSHARREFA AKTER
Author

Bangladesh University of Engineering and Technology
Dhaka
Department of Chemistry



Certification of Thesis

A thesis on

“ELECTROCHEMICAL PREPARATION OF COMPOSITE
ELECTRODES BASED ON ORGANIC/ORGANIC AND
ORGANIC/INORGANIC HYBRID STRUCTURE”

BY


MOSHARREFA AKTER

has been accepted as satisfactory in partial fulfillment of the requirements for the degree of Master of Philosophy (M. Phil) in Chemistry and certify that the student has demonstrated a satisfactory knowledge of the field covered by this thesis in an oral examination held on March 07, 2004.


Board of Examiners

1. **Dr. Al-Nakib Chowdhury**
Associate Professor
Department of Chemistry
BUET, Dhaka
2. **Dr. Md. Abdur Rashid**
Professor & Head
Department of Chemistry
BUET, Dhaka.
3. **Dr. Md. Rafique Ullah**
Professor
Department of Chemistry
BUET, Dhaka
4. **Dr. M. Yousuf Ali Mollah**
Professor
Department of Chemistry
Dhaka University, Dhaka.


07-03-04
Supervisor & Chairman


Member (Ex-officio)


Member


Member (External)

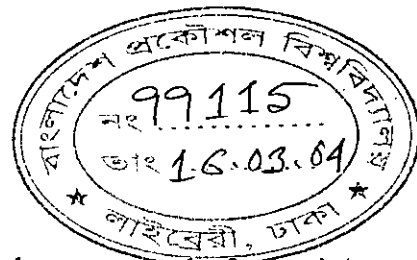
Contents

| | Page |
|--|------|
| Abstract | 1 |
| Chapter 1: Introduction | |
| 1.1 Fundamental aspects of Electrochemical process | |
| A. Design of Electrochemical Techniques | 4 |
| B. Processes at electrode surface | |
| 1.2 Some important electrode materials | |
| A. Metals | 11 |
| B. Semiconductors | 12 |
| C. Composites | 17 |
| 1.3 Organic materials | |
| A. Conductive Polymers | 18 |
| B. Dyes | 25 |
| 1.4 Theoretical of experimental techniques | |
| A. Cyclic voltammetry | 26 |
| B. Infra-red (IR) spectroscopy | 27 |
| C. Ultra violet-visible spectroscopy (UV-Vis) | 29 |
| D. X-ray diffraction | 29 |
| E. d. c. conductivity | 31 |
| F. SEM technique | 32 |
| 1.5 Aim of the present study | 33 |
| References | 34 |
| Chapter 2: Experimental | |
| 2.1 Materials and devices | |
| A. Chemicals | 37 |
| B. Instruments | 37 |
| 2.2 Electrochemical preparation of the film electrodes | 38 |
| A. Polyaniline | 38 |
| B. Polyaniline / Methylene blue | 38 |
| C. Polyaniline / Procion red | 40 |
| D. Polyaniline / Titanium (IV) oxide | 40 |
| 2.3 Spectral analysis | |
| A. Infra red spectra | 41 |
| B. Ultra violet-visible spectra | 41 |
| C. X-ray diffraction pattern | 42 |
| 2.4 Electrical conductivity measurements | 42 |
| 2.5 Analysis of surface morphology | 44 |
| 2.6 Doping-dedoping technique | 44 |
| 2.7 Electrochemical degradation study | 45 |
| References | 46 |

Chapter 3: Results and Discussions

| | | |
|-----|---|-----|
| 3.1 | Electrochemical synthesis | |
| | A. Organic electrode: PANI | 47 |
| | B. Organic /Organic composite electrode | 50 |
| | C. Organic/Inorganic composite electrode: PANI/TiO ₂ | 55 |
| 3.2 | Characterization of the electrode matrices | |
| | A. Infra red spectral analysis | 60 |
| | B. Ultra violet- visible spectroscopy | 73 |
| | C. X-ray diffraction pattern | 77 |
| | D. d. c. two point-probe conductivity | 85 |
| | E. Scanning electron microscopy | 87 |
| 3.3 | Electrochemical doping – dedoping process | |
| | A. PANI electrode | 88 |
| | B. PANI/MB electrode | 91 |
| | C. PANI/PR electrode | 95 |
| | D. PANI/TiO ₂ electrode | 98 |
| 3.4 | Electrochemical degradation | |
| | A. Oxidative degradation | 101 |
| | B. Degradation by repeating potential scan | 107 |
| | <i>References</i> | 112 |
| | Conclusion | 115 |

Abstract



Electrochemical preparations of composite film electrodes composed of organic/organic and organic/inorganic hybrid structures have been described. Organic film electrode, PANI was prepared electrochemically from an aqueous electrolytic solution by coating its film onto a Pt substrate. The organic/organic electrodes, PANI/MB and PANI/PR were also grown electrochemically as film from the same electrolytic solution that contain either MB or PR. The organic/inorganic film electrode PANI/TiO₂ was obtained electrochemically by polymerizing aniline in the presence of TiO₂ suspension in the same electrolytic media. The film electrodes thus grown electrochemically are free-standing and adhere to the substrate even in a deposit of sufficient thickness.

The rate of electrochemical polymerization in the presence of MB, PR and TiO₂ were evaluated from the observed slope of a straight line obtained in a plot of anodic peak current vs no. of potential scan. It was observed that, the line for the formation of PANI/TiO₂ film raises sharply compared to that of PANI, PANI/MB or PANI/PR films. The steeper line suggests that the electrochemical growth rate of PANI/TiO₂ is faster compared to the other films synthesized under the identical electrolytic and electrochemical condition employed.

IR spectral analysis of the film samples yielded useful information on the identification of the components present in the film electrodes of hybrid structure. In each electrode system, the corresponding components, viz., PANI, MB, PR, TiO₂ show characteristics bands confirming the presence of the components in each electrode matrix. UV-Vis optical spectra of the samples were recorded in their DMF solution. Strong absorption maxima in the ultra violet region and another band in the visible region were observed for the PANI sample. This optical phenomenon is identical to that of PANI and other conducting polymers reported previously suggesting an interband transition and mid-gap states transition occurring in the ultra violet and visible region, respectively. However, the peak responses in the optical spectra seem to be modified when MB or PR was embedded in the PANI matrix. TiO₂ was not dissolved in the DMF solution and thus optical

characterization of the PANI/TiO₂ matrix was not attempted. XRD spectra of PANI, PANI/MB, PANI/PR and PANI/TiO₂ samples showed diffused scattering indicating the amorphous nature of the materials.

The electrical conductivity of the film matrices was measured in their compressed solid formed by two point-probe method. The results of conductance measurement clearly provide evidence that the inclusion of MB, PR or TiO₂ into the PANI matrix affects the electrical properties of the matrix. The electrical conductivity of the PANI/TiO₂ was found to be significantly higher while the PANI/MB shows a considerably lower conductance than that of the parent PANI matrix. However, the measured conductance of all the samples indeed shows that their conductivity values still exist in the conductivity range of conventional inorganic semiconductors.

The surface morphology of the PANI was observed to be modified when either MB, PR or TiO₂ was embedded in it. The SEM image shows a granular morphology for the PANI surface. The granular morphology appears to be fibrillar on inclusion of MB in the PANI matrix. The PANI/PR surface seems to be consisted of agglomerates and stacked over the surface as deposit. The PANI/TiO₂, on the other hand, exhibits deposit of the particles that are aggregated and distributed non-uniformly over the substrate they grown. The film electrodes thus synthesized were found to be electroactive. The voltammetric features of the films show regular oxidation and reduction processes when cycled between -0.3 V and +0.6 V vs SCE in aqueous sulphuric acid. During oxidation and reduction, electrolytic anions are pushed in and out, respectively, of the film with its characteristics color changes. However, the redox reactivities of the films employed are found not to be identical. This may arises due to the inclusion of different chemical entities, viz., MB, PR, and TiO₂ into the PANI matrix and thus modifying the electrode surface behavior and hence shows dissimilar redox activity. The stability of the film electrodes, thus synthesized in repeated oxidation/reduction cycles and its degradation at highly positive potentials were examined. The results obtained from the current-voltage response (cyclic voltammogram) indicate that although over oxidation takes place with the composite electrodes (PANI/MB, PANI/PR and PANI/TiO₂), the extent of degradation is not as

drastic as with the PANI, suggesting a better electrochemical stability of the composite electrodes relative to the bulk PANI film electrode.

Chapter 1

INTRODUCTION

1.1 Fundamental aspects of Electrochemical process

A. Design of Electrochemical Techniques

Electrochemistry involves the study of spontaneous oxidation-reductions that generate an electrical current and the study of non-spontaneous oxidation-reduction reactions that are forced to occur by the passage of an electrical current. In both cases, the conversion between chemical and electrical energy is carried out by electrochemical cell.

i) Electrochemical cell: The electrochemical cell consist primarily of the electrodes and the electrolyte, together with a container. Commonly a glass frit, separator, or membrane may be incorporated to isolate the anolyte from the catholyte. Three electrodes are commonly employed: a working electrode which defines the interface under study, a reference electrode which maintains a constant reference potential, and a counter (or secondary) electrode which supplies the current. The cell must be designed so that the experimental data are determined by the properties of the reaction at the working electrode.

ii) Working electrode: Designs of working electrodes are diverse. Most commonly the working electrode is a small sphere, small disc, or a short wire, but it could also be metal foil, a single crystal of semiconductor or metal, an evaporated thin film, or a powder as pressed discs or pellets. An essential features is that the electrode should not react chemically with the solvent or solution components. In principle, the electrodes can be large or small, but there are commonly experimental reasons why the electrode area should be relatively small ($<0.25 \text{ cm}^2$). Moreover it should preferably be smooth, as the geometry and mass transport are then better defined. A wide range of solid materials are used as electrodes, but the most common 'inert' solid electrodes are lead, vitreous carbon, gold and platinum. In order to obtain consistent results with solid electrodes it is important to establish a satisfactory electrode pretreatment procedure which ensures a

reproducible state of oxidation, surface morphology and freedom from adsorbed impurities. Electrodes are polished on cloth pads impregnated with diamond particles down to 1 μm and then with alumina of fixed grain size down to 0.05 μm .

iii) Counter electrode: The purpose of the counter electrode is to supply the current required by the working electrode without in any way limiting the measured response of the cell. It is essential that the electrode process is decomposition of the electrolyte medium or oxidation/reduction of a component of the electrolyte so that current flows readily without the need for a large overpotential.

The counter electrode should not impose any characteristics on the measured data, and in consequence it should have a large area compared to the working electrode. Moreover, as also noted above, its shape and position are important since these determine whether the working electrode is an equipotential surface, and consequently it is preferable to avoid a separator in the cell.

iv) Reference electrodes: The role of the reference electrode is to provide a fixed potential which does not vary during the experiment (e.g. it should be independent of current density). In most cases, it will be necessary to relate the potential of the reference electrode to other scales, for example to the normal hydrogen electrode, the agreed standard for thermodynamic calculations.

In potentiostatic experiments the potential between the working electrode and reference electrode is controlled by a potentiostat, and as the reference half cell maintains a fixed potential, any change in applied potential to the cell appears directly across the working electrode-solution interface. The reference electrode serves the dual purpose of providing a thermodynamic reference and also isolates the working electrode as the system under study. In practice, however, any measuring device must draw current to perform the measurement, so a good reference electrode should be able to maintain a constant potential even if a few microamperes are passed through its surface.

In practice the main requirement of a reference electrode is that it has a stable potential and that it is not substantially polarized during the experiment. Hence it is common to use the highly convenient aqueous saturated calomel electrode (SCE) in many experiments in all solvents. Even so, a very wide range of reference electrodes have been used in non-aqueous solvents.

Potential of some common reference electrodes are listed in Table 1.1.1.

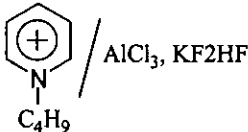
Table - 1.1.1 Potential of some typical reference electrodes in aqueous solutions at 298K.

| Common name | Electrode | Potential / V vs NHE |
|--------------------|--|----------------------|
| SCE | Hg/Hg ₂ Cl ₂ , sat KCl | +0.241 |
| Calomel | Hg/Hg ₂ Cl ₂ , 1 mol dm ⁻³ KCl | +0.280 |
| Mercurous sulphate | Hg/Hg ₂ SO ₄ , sat K ₂ SO ₄ | +0.640 |
| | Hg/Hg ₂ SO ₄ , 0.5 mol dm ⁻³ H ₂ SO ₄ | +0.680 |
| Mercurous oxide | Hg/HgO, 1 mol dm ⁻³ NaOH | +0.098 |
| Silver chloride | Ag/AgCl, sat KCl | +0.197 |

A great deal of modern electrochemistry is carried out in non-aqueous solvent media, and often aqueous reference electrodes can be used at the expense of an unknown aqueous-non aqueous junction potential. In acetonitrile, the calomel electrode is unstable, and the most frequently used reference electrodes are Ag/AgCl or Ag/Ag⁺.

v) The electrolytic solution: The electrolytic solution is the medium between the electrodes in the cell, and it will consist of solvent and a high concentration of an ionised salt as well as the electroactive species; it may also contain other materials, complexing agents, buffers, etc. The supporting electrolyte is present (a) to increase the conductivity of the solution and hence to reduce the resistance between the working and counter electrodes (to avoid undue Joule heating, to help maintain a uniform current and potential distribution, and to reduce the power requirement on the potentiostat), and also to minimise the potential error due to the uncompensated solution resistance. With appropriate precautions, electrochemical experiments are possible in almost any medium. Table 1.1.2 lists some widely used media.

Table 1.1.2. Common solvents and media for electrochemical experiments.

| |
|--|
| 1. Water |
| Aqueous solutions of many salts and/or complexing agents at various pH. Buffered and unbuffered media. |
| 2. Other protonic solvents |
| e.g. acetic acid, ethanol, methanol, liquid HF. |
| 3. Aprotic solvents |
| e.g. acetonitrile, dimethylformamide, dimethylsulphoxide, sulphur dioxide, ammonia, propylene carbonate, tetrahydrofuran. Many studies use as electrolytes $R_4N^+ X^-$, $R = CH_3, C_2H_5$ or C_4H_9 , $X = ClO_4^-, BF_4^-, PF_6^-$, or halide ion. Media difficult to buffer. |
| 4. Mixed solvents |
| Particularly mixtures of water with ethanol, acetonitrile, etc. Again, these media may be buffered or unbuffered, contain many electrolytes, etc. |
| 5. Molten salts |
| e.g. NaCl, KCl/NaCl/LiCl eutectics etc. |
| 6. Low temperature molten salts |
| e.g. |
|  |

Electrode reactions can be extremely sensitive to impurities in the solution; for example, organic species are often strongly adsorbed even at 10^{-4} mol dm^{-3} bulk concentration from aqueous solutions. Hence salts should be of the highest available purity and/or recrystallised, solvents should be carefully purified, and solutions must be carefully deoxygenated. Purification and drying of non-aqueous solvents have been described elsewhere [1, 2] in some detail.

vi) Instrumentation: The electrochemist's armoury is based on electronic apparatus designed to control/measure the charge passed (coulostat/integrator), current

(galvanostat/current follower) and potential (potentiostat/high impedance voltmeter) in an electrochemical cell.

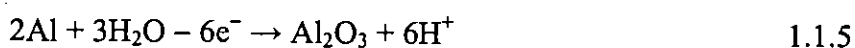
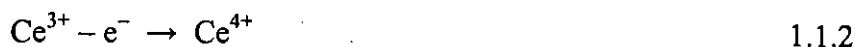
Potentiostat: The potentiostat is a device for controlling the potential between the working electrode and the reference electrode at a fixed and selected potential (commonly we also wish to programme this potential with time).

Galvanostat: The simplest way to obtain a constant current is to apply a voltage from a low output impedance voltage sources across a large resistor in series with the cell. The current will be given by the ratio E_{in}/R (provided resistance R is very large compared with the impedance of the cell).

B. Processes at electrode surface

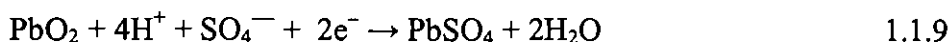
A solid conducting materials must be present to provide the site for each electrochemical reaction. These materials are called electrodes. The electrodes at which oxidation occurs is termed as the anode. The other electrode, the cathode, is the site of the reduction process.

i) Electrode reactions: An electrode reaction is a heterogeneous chemical process involving the transfer of electrons to or from a surface, generally a metal or a semiconductor. The electrode reaction may be an anodic process whereby a species is oxidised by the loss of electrons to the electrode, e.g.



By convention [3], the current density, I , for an anodic process is a positive quantity. Conversely, the charge transfer may be a cathodic reaction in which a species is reduced by the gain of electrons from the electrode, e.g.





and the current density for a cathodic process is a negative quantity. The diversity of electrode reactions can already be seen from Equation (1.1.1.–1.1.10): the electroactive species may be organic or inorganic, neutral or charged, a species dissolved in solution, the solvent itself, a film in the electrode surface, or indeed, the electrode materials itself. Moreover, the product may be dissolve in solution, in a gas, or a new phase on the electrode surface. The many type of electrodes reactions are also illustrated pictorially in Fig. 1.1.1.

Electrolysis is only possible in a cell with both an anode and a cathode, and, because of the need to maintain an overall charge balance, the amount of reduction at the cathode and oxidation at the anode must be equal.

ii) Mass transport: In general, in electrochemical systems, it is necessary to consider three modes of mass transport; namely,

(a) Diffusion: Diffusion is the movement of a species down a concentration gradient, and it must occur whenever there is a chemical change at surface. An electrode reaction converts starting material to product ($\text{O} \rightarrow \text{R}$), and hence close to the electrode surface there is always a boundary layer (up to 10^{-2} cm thick) in which the concentrations of O and R are a function of distance from the electrode surface. The concentration of O is lower at the surface than in the bulk, while opposite is the case for R, and hence O will diffuse towards and R away from the electrode.

(b) Migration: Migration is the moment of charged species due to a potential gradient, and it is the mechanism by which charge passes through the electrolyte; the current of electrons through the external circuit must be balanced by the passage of ions through the solution between the electrodes (both cations to the cathode and anions to the anode).

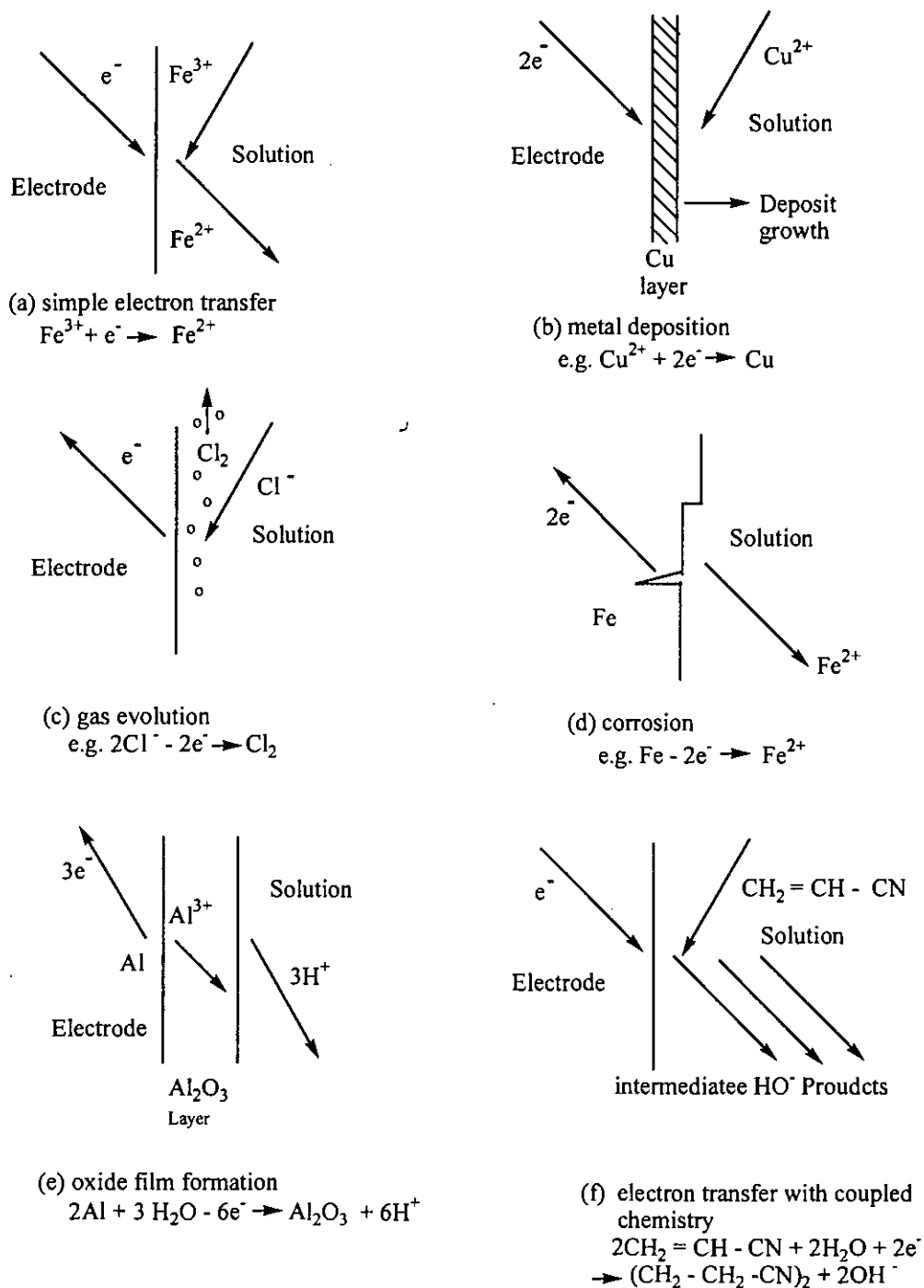


Fig. 1.1.1: Schematic view of some types of electrode reactions met in applied and fundamental electrochemistry.

It is, however, not necessarily an important form of mass transport for the electroactive species even if it is charged. The forces leading to migration are purely electrostatic, and hence the charge can be carried by any ionic species in the solution. As a result, if the electrolysis is carried out with a large excess of an inert electrolyte in the solution, this carries most of the charge, and little of the electroactive species is transported by migration.

(c) Convection: Convection is the movement of a species due to mechanical forces. It can be eliminated, at least on a short timescale (it is difficult to eliminate natural convection arising from density difference on a longer time, i.e. > 10s) by carrying out the electrolysis in a thermostat in the absence of stirring or vibration. In industrial practice it is much more common to stir or agitate the electrolyte or to flow the electrolyte through the cell. These are all forms of forced convection and, when present, they have a very large influence on the current density.

1.2 Some important electrode materials

A. Metals

Metals are crystalline solid materials consist of metal atoms distributed in a definite pattern resulting from their close packing. The types of close packing arrangement depends upon the size and electronic configuration of the atoms involved in the formation of crystal lattice. Since the metal atoms are all in direct contact with one another in the lattice and their valence electrons are in identical energy states, it is believed that the electrons are free to migrate between atoms. Metal atoms have an excess of low energy orbital vacancies. These vacancies enable valence electrons to move from near a certain nucleus to near any other nucleus where their position remains indistinguishable from the first. Thus, metals may be pictured as a collection of positive atomic cores embedded in a fluid of electrons or sea of electrons. For this fluid of electrons, metals are good conductors of electricity and heat. Metals have metallic luster; they are malleable, ductile and high melting points.

Metals have simple crystal lattices since metallic bonding envisages closest packing of atoms-one layer above another. Metals may have any system of seven common crystal system. Fe, Cu, Al, etc are the most common metals which are very useful to us.

B. Semiconductors

Semiconductors are special kind of materials which have the properties of semiconductivity. Semiconductivity is an electrical property of materials. A relatively small group of elements and compounds has an important electrical property, semiconduction in which they are neither good electrical conductors nor good electrical insulators. Instead, their ability to conduct electricity is intermediate. Si, Ge, impure ZnO, impure NiO are some examples of semiconductors.

The magnitude of conductivity in the simple semiconductors fall within the range 10^{-6} to $10^{-1} \Omega^{-1} \text{ cm}^{-1}$. This intermediate range corresponds to band gaps of less than $2e \text{ V}$. Both conduction electrons and electron holes are charge carriers in a simple semiconductor.

In a semiconductor element, the energies of the valence electrons which bind the crystal together lie in the highest filled energy band, called the valence band. The empty band above, called the conduction band, is separated from the valence band by an energy gap. The magnitude of the energy gap or the width of the forbidden energy zone, is characteristic of the lattice alone and varies widely for different crystals.

The transfer of an electron from the valence band to the conduction band requires high excitation energy to overcome the potential barrier of the forbidden energy zone. Consequently, such elements behave like an insulator at low temperatures. The application of heat or light energy may give enough energy to some electrons in the valence band to excite them across the forbidden zone into the conduction band. These electrons in the conduction band are now free to move and can carry electricity (Fig. 1.2.1).

Semiconductors are of two kinds such as

- (i) Intrinsic semiconductor
- (ii) Extrinsic semiconductor

(i) Intrinsic semiconductors : If a pure, elemental substance shows the semiconducting properties, it is called intrinsic semiconductor. Pure Si, Ge shows these semiconducting properties. For this semiconduction results from the thermal promotion of electrons from a filled valence band to an empty conduction band. There, the electrons are negative charge carriers. The removal of electrons from the valence band produces electron holes which are positive charge carrier and identical to the conduction electrons (Fig. 1.2.1 (a)). This overall conduction scheme is possible because of the relatively small energy band gap between the valence and conduction bands in silicon. If δ is the conductivity of semiconductor then for intrinsic semiconductor, we can write.

$$\delta = nq (\mu_e + \mu_n) \quad 1.2.1$$

Where, $n \rightarrow$ density of conduction electron

$q \rightarrow$ charge of single carrier

$\mu_e \rightarrow$ carrier mobility of electron

$\mu_n \rightarrow$ carrier mobility of hole

(ii) Extrinsic semiconductors: Extrinsic semiconduction result from impurity additions known as dopants, and the process of adding these components is called doping. These types of semiconductors are Extrinsic semiconductors. At room temperature the conductivity of semiconductors results from electrons and holes introduced by impurities in the crystal. The presence of an impurity lowers considerably the activation energy necessary to transfer an electron from the valence band to the conduction band. This indicates that the ground state energies of such easily excited electrons must lie in the forbidden energy region. Two such discrete energy levels, known as donor levels and acceptor levels, may be introduced into the forbidden energy zone at a small interval of energy below the conduction band or above the valence band (Fig.1.2.1 (b)). Donor levels give rise to electrons in the conduction band, whereas acceptor levels lead to the formation of holes in the valence band. Impurity of Si, with B, P, NiO, ZnO, are the examples of extrinsic semiconductors. Extrinsic semiconductors are of two kinds such as p-type extrinsic semiconductor and n-type extrinsic semiconductor.

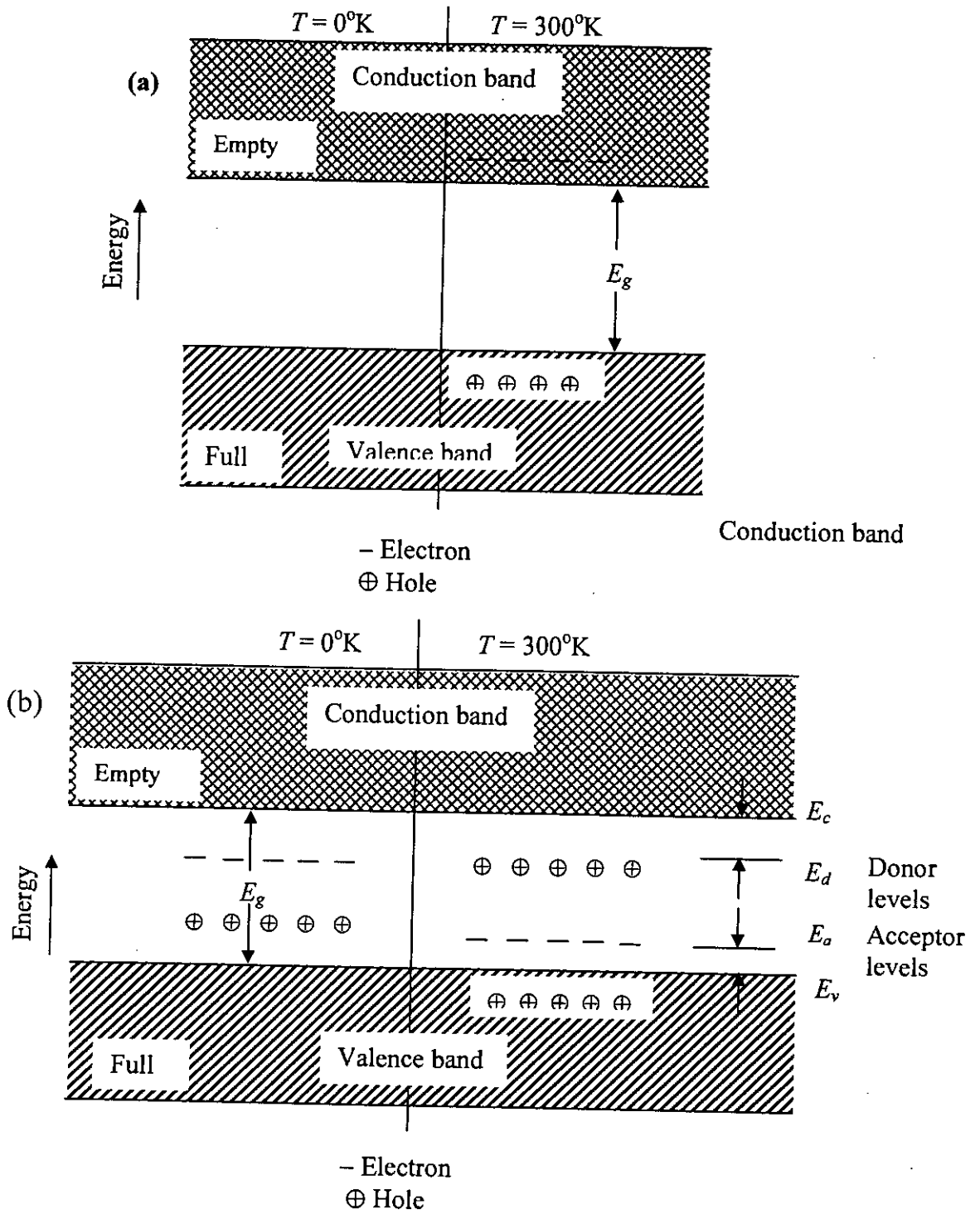


Fig. 1.2.1 A pictorial representation of an (a) intrinsic and (b) extrinsic semiconductor.

p-type extrinsic semiconductors: The p-type semiconductor is obtained when the impurity atoms have fewer valence electrons than the silicon or germanium atoms of the original crystal. When a trivalent element such as B, Al, Ga, In is substituted for Si atom, the structure will be locally incomplete and the impurity atom will acquire an extra electron from a nearby bond in the lattice to approximate the tetrahedral cloud distribution of the lattice. This creates a positive hole localized near the impurity, which will attempt to neutralize itself by taking an electron from another neighboring bond. Then again a hole is formed in place of this electron and it will neutralize itself by taking another electron from the next neighboring bond. Such way the positive holes carry electricity in the extrinsic semiconductor. So it is called p (i.e. positive) type semiconductor (Fig. 1.2.2 (b) Cu_2O also p-type semiconductor).

n-type semiconductors: They n-type semiconductor arises from substitution of impurity atoms having more valence electrons than Si or Ge atoms. Elements such as P, As, Sb, and Bi have five valence electrons. When such an element is substituted for a silicon atom, four of its five electrons will enter the inter-atomic bonds, but the fifth electron will be only slightly attracted by the excess of the positive charge on the nucleus. Thermal agitation even at room temperature is sufficient to transfer this electron to the conduction band. Since conductivity is due to the motion of electrons in the conduction band, this semiconductor is called n-type and the impurity is called the donor (Fig. 1.2.2 (a)). Titanium dioxide or titania is a non-stoichiometric transition metal oxide and behaves as n-type semiconductor [4].

There are three naturally occurring crystal phases of titanium dioxide: rutile, anatase, and brookite. Most of the electrochemical and photocatalytic work to date have been performed on rutile or anatase, or a mixture of the two. Both rutile and anatase have tetragonal unit cells, and both structures contains slightly distorted TiO_6 octahedral. Rutile is thermodynamically more stable than anatase at room temperature; the free energy change for anatase to rutile is $-5,4 \text{ kJ/mol}$ [5].

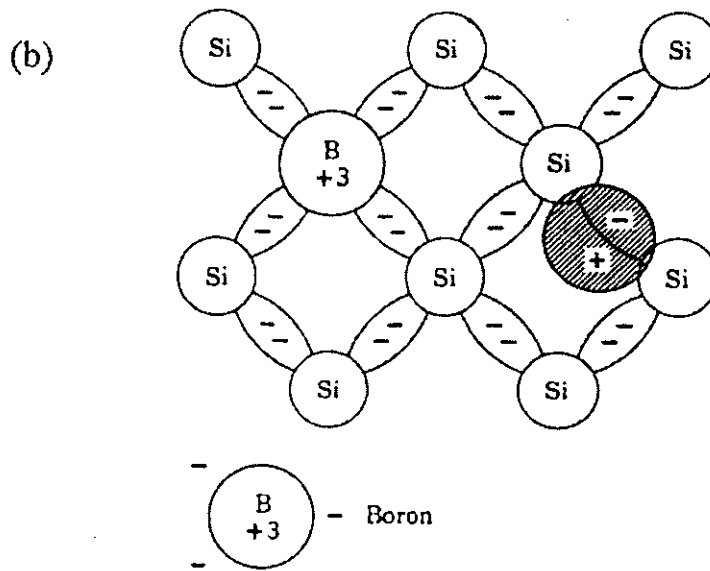
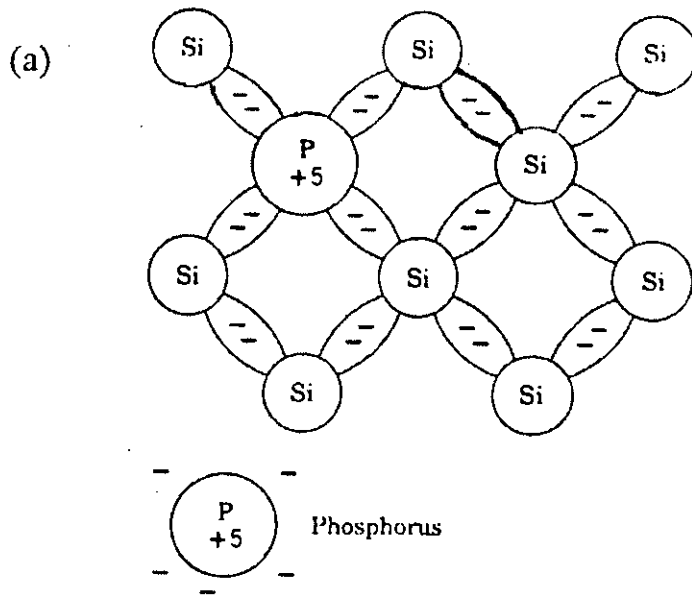
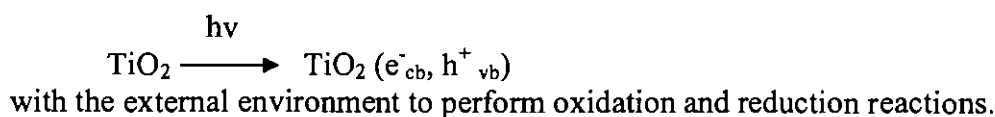


Fig. 1.2.2: Types of impurity semiconductors (a) n-type (b) p- type.

The absorption and reflection properties of rutile have been studied extensively. At 4K, the short wavelength absorption edge for rutile is 410 nm (bandgap energy = 3.05 eV) [6, 7]. The lowest energy electronic absorption at 3.05 eV is an indirect transition. On the other hand, the bandgap of anatase is reported as 3.2 eV [8]. The absorption coefficients for both crystal phases are reported as $\sim 10^5 \text{ cm}^{-1}$ at 340 nm [9].

Ultraviolet radiation below $\sim 390 \text{ nm}$ stimulates valence-band electrons in TiO_2 particles that are suspended in contaminated water. These electrons are promoted to the conduction band (e^-_{cb}), creating holes in the valence band (h^+_{vb}). These electron / hole pairs can either recombine, producing thermal energy, or interact



C. Composites

Since 1965 a distinct discipline and technology of composite materials begun to emerge. That is 80% of all research and development on composites have been done since 1965 when the Air Force launched its-all out development program to make high performance fiber composites a practical reality. There are two major reasons for the revived interest in composite materials. One is that the increasing demands for higher performance in many product areas specially in the aerospace, nuclear energy and aircraft fields is taxing to the limit our conventional monolithic materials. The second reason, the most important for the long run is that the composites concept provides scientists and engineers with a promising approach to designing, rather than selecting, materials to meet the specific requirements of an application.

The term 'composite' refers to something made up of various parts or elements. In definition of composite depends on the structural level of the composite we are thinking about. At the submicroscopic level that of simple molecules and crystal cells all materials composed of two or more different atoms or elements would be regarded as composites. This would include compounds, alloys plastics and ceramics. Only the pure elements

would be excluded. At the microscopic level (or microstructural level) that of crystals, polymers, and phases a composite would be a material composed of two or more different crystals, molecular structures, or phases. By this definition most of our traditional materials which have always been considered monolithic would be classified as composites. At the macrostructural level which is most useful for composites, the definitions of composites is that they are a mixture of macroconstituent phase composed of materials which are in a divided state and which generally differ in form and/or chemical composition. Note that, contrary to a widely held assumption, this definition does not require that a composite be composed of chemically different materials, although this usually the case. The more important distinguishing characteristics of a composite are its geometrical features and the fact that its performance is the collective behavior of the constituents of which it is composed. A composite material can vary in composition, structure, and properties from one point to the next inside the material.

The major constituents used in structuring composites are fibers, particles, laminas, flakes, filters and matrix. The matrix which can be thought of as the body constituent gives the composite its bulk form. The other four, which can be referred to as structural constituents determine the character of the composites internal structure. An special type of composite, fiber glass embedded in a polymer matrix is a relatively recent invention but has in a few decades, become a common place material. Characteristic of good composites, fiber glass, provides the 'best of both worlds', it carries along the superior properties of each component, producing a product that is superior to either of the components separately. The high strength of the small diameter glass fibers is combined with the ductility of the polymer matrix to produce a strong material capable of withstanding the normal loading required of a structural material.

1.3 Organic materials

A. Conductive Polymers

The discovery in 1973 that poly sulfur nitride $(SN)_x$ was intrinsically conducting provided a proof that polymers could be conducting and thus greatly stimulated the search for other conducting polymer [10]. During the last two decades, a new class of organic

polymers has been devised with the remarkable ability to conduct electrical current. These class of materials are called conducting polymers [11].

One of the earliest approaches to make the polymers conductive is to prepare a composite of polymers and conductive filler, such as, metal powder, graphite powder, flake or wire etc. Conductive fillers remain embedded more or less evenly dispersed in the polymer matrix and conduct electric current. But these composites cannot be regarded as conducting polymers because the polymers presents in such composites are non-conducting [12-15].

In 1964, W. A. Little [16] synthesized a superconductor at room temperature with polymeric backbone and large polarizable side groups which led the discovery of new organic compounds with high electrical conductivity.

In the early 1980s, excitement ran high when several prototype devices based on conductive polymers, such as rechargeable batteries and current rectifying *p-n* junction diodes [17] were announced. Among the many polymers known to be conductive, polyacetylene (PAT), polyaniline (PANI), polypyrrole (PP) and polythiophene (PT) have been studied most intensively [18-24]. However, the conductive polymer that actually launched this new field of research was PAT.

Research has been expanded into the studies of heteroatomic conductive polymers because of their better chemical stability and the interest in the polaron and bipolaron conduction mechanism [25, 26]. Among the heteroatomic polymers PP, PT and PANI have been studied extensively.

During the 1980s, PANI was subjected to intense structural, physical, and electrical characterization, using modern experimental techniques. A brief survey, out of numerous features and studies made on PANI is presented below:

Structural features

Organic conducting polymer, PANI, is being studied more and more, and up to the recent years has been the centre of considerable scientific interest. However, PANI is not really a new material and its existence has been known for the past 150 years or over, since it had already been made by Runge in 1834.

PANI has been described in many papers [27] usually as ill-defined forms such as 'aniline black' emeraldine, nigraniline, *etc.* synthesized by the chemical or electrochemical oxidation of aniline. Figure 1.3.1 shows the

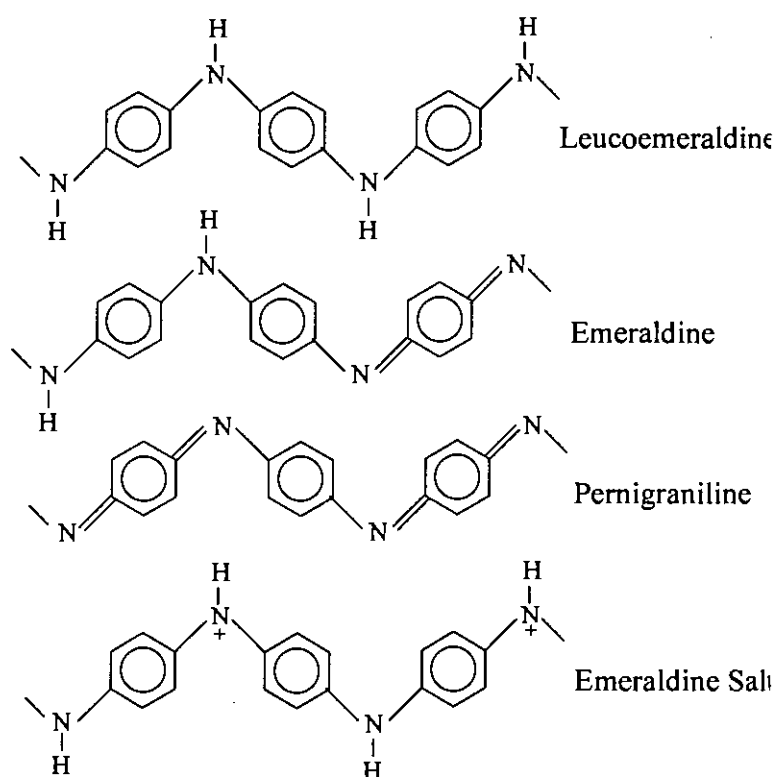
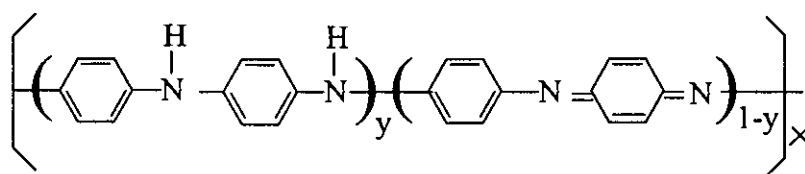


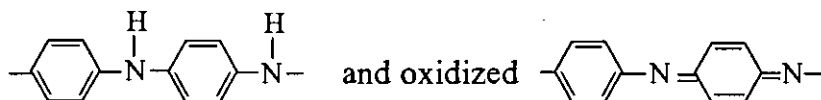
Fig. 1.3.1 Representation of idealized oxidation states of PANI.

idealized oxidation state of PANI: leucoemeraldine, emeraldine, pernigraniline and emeraldine salt. Different structures result in different electrical behaviours of the material. Emeraldine salt is a partially oxidized compound, protonated, with electrical

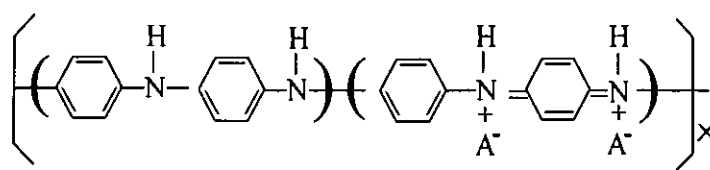
conducting characteristics. Leucoemeraldine is a fully reduced compound with electrical insulating characteristics. There are no double bonds between the aromatic rings and the N-H groups. Emeraldine base is an insulating compound, partially oxidized with few N-H groups in the main chain. Emeraldine changes from insulator to conductor when it is protonated with proton donor acids, such as, hydrochloric acid. This change is one of the most interesting properties of PANI. The structure of emeraldine PANI can be changed to emeraldine salt by removing an electron from the N-H group. Pernigraniline is a fully oxidized compound without conducting characteristics. There are no N-H groups in the structure. The level of protonation in the structure causes dramatic changes in the conductivity. The base form of the polymer in the emeraldine oxidation state ($y = 0.5$)



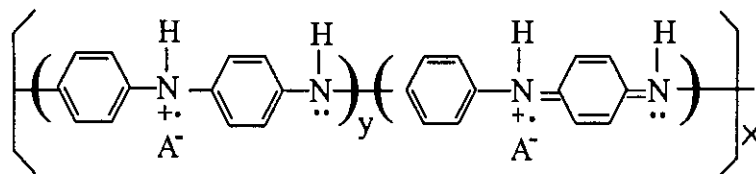
which contains equal number of alternating reduced,



repeat units can be protonated by dilute aqueous acid to produce the corresponding salt (A=anion)



which is believed to exist as polysemiquinone radical cation [28-30].



The polymer exhibits conductivities of $\sim 1\text{-}5 \text{ S cm}^{-1}$ when approximately half of its nitrogen atoms are protonated as shown above.

Methods of preparation

PANI is generally prepared by direct oxidation of aniline using an appropriate chemical oxidant or by electrochemical oxidation on different electrode materials.

Various chemical oxidizing agents have been used by different authors: potassium dichromate [31, 32], ammonium persulfate or peroxydisulfate [33, 34], hydrogen peroxide, ceric nitrate and ceric sulfate [35, 36]. The reaction is mainly carried out in acid medium, in particular sulfuric acid, at a pH between 0 and 2 [31, 32]. However, MacDiarmid *et al.* [33, 34] used hydrochloric acid at pH 1. Genies *et al.* [37] used a eutectic mixture of hydrofluoric acid and ammonia, the general formula of which is $\text{NH}_4\text{F} : 2.3 \text{ HF}$, for which the pH is probably less than 0.

When aniline is mixed with the chemical oxidant in a reaction vessel and left for a certain period of time (the duration of which depends on the temperature and the concentration of active species), the solution gradually becomes colored and a black precipitate appears [38]. The coloration of the solvent is possibly due to the formation of soluble oligomers.

Anodic oxidation of aniline on an inert metallic electrode is the most current method for the electrochemical synthesis of PANI. This method offers the possibility of coupling with physical spectroscopic technique such as visible, IR, Raman, ellipsometry and conductimetry, for *in situ* characterization.

The anodic oxidation of aniline is generally effected on an inert electrode material which is usually Pt [39, 40]. However, several studies have been carried out with other electrode materials: iron [41], copper [42], zinc and lead [43], chrome-gold [44], palladium [45] and different types of carbon vitreous, pyrolic or graphite [46] or on semiconductor [47, 48]. When the polymerization is carried out at constant current, a maximum current density of 10 mA cm^{-2} is rarely exceeded.

Morphology and structure

The adherence and the homogeneity of a PANI film on an electrode varies according to the method of synthesis employed. Diaz [49] has observed weak adherence for a polymer prepared by electrochemical oxidation at constant potential, whereas good adherence results when potential cycling is employed. Kitani *et al.* [50] have reported that, using the same method, a thin homogenous film is initially deposited on the electrode, followed by the formation of an amorphous powder which eventually becomes detached from the electrode surface. Electrochemical investigations on the polymer growth by Thyssen *et al.* [51] yielded evidence for cross-linking reactions leading to the formation of hemispheres.

There is, therefore, a myriad of possible chemical structures for the polymeric backbone of PANI. Elucidation of the precise molecular arrangement is complicated by the fact that these structures are affected by both electronic excitation and reduction and by concomitant protonation and deprotonation of the nitrogen atoms in the polymer.

Optical properties

A wide range of colors from pale yellow to blue for the PANI is observed. From the optical data obtained for PANI, it is possible to assign three absorption zones which are dependent on the oxidation state of the polymer. In the reduced state, PANI is an insulating material, the energy band structure of which is comparable to that of an intrinsic semiconductor, with the resulting absorption being associated with the transition between the valence band and the conduction band. However, when the potential is increased, the polymer oxidizes and intermediate mid-gap states appear in the forbidden band (radical cations and then dications) and thus results absorption in the longer wave length. Elucidation of band model of a polymer can be made based on optical data.

Conductivity

From conductivity measurements, Travers *et al.* [32] have observed that the PANI exhibits a metal-to-insulator transition which is a function of the pH. The conductivity of the polymer is $5 \text{ ohm}^{-1} \text{ cm}^{-1}$ when the polymer is previously equilibrated at pH 6.

MacDiarmid *et al.* [33, 34] has also described a variation in the conductivity of both chemically and electrochemically prepared polymers with the pH of the aqueous solution to which the polymer was exposed before drying. The polymer exhibits a conductivity of $1 \text{ ohm}^{-1} \text{ cm}^{-1}$ when it is equilibrated at a pH between -1 and $+1$, and $10 \text{ ohm}^{-1} \text{ cm}^{-1}$ when it is equilibrated at a pH between 5 and 6. Elsewhere, they indicate that the conductivity of the polymer is a function of the level of doping, with a value of $1 \text{ ohm}^{-1} \text{ cm}^{-1}$ for 15% doping, and varying from 10^{-10} to $10^{-1} \text{ ohm}^{-1} \text{ cm}^{-1}$ for 0% to 10% doping. Measurements carried out by Brahma [52] revealed that PANI doped with iodine exhibits a conductivity four orders of magnitude greater than the undoped polymer.

Solubility

It is generally accepted that PANI is insoluble in most common organic and aqueous solvents, irrespective of the method of synthesis. Nevertheless, Mohilner *et al.* [39] have shown that the polymer is easily dissolved in pyridine and DMF, strongly tinting the solutions blue.

The synthesis of soluble PANI is of great interest since the formation of a soluble material is essential in order to post-synthesis processing. There are two possible methods for preparing soluble polymers: (i) formation of the polymer salt using an anionic dopant which favors dissolution, or (ii) prefunctionalization of the starting monomer with a suitable group prior to polymerization. Chemical synthesis of soluble PANI by the former method has been successfully accomplished by Li *et al.* [53] and involves proton acid dopants of large molecular size such as toluene-*p*-sulfonic acid, sulfanilic acid or polymeric electrolyte-polystyrene sulfonic acid.

Applications

PANI can be used as material for modified electrodes [46, 49], as a corrosion inhibitor for semiconductors in photoelectrochemical assemblies [54], in microelectronics [55] and as electrochromic material [56]. The application which has inspired most interest is in the area of electrochemical batteries. The possible use of PANI as active anodic material is in rechargeable batteries [57].

More recent systematic studies have been undertaken by numerous groups [33, 34, 54] on the possible use of PANI as an active electrode material. These investigations deal with the behavior of PANI in aqueous and organic media as a function of the mode of synthesis.

B. Dyes

A dye must be colored, but it must also be able to impart color to something else on a reasonably permanent basis before it can be considered as a dye.

A dye consists of a color producing structure, the chromogen (electron acceptor), and a part to regulate the solubility and dyeing properties, the auxochrom (electron donor). Without both parts, the material is simply a colored body.

The Chromogen is an aromatic body containing a color-giving group, called the chromophore. Chromophore groups cause color by altering absorption bands in the visible spectrum. Common chromophores are: nitroso group ($-NO$), nitro group ($-NO_2$), azo group ($-N=N-$), ethylene group ($>C=C<$), carbonyl group ($>C=O$), carbon nitrogen groups ($>C=NH$ and $-CH=N-$), carbon sulphur groups ($>C=S$ and $\rightarrow C-S-S-C\leftarrow$) etc.

These groups add color to aromatic bodies by causing displacement of, or an appearance of absorption bands in the visible spectrum. In modern point of views, these groups place the ground and excited state in the range that corresponds to the visible range of the spectrum.

The auxochrome, an essential part of a dye molecule, cause the dye to adhere to the material which it colors, enhance the color of dye, improve solubility in the solvent which is important for application on the materials.

Common auxochrome are: $-NH_2$, $-OH$, $-NR_2$, $-COOH$, $-SO_3H$ etc.

Methylene blue (MB) and procion red (PR) are the typical organic ionic dyes. MB is cationic in nature while PR is an anionic one. Their chemical structures are shown in Fig. 3.1.2.

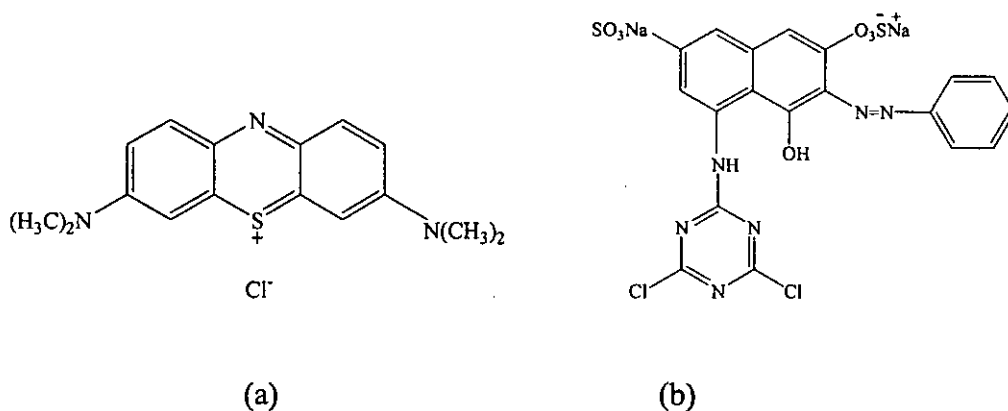


Fig. 1.3.2: Chemical structure of (a) MB and (b) PR.

1.4 Theoretical of experimental techniques

A. Cyclic voltammetry

Electrochemical process is widely used in the polymerization of organic polymer. Most of the system for electrochemical polymerization consists of compartment where three electrodes are dipped into the solution containing monomer and electrolyte solution. Appropriate potential is applied to the working electrode for polymerization of the monomers. The potential of the working electrode, where deposition of the polymer film takes place, is controlled versus the reference electrode using a feed-back circuit or a potentiostat. Feed-back circuit drives the circuit between the working and counter electrode while ensuring that none passed through the reference electrode circuit.

The nature of the working electrode is a critical consideration for the preparation of these films. Since the films are produced by an oxidative process, it is important that the electrode is not oxidized concurrently with the aromatic monomer. For this reason, most of the available films have been prepared using a platinum or a gold electrode.

Potentiostatic, galvanostatic and potential sweep techniques such as cyclic voltammetry are widely used for electrochemical polymerization of aromatic compounds. In potentiostatic technique, a constant potential is applied to the working electrode which is sufficient to oxidize the monomers to be polymerized on the electrode. In galvanostatic process, a constant current density is maintained to polymerize the monomers while film thickness can be monitored in the similar way as described for potentiostatic technique. On the other hand, cyclic voltammetry involves sweeping the potential between potential limits at a known sweep rate. On reaching the final potential limit, the sweep is reversed at the same scan rate to the initial potential and the sweep may be halted, again reversed, or alternatively continued further. In such experiments, cell current is recorded as a function of the applied potential.

B. Infra-red (IR) spectroscopy

Emission or absorption spectra arise when molecules undergo transition between quantum states corresponding to two different internal energies. The energy difference ΔE between the states is related to the frequency of the radiation emitted or absorption by the quantum relation

$$\Delta E = h\nu \qquad 1.4.1$$

where $h \rightarrow$ planck's constant, $\nu \rightarrow$ frequency. Infrared frequencies have the wave length range from 1 μm to 50 μm and are associated with molecular vibration and vibration-rotation spectra. Detection of chemical groups and bonding are done by the typical spectra.

In polymer, the IR absorption spectrum is often surprisingly simple, if one considers the number of atoms involved. This simplicity results first from the fact that many of the normal vibrations have almost the same frequency and therefore appear in the spectrum as one absorption band and second, from the strict selection rules that prevent many of the vibrations from causing absorptions. Samples were introduced as KBr pellets. A block diagram of an IR spectrophotometer is shown in Fig. 1.4.1.

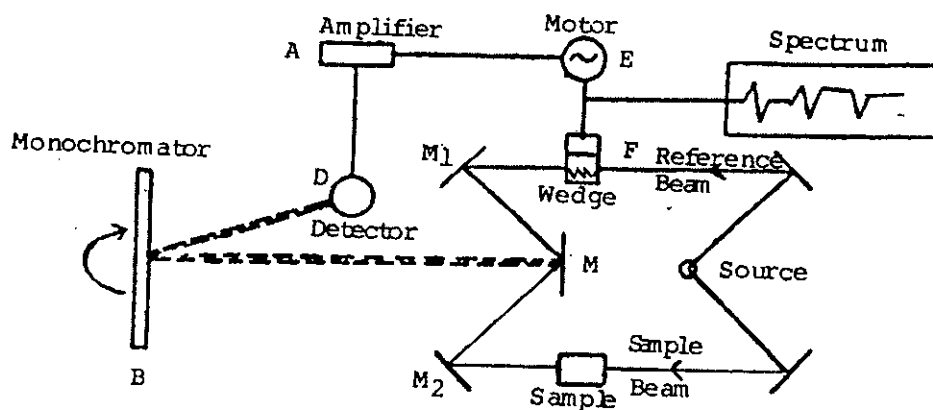


Fig. 1.4.1: A block diagram of an IR spectrophotometer.

C. Ultraviolet-visible spectroscopy (UV-Vis)

Electromagnetic radiation of suitable frequency can be passed through a sample so that photons are absorbed by the samples and changes in the electronic energies of the molecules can be brought about. So it is possible to effect the changes in a particular type of molecular energy using appropriate frequency of the incident radiation. When a beam of photons passes through a system of absorbing species, then we can write

$$-\frac{dI}{dx} = \alpha I \quad 1.4.2$$

where, $I \rightarrow$ intensity of photon beam

$dI \rightarrow$ reduction of intensity

$dx \rightarrow$ rate of photon absorption with distance (x) traversed

$\alpha \rightarrow$ absorption co-efficient of the material

Now if I_0 is the initial intensity at thickness $l = 0$ and I is the transmitted radiation at $x = l$, then by integration, we can write

$$\ln \frac{I_0}{I} = \alpha l \quad 1.4.3$$

For polymers and polymeric composites, UV-Vis spectrum is taken to measure the impurity level, band gap energy etc. The electrode spectra of the prepared compounds were recorded on a UV-Vis recording spectrophotometer in the wave length range 300-800 nm. A schematic diagram of UV-Vis spectrophotometer is shown in Fig. 1.4.2.

D. X-ray diffraction

The X-ray diffraction (XRD) provides substantial information on the crystal structure. This method is applied for the investigation of orderly arrangements of atoms or molecules through the interaction of electromagnetic radiation to give interface effects with structures comparable in size to the wave length of the radiation. Studies on the crystal structures developed, based on methods using single crystals after the discovery of X-ray diffraction by crystals made by the Von Laue [58]. Now a days XRD is used not only for the determination of crystal structure but also chemical analysis, such as chain conformations and packing for polymers, for stress measurements and for the

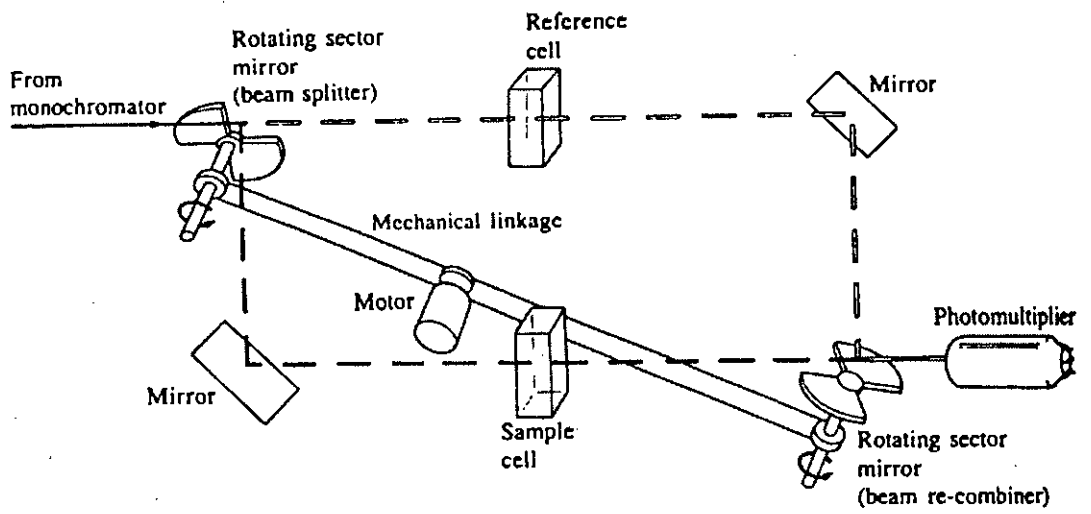


Fig. 1.4.2: A block diagram of an UV-Vis spectrophotometer.

measurement of phase equilibria and the measurement of particle size, for the determination of the orientation of the crystal and the ensemble of orientations in a polycrystalline material.

X-rays are the electromagnetic radiation whose wavelength are in the neighborhood of 1° A. The wave length of an X-ray is thus of the same order of magnitude as the lattice constant of crystals, and it is this which makes X-rays so useful in structures analysis of crystals whenever X-ray are incident on a crystal surface they are reflected. The reflection abides by the celebrated Bragg's law as given below:

$$2d \sin\theta = n\lambda \quad 1.4.4$$

where d is distance between crystal planes, θ is the incident angle, λ is the wave length of X-ray and n is a positive integer. The diffracted X-ray may be detected by their action on photographic films or plates or by means of a radiation counter or electronic equipment feeding data to a computer [59].

The main purpose of using this technique for the analysis of the studied polymeric samples is to observe, from the X-ray diffraction pattern, the change in crystallinity in the series upon same condition.

E. d. c. conductivity

The conductivity of polymer or polymeric composites depends on dopant level, protonation level of oxidation morphology and moisture content of the sample. Electrical resistivity of the polymer samples may be measured by two probe and four probe techniques. The electrical conductivity may be measured by using ohm's law

$$E/I = R \quad 1.4.5$$

where I is the current in amperes, E is the potential difference in volts, R is the resistance in ohms. The reciprocal is termed the conductance, this is measured in Siemens (S) which is reciprocal of ohms (ohm^{-1}). The resistance of a samples of length L , and cross-sectional area A , is given by

$$R = \rho L/A \quad 1.4.6$$

where ρ is a characteristic property of the material termed the resistivity. If L and A will be measured respectively in cm and then ρ refers to cm cube of the material and

$$\rho = RA/L \quad 1.4.7$$

The reciprocal of resistivity is the conductivity, (formerly specific conductance)

$$K = 1/\rho \quad \text{or} \quad K = L/RA \quad 1.4.8$$

which in SI units is the conductance of a one cm cube of substance and has the units $\text{ohm}^{-1} \text{cm}^{-1}$ or S cm^{-1} [60].

In this experiment, the powdered samples were pressed to rigid solid mass by pressing from the both sides of the mass. The two electrodes of microvolt were then connected with solid mass and resistivity was measured directly from the microvolt.

SEM technique

The scanning electron microscope (SEM) uses a finely focused beam of electrons to scan over the area of interest. The beam-specimen interaction is a complex phenomenon. The electrons actually penetrate into the sample surface, ionizing the sample and cause the release of electrons from the sample. These electrons are detected and amplified into a SEM image that consists of Back Scattered Electrons and Secondary Electrons. Since the electron beam has a specific energy and the sample has a specific atomic structure, different image will be collected from different samples, even if they have the same geometric appearance.

The specimen stage of SEM allows movement of the specimen along 5 axis. The basic stage is controlled manually by micrometers and screw-type adjusters on the stage door. The motorized stage has motors driving the X, Y, Z and rotation controls, all with manual over ride.

The stage can be tilted over 90° . The tilt axis always intersects the electron optical axis of the column at the same height (10 mm). When the specimen positioned at this height, the specimen can be tilted in the eucentric plane. This means that during tilt, almost no image

displacement occurs. The tilting mechanism can be locked for more stability at high magnification.

1.5 Aim of the present study

Metal and semiconductor particles comprise a fundamentally and technologically interesting class of materials because of their interesting physico-chemical and opto-electronic behaviors. The properties of these materials, their free electron behavior and straight forward surface modification are of potential utility in chemical sensing, linear and non-linear optics and in a variety of nanoscale electronic devices scheme. Taking into account the early works, it is evident that a good progress has also been made in preparing conductive polymers with well-defined structures. PANI is unique among the other conducting polymers that its electrical properties can be reversibly controlled both by charge-transfer doping and by protonation. The wide range of associated electrical, electrochemical and optical properties coupled with good stability made PANI potentially attractive for application as an electronic material. The possibility of dispersing metallic and semiconductor particles inside the conducting polymer to form hybrid conducting matrices has received a special attention in recent times. Inorganic oxide such as TiO_2 and organic dye, viz. MB or PR are very important class of opto-electronic materials because of their uses in many important photochemical and opto-electrochemical reactions. In the present work, attempt was made to embed TiO_2 , MB, or PR in the PANI matrix and thus to construct a non-conventional new electrode system of hybrid structure. The new electrode based on organic/organic and organic/inorganic hybrid structure would be examined for their performance toward electrochemical redox processes. It is expected that hybrid structure composite matrix could be used as an electrode both in aqueous and non-aqueous medium. Thus, it could be good replacement for the very costly conventional metal and semiconductor electrodes. Structural, optical and electrical properties of the new electrode matrices are also planned to be undertaken. These results could provide useful information for the possibility of their uses in electronic and opto-electronic processes.

References

1. H. Lund, in organic electrochemistry, Eds., M. M. Baizer and H. Land, Marcel Dekker, 1983.
2. S. Barnartt, *J. Electrochem. Soc.*, **99** (1952) 549.
3. Reports on the IUPAC Convention on Electrochemistry, *Electrochim. Acta*, **27** (1982) 629 and *Pure and Appl. Chem.*, **37** (1974) 503, **51** (1979) 1159.
4. L. Smart and E. Moore, *Solid State Chemistry*, Chapman and Hall, (1992) 126.
5. *The Oxide Handbook*, Samsonov, G. V. Ed.; IFI / Plenum, New York, p23, 1982.
6. Grant, F. A. *Riv. Modern Phys.*, **31** (1959) 646.
7. Cronmeyer, D.C. *Phys. Rev.* **87** (1952) 876.
8. Bickley, R. I. *Chem. Phys. of Solids and Their Surface* **7** (1978) 118.
9. Salvador, P. *Solar Energy Matter.*, **6** (1982) 241.
10. V. V. Walatka, M. M. Labes and J. H. Perlstein, *J. Phys. Rev. Lett.*, **31** (1973) 1139.
11. A. J. Heeger, G. B. Street and G. Tourillon, *Hand Book of Conducting Polymers* (T. A. Skotheim, ed.), Marcel Dekker, Inc., New York, vol. 1 (1986) 265, 293.
12. R. B. Seymour, *Conducting Polymers*, Plenum Press, New York, (1981) 23.
13. E. K. Sickel, *Carbon Black Polymer Composites*, Marcel Dekker, New York, (1982).
14. A. Malliaris and D. T. Turner, *J. Appl. Phys.*, **42** (1971) 614.
15. H. Inokushi and H. Akamatu, *Solid State Physics*, (F. Seitz and D. Turnbull, ed.), **12** (1955) 93.
16. W. A. Little, *Phys. Rev.* **134A** (1964) 1416.
17. C. K. Chiang, A. J. Heeger and MacDarmid, *Ber. Bunsenges. Phys. Chem.*, **83** (1979) 407.
18. R. de Surville, M. Jozefowicz, L. T. Yu, J. Perichon and R. Buvet, *Electrochim. Acta.*, **13** (1968) 1451.
19. A. G. MacDiarmid, J.-C. Chiang, M. Halpen, W.-S. Huang, S.-L. Mu, N. L. D. Somasiri, W. Wu and S. I. Yaniger, *Mol. Cryst. Liq. Cryst.*, **121** (1985) 173.
20. E. M. Genies, A. A. Syed and C. Tsintavis, *Mol. Cryst. Liq. Cryst.*, **121** (1985) 181.
21. E. W. Paul, A. J. Ricco and M. S. Wrington, *J. Phys. Chem.*, **89** (1985) 1441.
22. P. M. McManus, S. C. Yang and R. J. Cushman, *J. Chem. Soc., Chem Commun.*, (1985) 1556.

23. D. McInnes, M. A. Druy, P. J. Nigrey, D. P. Nairns, A. G. MacDiarmid and A. J. Hegger, *J. Chem. Soc., Chem. Commun.*, (1981) 317.
24. A. G. Hegger, G. B. Street and G. Tourillon, in *Hand Book of Conducting Polymers* (T. A. Skotheim, ed.), Marcel Dekker, Inc., New York, vol 1 (1986) 46, 51.
25. J. L. Bredas, G. B. Street, *Acc. Chem. Res.*, **18** (1985) 309.
26. M. G. Kanatzldls, *Chemical Engineering News*, Dec. 03 (1990) 38- 42.
27. A. G. Green and A. E. Woodhead, *J. Chem. Soc.*, (1910) 2388; R. de Surville, M. Josefowicz, L. T. Yu, J. Perichon and R. Buvet, *Electrochem. Acta*, **13**, (1968) 1451; F. Cristofini, R. de Surville, M. Josefowicz, L. T. Yu and R. Buvet, *C. R. Acad. Sci. Paris, Ser. C*, **268** (15), (1969) 1346; A. F. Diaz and J. A. Logan, *J. Electroanal. Chem. Interfacial Electrochem.*, **111** (1980) 111; R. Noufi and A. J. Nozic, *J. Electrochem. Soc.*, **129**, (1982) 2261.
28. A. J. Epstein, J. M. Ginder, F. Zuo, H.-S. Woo, D. B. Tanner, A. F. Richter, M. Angelopoulos, W. S. Hung and A. G. MacDiarmid, *Synth. Met.*, **21**, (1987) 63.
29. A. G. MacDiarmid, J.-C. Chiang, A. F. Richter, N. L. D. Somasiri and A. J. Epstein, (L. Alcacer, ed.), *Couducting Polymers*, D. Redel Publishing Co., Dordrecht, The Netherlands (1987).
30. A. G. MacDiarmid, J.-C. Chiang, A. F. Richter and A. J. Epstein, *Synth. Met.*, **18** (1987) 285.
31. E. M. Genies and C. Tsintavis and A. A. Syed, *Mol. Cryst. Liq. Cryst.*, **121** (1985) 181.
32. J. P. Travers, J. Chroboczek, F. Devreux, F. Genoud, M. Nechtschein, A. A. Syed, E. M. Genies and Tsintavis, *Mol. Cryst. Liq. Cryst.*, **121** (1985) 195.
33. A. G. MacDiarmid, J. C. Chiang, M. Halpern, W. S. Huang, S. L. Mu, N. L. D. Somasiri, W. Wu and S. I. Yaniger., *Mol. Cryst. Liq. Cryst.*, **121** (1985) 173.
34. A. G. MacDiarmid, N. L. D. Somasiri, W. R. Salaneck, I. Lundstrom, B. Liedberg, M. A. Hasan, R. Erlandsson and P. Konrasson, *Springer Series in Solid State Sciences*, Vol. 63, Springer, Berlin, 1985, p-218.
35. R. L. Hand and R. F. Nelson, *J. Electrochem. Soc.*, **125** (1978) 1059.
36. R. L. Hand and R. F. Nelson, *J. Am. Chem. Soc.*, **96** (1974) 850.
37. *Fr. Patent No. EN 8307958* (1983); *U.S. Patent No. 698 183* (1985).
38. L. T. Yu, M. S. Borredon, M. Jozefowicz, G. Belorgey and R. Buvet., *J. Polym. Sci.*, **10** (1987) 2931.
39. D. M. Mohilner, R. N. Adams and W. J. Argersinger, *J. Am. Chem. Soc.*, **84** (1962) 3618.

40. J. Bacon and R. N. Adams, *J. Am. Chem. Soc.*, **90** (1968) 6596.
41. G. Mengoli, M. T. Munari, P. Bianco and M. M. Musiani, *J. Appl. Polym. Sci.*, **26** (1981) 4247.
42. G. Mengoli, M. T. Munari and C. Folonari, *J. Electroanal. Chem.*, **124** (1981) 237.
43. E. M. Genies and C. Tsintavis, unpublished work.
44. E. W. Paul, A. J. Ricco and M. S. Wrighton, *J. Phys. Chem.*, **89** (1981) 1441.
45. B. Pfeiffer, A. Thyssen, M. Wolff and J. W. Schultze, *Int. Workshop – Electrochemistry of Polymer Layers, Dutsburg, F. R. G., Sept. 15-17, 1986*.
46. C. M. Carlin, L. J. Kepley and A. J. Bard, *J. Electrochem. Soc.*, **132** (1985) 353.
47. R. Noufi, A. J. Nozik, J. White and L. F. Warren, *J. Electrochem. Soc.*, **129** (1982) 226.
48. B. Aurian-Blajeni, I. Taniguchi and J. O'M. Bockris, *J. Electroanal. Chem.*, **149** (1983) 291.
49. A. F. Diaz and J. A. Logan, *J. Electroanal. Chem.*, **111** (1980) 111.
50. A. Kitani, J. Yano and K. Sasaki, *Chem. Lett.*, (1984) 1565.
51. A. Thyssen, A. Hochfeld, R. Kessel, A. Meyer and J. W. Schultze. *Synth. Met.*, **29** (1989) E357; T. A. Borgerding and J. W. Schultze, *Makromol. Chem., Macromol. Symp.*, **8** (1987) 143.
52. A. Brahma. *Solid State Commun.*, **57** (1986) 673.
53. S. Li. Y. Cao and Z. Xue., *Synth. Met.*, **20** (1987) 141.
54. E. M. Genies, M. Lapkowski, C. Santier and E. Vieil, *Synth. Met.*, **18** (1987) 631.
55. (a) E. P. Lofton, J. W. Thackeray and M. S. Wrighton, *J. Phys. Chem.*, **90** (1986) 6080; (b) S. Chao and M. S. Wrighton, *J. Am. Chem. Soc.*, **109** (1987) 6627.
56. T. Kobayashi, H. Yoneyama and H. Tamura, *J. Electroanal. Chem.*, **161** (1984) 419; **177** (1984) 281, 293.
57. F. Cristofini, R. De Surville, M. Josefowicz, L. T. Yu and R. Buvet, *C. R. Acad. Sci., Ser. C*. **268** (1969) 1346.
58. M. J. Buerger and L. V. Azraf, the powder method in X-ray crystallography, McGraw. Hill, New York, (1958).
59. B. D. Cullity, Elements of X-ray diffraction, Weseley publishing Inc., Philippines, (1978).
60. G. H. Jeffery, J-Bassett, J. Mendham and R. C. Denney, Vogel's Text book of Quantitative Chemical Analysis, 5th edition ed. ELBS, England, (1991), p-519.

Chapter 2

EXPERIMENTAL

2.1 Materials and devices

A. Chemicals

Analytical grade chemicals and solvents were used throughout the work and were used as received unless stated otherwise. The monomer aniline was distilled twice prior to its use in polymerization reactions. Doubly distilled water (H₂O) was used as solvent to prepare most of the solutions utilized in this work except for optical analysis where N, N-dimethyl formamide (DMF) was employed as solvent. The important chemicals and solvents utilized throughout the experiments are listed below:

- i) Aniline [E. Merck, Germany]
- ii) Sulphuric acid (97%) [E. Merck, Germany]
- iii) N, N-dimethyl formamide [E. Merck, Germany]
- iv) Methylene blue [Fluka, England]
- v) Procion red [Fluka, England]
- vi) Titanium (IV) oxide [E. Merck, Germany]

B. Instruments

Analysis of the samples performed in this work employed the following devices:

- i) Potentiostat / Galvanostat / Coulombmeter [HABF 501, Hokuto Denko, Japan]
- ii) X-Y recorder [F-5C, Riken Denshi Co. Ltd, Japan]
- iii) Infra red spectrophotometer [IR-470, Shimadzu, Japan]
- iv) UV-visible spectrophotometer [UV-1601 PC, Shimadzu, Japan]
- v) Automatic X- ray diffractometer [JDX-8P, JEOL Ltd., Japan]
- vi) Scanning electron microscope [Philips XL 30, Holland]
- vii) Autoranging microvolt [Keithley 197 A, USA]
- viii) Digital balance [FR-200, Japan]
- ix) Controlled heating vacuum oven [Gallencamp, England]

2.2 Electrochemical preparation of the film electrodes

The electrochemical synthesis and characterization of the organic (e.g. PANI), organic/organic (e.g. PANI/MB, PANI/PR) and organic/inorganic (e.g. PANI/TiO₂) films were carried out at room temperature in a standard three-electrode one compartment electrolysis cell. A schematic representation of the electrochemical cell employed in this work is illustrated in Fig. 2.2.1. The cell consisted of a 0.25 cm² working electrode (WE) made of platinum (Pt), a 0.50 cm² Pt foil counter electrode (CE) and a saturated calomel electrode (SCE) as the reference (RE). Prior to each experiment, the working Pt electrode was carefully polished with fine-grained abrasive paper, followed by rinses in distilled water and 5 min immersion in concentrated nitric acid (HNO₃), before it was finally dried on clean laboratory tissues. The reproducibility of experimental results was greatly improved with this pretreatment of the working electrode. The films were grafted onto the working Pt electrode either by sweeping the potential or constant potential mode. Voltammetric sweeps were always started in the anodic direction from 0.0V at 100 mV/s, unless stated otherwise. A Hokuto Denko (HABF 501) electrochemical measurement system provided necessary potential and current control.

A. Polyaniline:

PANI film was prepared on the Pt working electrode by the ordinary anodic polarization method [1-7]. The working Pt was the anode and counter Pt foil was used as the cathode. A 0.8M sulphuric acid (H₂SO₄) in distilled H₂O containing 0.5 M aniline was used as the electrolytic solution. Electrolysis was carried out either by sweeping the potential between -0.3 V and +1.0 V vs SCE or by constant potential made at +1.0 V. After polymerization, the potential of the PANI film coated Pt electrode was held at 0.0V until the cathodic current disappeared to dedoped the PANI film. The film as grown and dedoped, was washed several times in 0.8M H₂SO₄ to remove any traces of monomer or any other reactants or by-products that might be produced during electrolysis.

B. Polyaniline / Methylene blue :

PANI/MB films were deposited on the Pt electrode from an aqueous electrolytic solution containing 0.5 M aniline, 0.8M H₂SO₄ and 1.93×10^{-5} M methylene blue (MB) at room

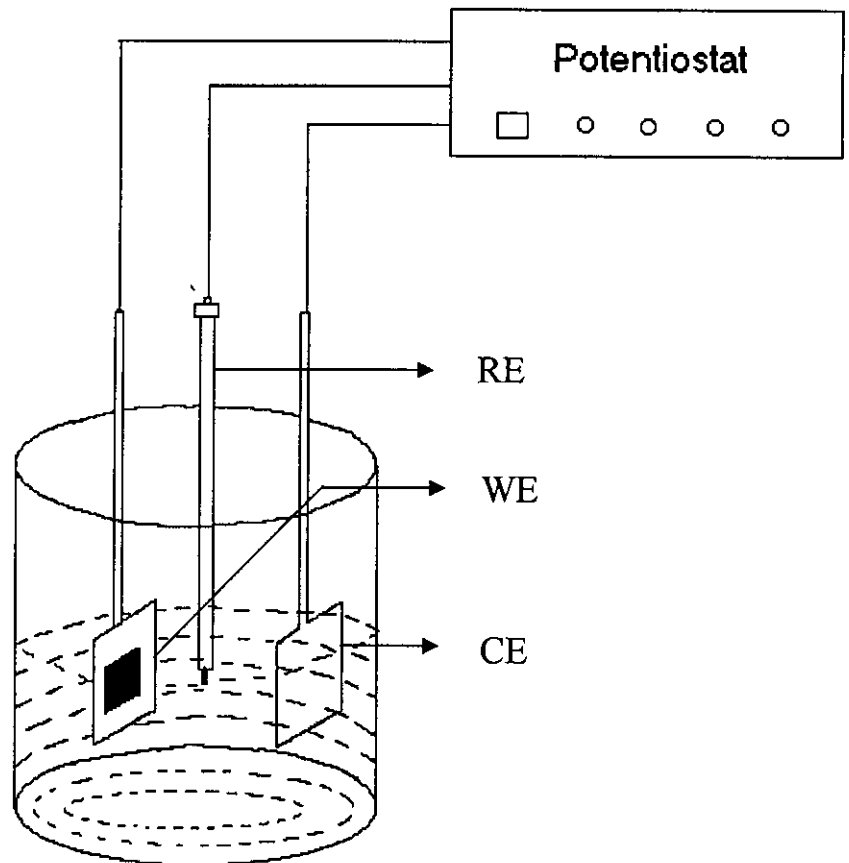


Fig. 2.2.1: Three electrode system for electrochemical measurements.

temperature. The film was coated onto the Pt surface either by cycling the potential or by a controlled potential method. In the cycling method, the potential was swept from -0.3 V to $+1.0$ V at a scan rate of 100 mV/sec. In the preparation of the film, a potentiogalvanostat (Hokuto HABF 501) with function-generating ability were used for generation of potential and supply of current. The current-potential response was recorded in a X-Y recorder (F-5C, Riken Denshi). The film grown onto the Pt electrode was dedoped and washed several times in 0.8 M H_2SO_4 as stated previously.

C. Polyaniline / Procion red:

Electrochemical deposition of the PANI/PR film on the Pt substrate employed either potential sweeping or controlled potential method. The former technique involves scanning between the potential range -0.3 and $+1.0$ V vs SCE while the latter one was operated at $+1.0$ V. The PANI/PR film was grown by anodic oxidation of aniline from an aqueous electrolytic solution containing 0.8 M H_2SO_4 and 1.93×10^{-5} M procion red (PR). A deep blue film appeared on the working electrode when the scanning reached to $+0.8$ V and above or a constant potential of $+1.0$ V was applied to the electrode. The film thus formed was dedoped and washed carefully, according to the procedure described earlier. The potentiostat/galvanostat employed provide the necessary current and potential generation.

D. Polyaniline / Titanium (IV) oxide:

The electrochemical formation of the PANI/TiO₂ film employed an electrolytic aqueous solution containing 0.8 M aniline, 0.8 M H_2SO_4 and a TiO₂ suspension. TiO₂ suspension was made by adding 0.5 g TiO₂ in 400 ml distilled H₂O and then mixing the content by beating for an hour. The mixture was then kept undisturbed for 10 minutes. The TiO₂ suspension was then decanted for use in the PANI/TiO₂ synthesis.

The content of the electrolytic solution was then subject to electrolysis in the electrochemical cell. Electrolysis was performed as before by sweeping the potential between -0.2 V and $+1.0$ V. During electrolysis, anodic polymerization of the Pt electrode in the electrolytic media results a deposition of a compact film on the electrode.

Multiple scanning allowed the film to be grown thicker. Similar film was also grafted on the electrode when a constant potential of +1.0 V was applied. The film thus formed was dedoped and washed repeatedly to remove undesired species.

2.3 Spectral analysis

A. Infra red spectra

The samples, PANI, PANI/MB, PANI/PR and PANI/TiO₂ were obtained electrochemically, as described in section 2.2, either as thin films grafted on the Pt electrode or as thick deposits, which can be scratched off the Pt electrode, rinsed and dried. They were crushed to powder and used for IR measurements. IR spectra of the studied solids were frequently obtained by mixing and grinding a small portion of the materials with dry and pure KBr crystals. Thorough mixing and grinding were carried out in a mortar by a pestle. The powder mixture was then compressed in a metal holder under a pressure of 8–10 tons to make a pellet. The pellet was then placed in the path of IR beam for measurements. IR spectra of all the studied samples were recorded by an IR spectrophotometer in the region of 4000–400 cm⁻¹.

B. Ultra violet–visible spectra

UV-Vis spectra of the samples were recorded by dissolving the solids in DMF. The solutions of MB, PANI and PANI/MB were made by dissolving small amount of each solid in 50 mL of DMF. The dissolution employed 30 min sonication in an ultrasonic bath to allow appreciable extent of dissolution. The sample solutions exhibited deep color in some cases. Thus, to ensure preferred dilution of the sample solutions for this spectral measurement, the solutions were diluted with DMF to a visible extent in such a way that the optical density remains within the range 0.5 to 1.0. The sample solution was placed in the sample holder while the reference holder was filled with the DMF solvent. The UV-Vis spectral analysis of the samples employed a double beam spectrophotometer attached with a synchronized personal computer (PC) for recording the spectral data. All the optical analysis were performed at room temperature to within 30° (± 2°)C.

C. X – ray diffraction pattern:

The samples examined for their structural analysis were obtained either as films or thick deposits as described previously. The dried samples were thoroughly crushed to powder for X-ray diffraction (XRD) measurements. The powdered samples were pressed in a square aluminum sample holder (40 mm× 40 mm) with a 1 mm deep rectangular hole (20 mm × 15 mm) and pressed against an optically smooth glass plate. The upper surface of the sample was labeled in the plane with its sample holder. The sample holder was then placed in the diffractometer. The XRD pattern was recorded in an automatic X-ray diffractometer using Mo(Zr) radiation having wave length of 1.5 Å. The diffractometer was operated at 30 KV, 20 mA with a scan speed of 2° min⁻¹. The samples, thus examined for XRD characteristics were processed and operated under ambient atmospheric conditions.

2.4 Electrical conductivity measurements

The study of electrical conductivity of the solids at room temperature was carried out by a conventional two point-probe method [8,9]. For this purpose, the dried and powdered solids were compressed mechanically in a transparent plastic tube as illustrated in Fig. 2.4.1. A few centimeters long plastic tube having diameter 1.75 mm was taken for loading the solids in it. One end of the tube was tightly closed with a copper (Cu) wire having the same diameter as that of the tube. The sample was then pushed gradually inside the tube and compressed mechanically from the other end of the tube by another piece of same wire. Eventually the mass become tightly compressed having a very rigid structure that on further pressing did not change the length of the compressed mass. In this position, the other end of tube was made closed by the similar wire. The two Cu wires at the two ends pressed tightly in such a way that ensures an adequate contact between the sample and the wires. The wire poles were used for electrical contact to get the voltage drop between the two ends of the sample under investigation. An auto ranging microvolt was employed for the conductivity measurements. This equipment allows reading directly the resistance of the sample. Thus, knowing the observed resistance, the specific conductance of each studied sample was calculated out by using the standard

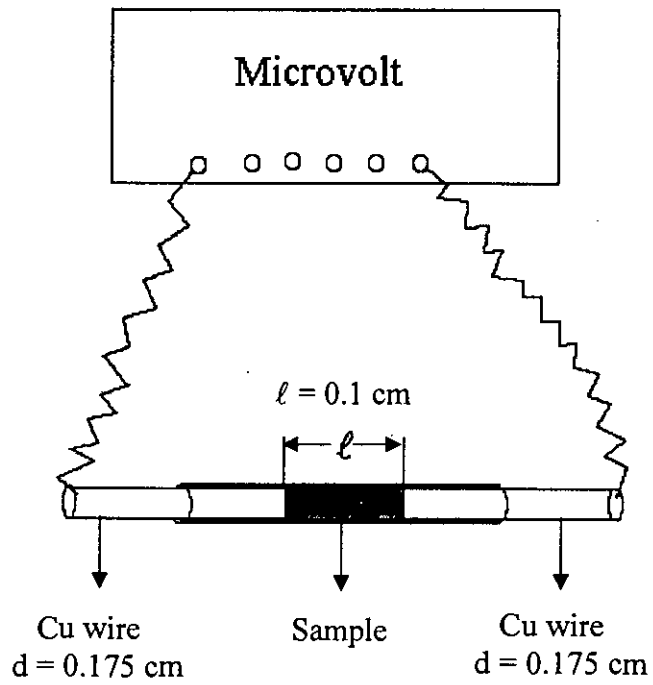


Fig. 2.4.1: The construction for the measurement of the two point-probe conductivity.

relation mentioned in chapter 1. The measurement was conducted at laboratory temperature ($\sim 30^{\circ}\text{C}$).

2.5 Analysis of surface morphology

Scanning electron microscopic technique was adapted to analyze the surface morphology of the samples. The PANI, PANI/MB, PANI/PR and PANI/TiO₂ as prepared onto the Pt electrode as films were utilized for SEM analysis. The films thus grown were rinsed and dried under vacuum before subjected to their surface analysis. The samples were loaded to the SEM chamber where these were kept under evacuation of 10^{-3} to 10^{-4} torr for ~ 30 min. Then a very thin layer of gold, \sim few nanometers thick, was sputtered onto the sample surface to ensure electrical conductivity of the sample surface under studied. The sample was then placed in the main chamber to view its surface image. A Philips XL 30 SEM arrangement was employed for this analysis. The image of the surface morphology is recorded in a PC that interfaced with the main SEM system. The operation system performed all the analysis under ambient atmospheric conditions.

2.6 Doping-dedoping technique

The synthesized film electrodes, *viz.*, PANI, PANI/MB, PANI/PR and PANI/TiO₂ were doped and dedoped electrochemically by the conventional anodic and cathodic treatment of the working electrode [10]. The doping-dedoping process was performed in a single compartment three-electrode cell under ambient atmosphere (Fig. 2.2.1). The films were grown onto the Pt electrode either as thin (6 cycle) or thick (25 cycle) deposits. The film thus deposited was then rinsed repeatedly to remove any traces of monomer or other by-products. To perform doping-dedoping process, the rinsed film electrode was then placed in the cell containing monomer free electrolytic solution only. The doping-dedoping processes of the films were examined by the cyclic voltammogram in an aqueous electrolytic solution of 0.8 M H₂SO₄. A potential sweeping from -0.3 to $+0.6$ V was allowed with a scan rate of 100 mV/sec. Indeed, the doping and dedoping process of the films were observed to be occurred within the potential range scanned in this experiment.

2.7 Electrochemical degradation study

In this work, electroactive matrices were synthesized to examine their ability to act as electrodes in the electrochemical system. The durability and stability are the prerequisites for their potential use as electrodes in the electrochemical systems. Thus, the study of the electrode degradation was carried out with the film of PANI, PANI/MB, PANI/PR and PANI/TiO₂. The films were grown onto the Pt substrate either as thin or thick structured as described in section 2.2. In order to study their electrochemical degradation, the voltammetric behavior of the film coated electrodes was followed. This was done in the electrochemical one compartment cell (Fig. 2.2.1) connected with a potentiostat/galvanostat and a X-Y recorder. The potential was swept between either -0.3 and +1.0 V or -0.3 and +2.0 V vs SCE. One set of degradation study was dealt with the multiple sweeping and observing any degradation, *i.e.* if any change in the peak position and current response, occur than observed in the original voltammogram. The other set of degradation was attempted by applying high anodic potentials, such as, +1.0 and +2.0 V vs SCE and then recording the voltammogram to detect any changes either in peak position and / or current response. For degradation studies, monomer free electrolytic solution of 0.8 M H₂SO₄ was used throughout the work. The voltammograms of the films were measured by scanning the potential first in the positive direction and then in the negative side with a scan rate of 100 mA/sec, unless otherwise stated.

References

1. Y. Ohnuki, T. Ohsaka, H. Matsuda and N. Oyama, *J. Electroanal. Chem.*, **158** (1983) 55.
2. N. Oyama, Y. Ohnuki, K. Chiba and T. Ohsaka, *Chem. Lett.*, (1983) 1759.
3. R. Noufi, A. J. Nozik, J. White and L. F. Warren, *J. Electrochem. Soc.*, **129** (1982) 2261.
4. A. Volkov, G. Tourillon, P. C. Lacaze and J. E. Dubois, *J. Electroanal. Chem.*, **115** (1980) 279.
5. A. F. Diaz and J. A. Logan, *J. Electroanal. Chem.*, **111** (1980) 111.
6. A. Kitani, J. Izumi, J. Yano, Y. Hiromoto and K. Sasaki, *Bull. Chem. Soc. Jpn.*, **57** (1984) 2254.
7. A. G. MacDiarmid, J.-C. Chiang, M. Halpern, W-S. Huang, S-L. Mu, N. L. D. Somasiri, W. Wu and S. I. Yaniger, *Mol. Cryst. Liq. Cryst.*, **121** (1985) 173.
8. I. J. van der Pauw, *Philips Res. Repts.*, **13** (1958) 1.
9. J. Lange, *J. Appl. Phys.*, **35** (1964) 2659.
10. See, for example, A.-N. Chowdhury, Y. Kunugi, Y. Harima and K. Yamashita, *Thin Solid Films*, **271** (1995) 1.

Chapter 3

RESULTS AND DISCUSSION

3.1 Electrochemical synthesis

A. Organic electrode: PANI

Anodic oxidation of the monomers on the inert metallic electrodes to yield polymer is the most current electrochemical method for the synthesis of conductive polymer films, such as, PANI, polypyrrole (PP), polythiophene (PT) etc. The anodic oxidation of aniline is generally effected on an inert material which is generally Pt [1-7]. In the present work, electrochemical synthesis of PANI was carried out by anodic oxidation of aniline onto a Pt electrode. Typical CV of electrochemical polymerization of aniline is given in Fig. (3.1.1). On sweeping the first potential cycle from -0.3 to $+1.0$ V vs SCE, a sharp rise in current is seen at a potential *ca.* $+0.8$ V indicating the oxidation of aniline to yield PANI [8, 9]. A thin deep blue film is seen on the Pt surface. As the sweeping repeated, i.e., in the second and subsequent cycles, the peak current increases further indicating the formation of more deposits of PANI on the substrate. Potential cycling was repeated upto 6 cycles for the deposition of a thin film of PANI. The anodic peak *at ca.* $+0.18$ V is observed from the second scan. This peak can be assigned to the oxidation of PANI film deposited on the electrode corresponding to the conversion of amine units to radical cations in the polymer chain [10-11]. The deep blue color of the film turned to greenish-yellow when potential sweep approached to the cathodic direction at *ca.* $+0.0$ V or lower. Figure 3.1.2 also represents the CV of electrochemical polymerization of aniline under similar electrolytic conditions; here polymerization was allowed to grow on the Pt upto 25 cycles. As the PANI film got thicker, the characteristic peaks seem to be less prominent or at least broadened and also their positions are shifted. However, the colour changes of the thick film also occur in the similar fashion as described for the thin PANI film. The Pt electrode thus coated with the PANI film is referred to as PANI electrode.

The mechanism for the electrochemical formation of PANI as proposed by Y. Wei *et. al.* [12], is presented in Scheme -1. The oxidation of aniline to form the diamer is a slow reaction [12, 13]. Since the diamer has a lower oxidation potential than does aniline [1, 14], it will undergo oxidation immediately after its formation to yield a diiminium ion [13]. An electrophillic attack of aniline monomer by the diiminium or by a nitrenium

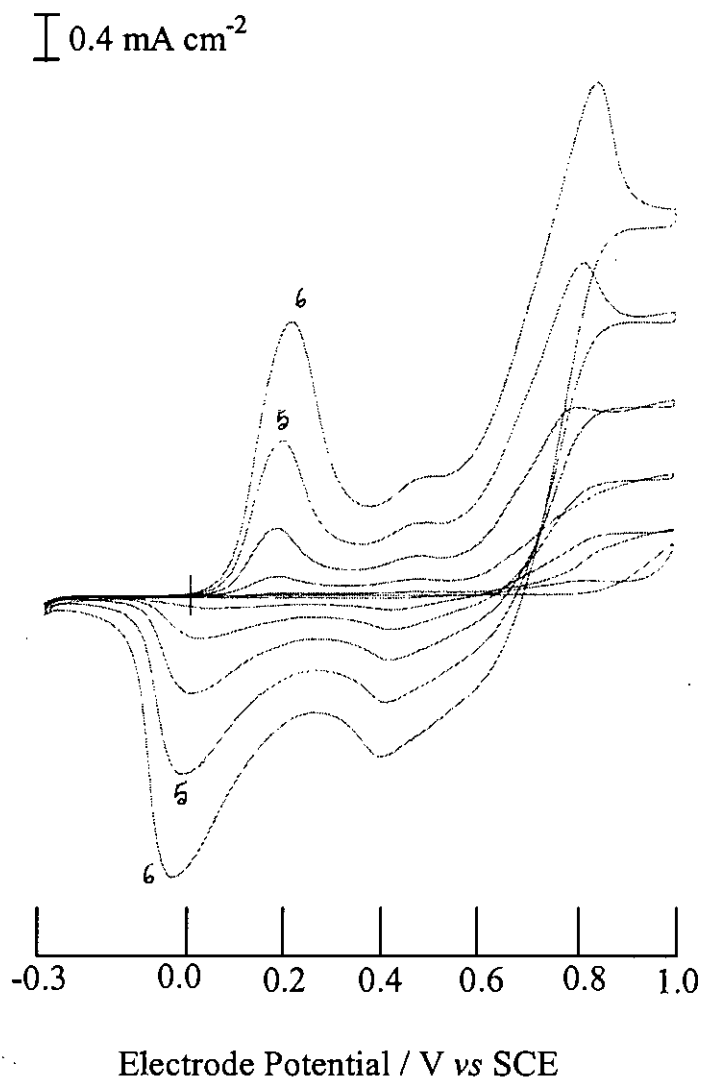


Fig. 3.1.1: CV (6th cycle) during electrochemical synthesis of PANI.

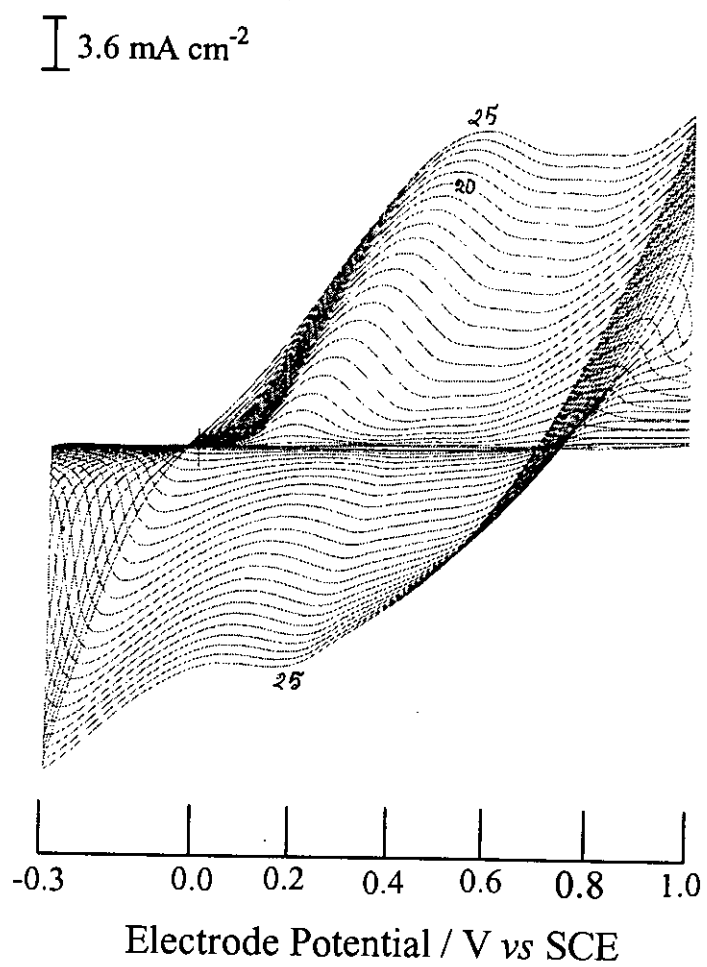
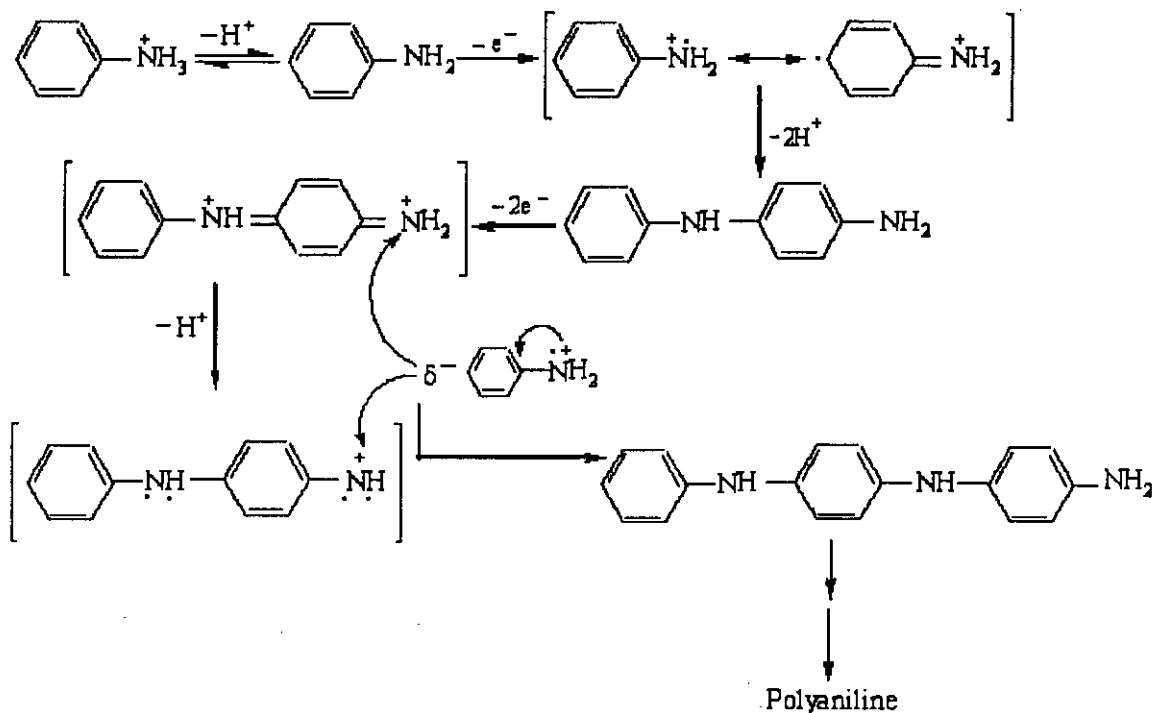


Fig. 3.1.2: CV (25th cycle) during electrochemical synthesis of PANI.

Scheme- 1: Mechanism for the electrochemical formation of PANI



ion [15], which could be generated from a deprotonation of the diiminium ion [13], would accomplish a growth step and lead eventually to the final polymer.

B. Organic /Organic composite electrode:

i) PANI/MB: Synthesis of this electrode matrix was accomplished electrochemically by coating the polymer-dye film onto an inert Pt electrode surface from an aqueous electrolytic solution containing aniline monomer, sulfuric acid and the organic cationic dye, MB. Figure 3.1.3 shows the CV of electrochemical co-deposition of PANI/MB film on the Pt electrode. The CV shows the growth of a film with two important electrochemical systems that are also observed during PANI synthesis (Fig. 3.1.1). The prepeak in the middle is attributed to a solvation- desolvation phenomenon of ions insertion [16]. The most significant phenomena observed in this case is the redox processes at *ca.* -0.3 V. This process is not seen when the film was prepared in absence of dye in the electrolytic solution (Fig. 3.1.1). Thus the electrochemical responses as

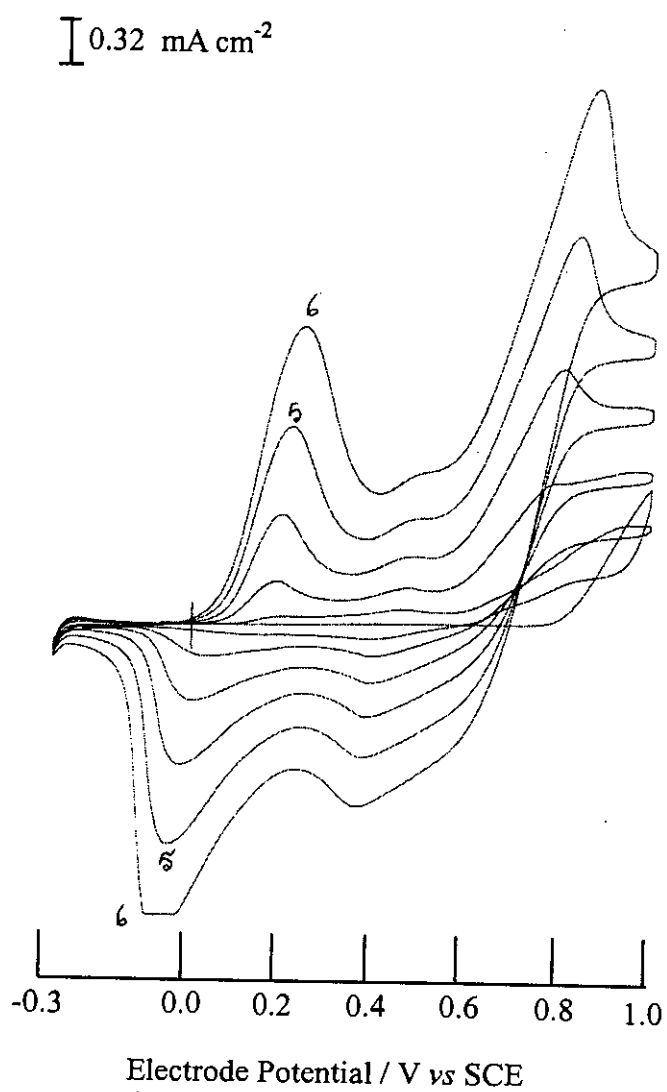


Fig. 3.1.3: CV(6th cycle) during electrochemical synthesis of PANI/MB.

observed in the CVs (Fig. 3.1.1 and Fig. 3.1.3), clearly indicate the presence of MB in the system during the PANI/MB film formation. Thus, it is expected that MB is incorporated into the PANI matrix and yielded PANI/MB film during the course of polymerization. The anodic peak around 0.8 V is assigned to the formation of the radical cations of aniline by electrochemical oxidation. The anodic peak intensity gradually increased with increasing cycle number due to the further deposition of PANI/MB films on the Pt electrode [17]. The anodic peak at *ca.* +0.18 V is also clearly visible as was also observed for PANI films. Hence, the composite PANI/MB film thus synthesized also indicates electroactive site similar to PANI matrix prepared electrochemically. CV for the PANI/MB was also recorded for the thick deposition as high as 25 cycles. This has been shown in Fig. 3.1.4. For the thick film, electrochemical processes are also observed although not as sharp as visible as in the CV depicted in Fig. 3.1.3 that recorded for a few cycle deposition. Both the thin and thick PANI/MB films shows usual color changes as PANI does.

ii) PANI/PR: The PANI/PR film was prepared by scanning the potential from -0.3 to +1.0 V vs SCE. Figure 3.1.5 shows the CV observed with a Pt electrode immersed in 0.8 M H₂SO₄ containing 0.5M aniline and 1.93×10^{-5} M PR. The redox current response of the system continued to grow with the repetition of potential cycles. This indicates that the growth of the film matrix onto the Pt surface is proportional to the number of potential cycles. As soon as the first potential scan reached to *ca.* +0.8 V, a tightly held thin film having deep blue color appeared even at the first scan. At least up to 25 cycles, the PANI/PR film was seen to be adhering onto the Pt surface and seemed to grow progressively. The CV's exhibited the peaks at *ca.* +0.8 V and +0.18 V (starting from second cycle) are identical to those of PANI and PANI/MB electrodes suggesting that the electrochemical oxidation of aniline and the polymer films took place at those potentials. Like PANI color of the present film was also changed from deep blue to greenish yellow when potential was switched from +0.18 V to +0.0 V, respectively. It is noticeable that a redox peak is also observed at *ca.* -0.3 V when the scanning was performed in the negative direction. This peak is absent when PANI was synthesized from an electrolytic solution without PR (Fig. 3.1.1). This observation suggests that the redox response seen

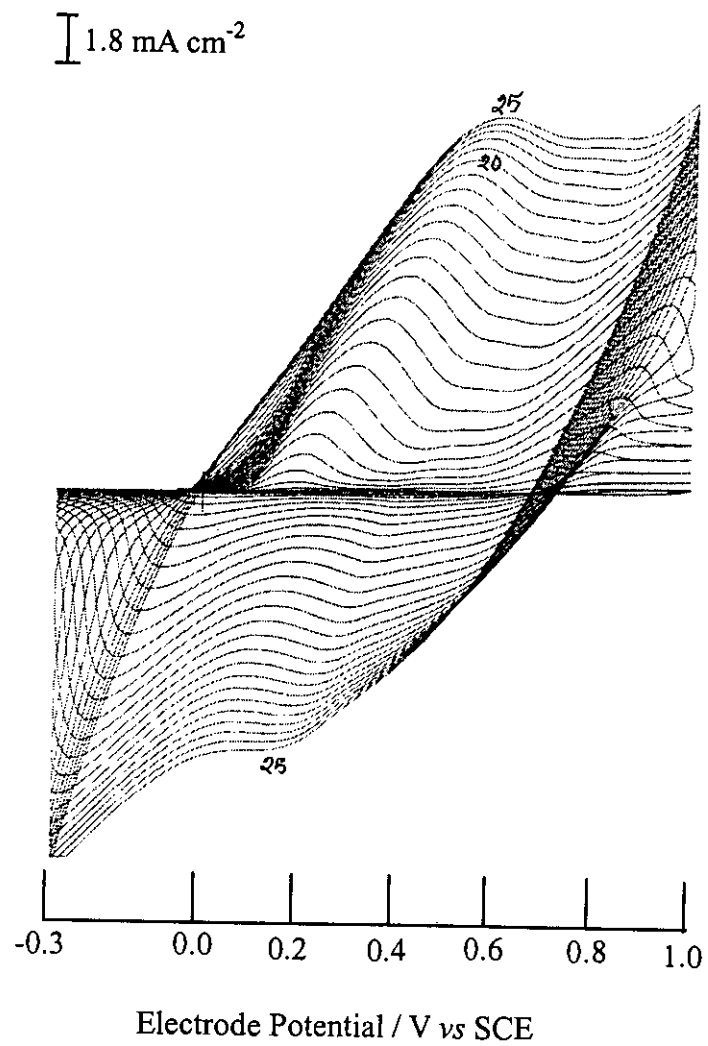


Fig. 3.1.4: CV (25th cycle) during electrochemical synthesis of PANI/MB.

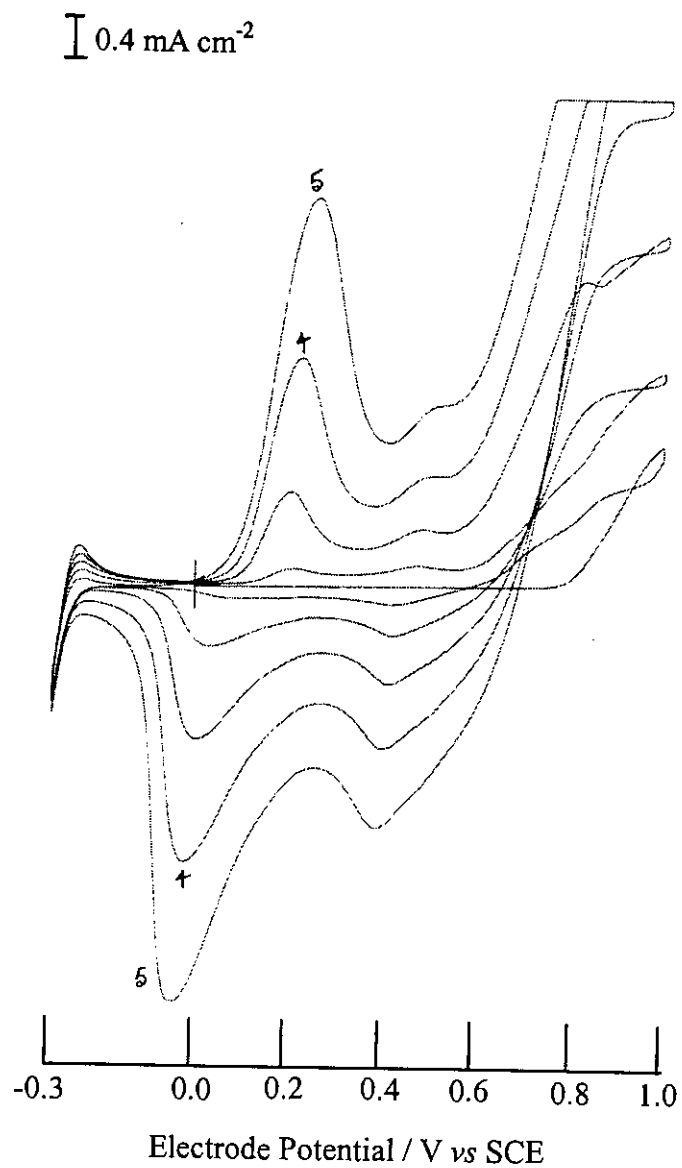


Fig. 3.1.5: CV (5 th cycle) during electrochemical synthesis of PANI/PR.

response seen at -0.3 V is due to the PR dye that incorporated in the electrolytic solution in order to prepare the PANI/PR matrix. This result also indicates that the PANI/PR film thus expected to be coated onto a Pt substrate is electroactive and performs the electrochemical processes as unique as the PANI film electrode does. The CV of the thicker PANI/PR film electrode is presented in Fig. 3.1.6. Instead of the massive structure, the CV of the thicker PANI/PR film seems to be identical to that of the thin PANI/PR film presented in Fig. 3.1.5, although broadening and slight shifting of the peaks for the thicker film are observed. Similar phenomenon was also observed for the thick PANI/MB system.

C. Organic/Inorganic composite electrode: PANI/TiO₂

The PANI/TiO₂ composite film electrode was prepared by oxidizing aniline at a Pt electrode in the presence of aqueous TiO₂ suspension in 0.8 M H₂SO₄. Figure 3.1.7 shows current–potential curve *i.e.* CV obtained in the course of the PANI/TiO₂ film formation on the Pt substrate. In the first cycle, from 0 to $+0.7$ V range, the current remains very low. Above $+0.7$ V, current increases rapidly and the CV shows a large anodic peak with a maximum at $+0.8$ V at which point, a deep blue color of the film thus deposited is observed. On the reverse sweep, the anodic current decrease continuously and then cathodic current appears, showing a peak maxima at about 0.0 V. The cathodic current decreases until the sweeping reached at -0.2 V. At this point, color of the film changes to greenish-yellow. In the second and subsequent cycles, another new peak appears at $+0.18$ V indicating the oxidation of the PANI/TiO₂ film electrode. The redox process as observed in this CV clearly indicates that the film thus obtained is electroactive. The electroactivity of the film even remains with thicker structure (25 cycle) as can be realized from the CV depicted in Fig. 3.1.8.

The above results of CV during electrochemical preparations of PANI, PANI/MB, PANI/PR and PANI/TiO₂ film electrodes clearly indicate that the matrices thus synthesized are capable of performing redox processes onto their surfaces in an appropriate electrolytic medium that employed. The redox activity of the electrode matrices are evaluated from the results of their corresponding CV are described below:

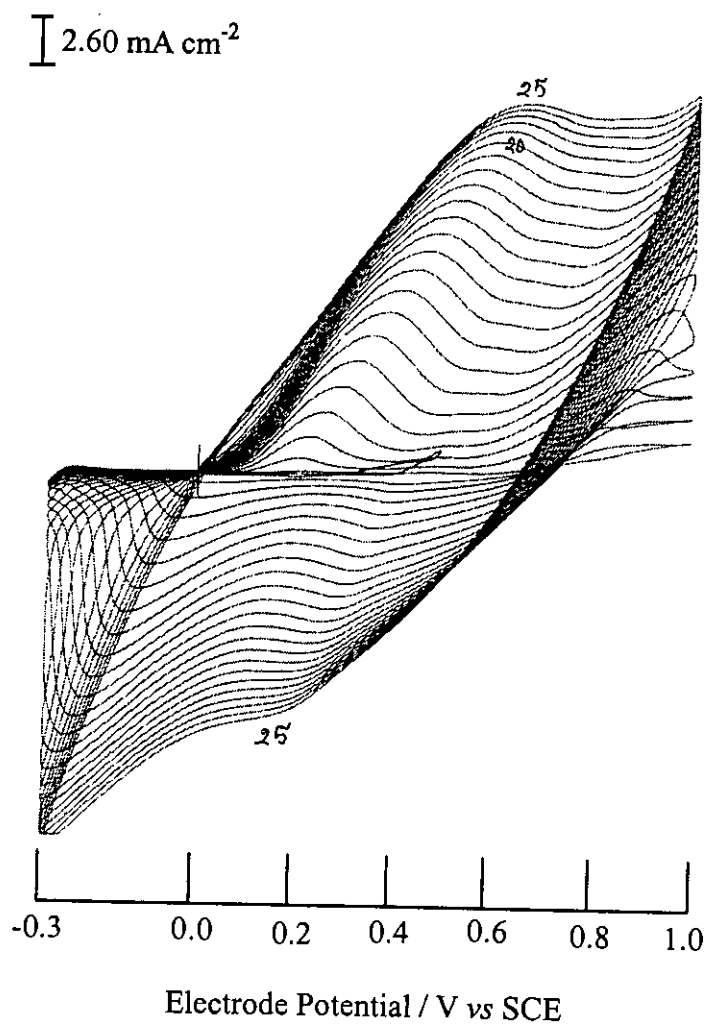


Fig. 3.1.6: CV (25th cycle) during electrochemical synthesis of PANI/PR.

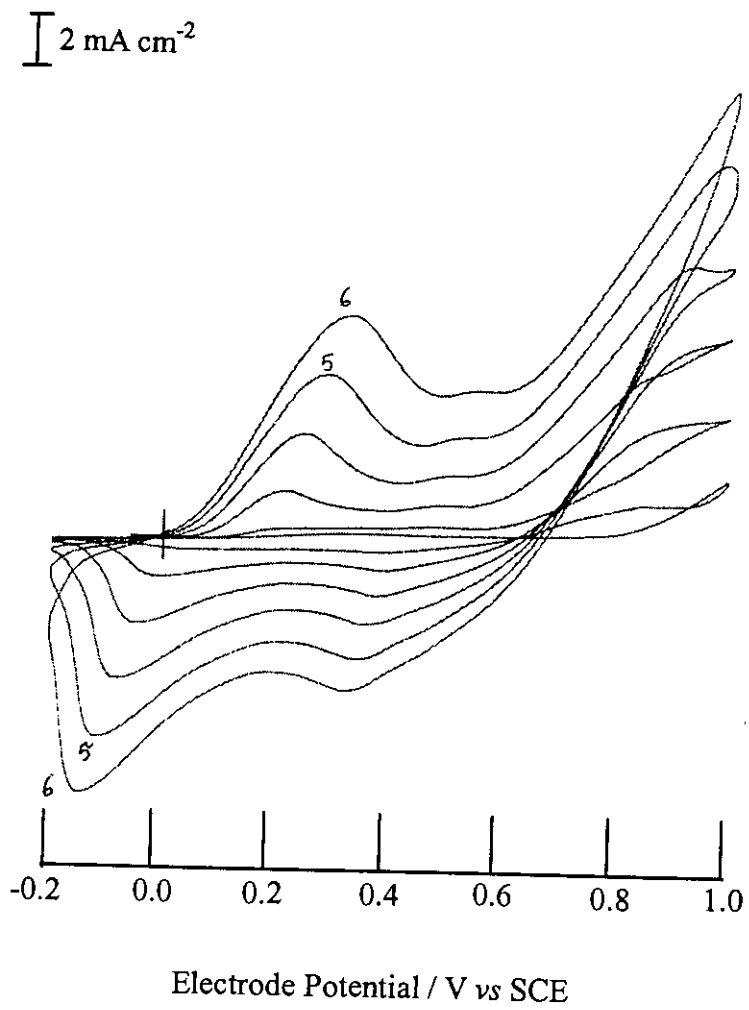


Fig. 3.1.7: CV (6th cycle) during electrochemical synthesis of PANI/TiO₂.

$\int 3.2 \text{ mA cm}^{-2}$

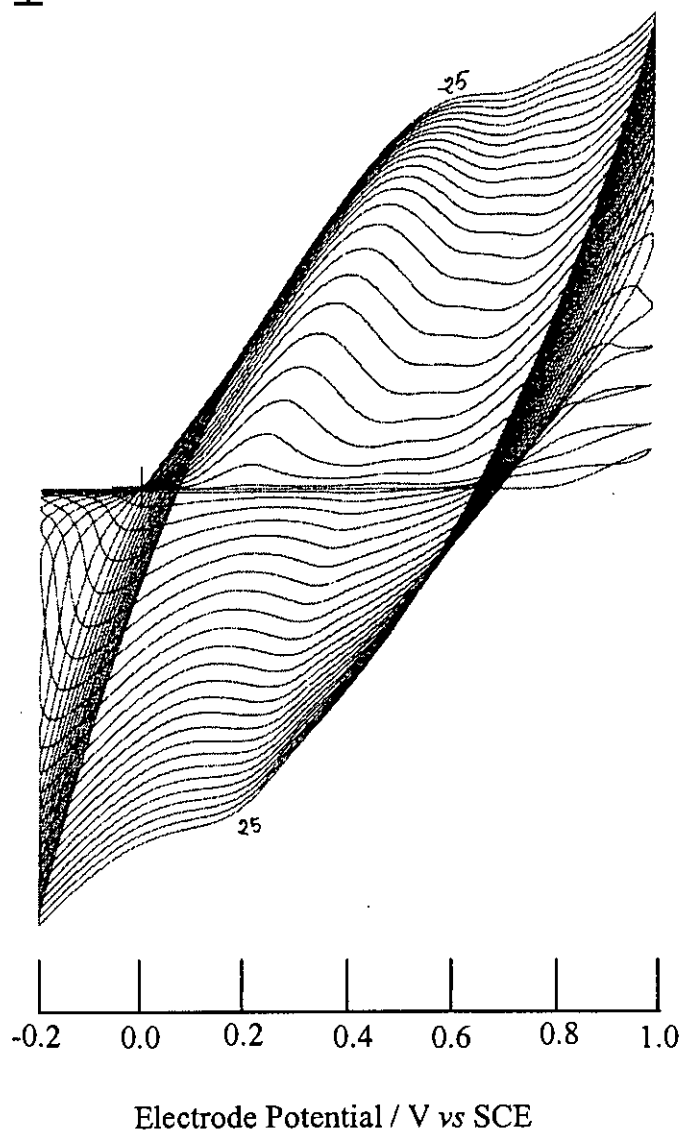


Fig. 3.1.8: CV (25th cycle) during electrochemical synthesis of PANI/TiO₂.

In the 5th cycle of potential scan under polarization between -0.3 and $+1.0$ V, the anodic (I_{pa}) and cathodic (I_{pc}) peak currents appear at the potentials E_{pa} and E_{pc} , respectively, where

i) for PANI (Fig. 3.1.1)

$$I_{pa} = 2.32 \text{ mA cm}^{-2} \text{ at } E_{pa} = +0.19 \text{ V}, I_{pc} = 1.52 \text{ mA cm}^{-2} \text{ at } E_{pc} = -0.03 \text{ V}$$

ii) for PANI/MB (Fig. 3.1.3)

$$I_{pa} = 1.38 \text{ mA cm}^{-2} \text{ at } E_{pa} = +0.21 \text{ V}, I_{pc} = 1.56 \text{ mA cm}^{-2} \text{ at } E_{pc} = -0.05 \text{ V}$$

iii) for PANI/PR (Fig. 3.1.5)

$$I_{pa} = 3.28 \text{ mA cm}^{-2} \text{ at } E_{pa} = 0.26 \text{ V}, I_{pc} = 3.6 \text{ mA cm}^{-2} \text{ at } E_{pc} = -0.04 \text{ V}$$

iv) for PANI/TiO₂ (Fig. 3.1.7)

$$I_{pa} = 5.8 \text{ mA cm}^{-2} \text{ at } E_{pa} = +0.28 \text{ V}, I_{pc} = 6.8 \text{ mA cm}^{-2} \text{ at } E_{pc} = -0.12 \text{ V}$$

For comparison, the results are presented in a tabular form given below:

Table-1: Redox reactivity of different electrode matrices

| Electrode matrix | Anodic peak current, I_{pa} (mA cm^{-2}) | Anodic peak potential, E_{pa} (V) | Cathodic peak potential, E_{pc} (V) | Cathodic peak current, I_{pc} (mA cm^{-2}) | I_{pc} / I_{pa} |
|-----------------------|---|-------------------------------------|---------------------------------------|---|-------------------|
| PANI | 2.32 | +0.19 | -0.03 | 1.52 | 0.655 |
| PANI/MB | 1.38 | +0.21 | -0.05 | 1.56 | 1.130 |
| PANI/PR | 3.28 | +0.26 | -0.04 | 3.6 | 1.097 |
| PANI/TiO ₂ | 5.8 | +0.28 | -0.12 | 6.8 | 1.172 |

From the above data, it is clear that all the matrix synthesized in this work are redox active. The redox reactivities of the matrices are also seen to be reversible although the extent of reversibility varies considerably from matrix to matrix. Peak separation between E_{pa} and E_{pc} and the ratio of I_{pc} to I_{pa} are the measures of reversibility. The differences of the reversibility indicate that the redox reaction on these surfaces did not proceed in similar way. The differences of the reversibility of the matrices may occur due to the presence of different entities, viz. MB, PR and TiO₂ in the matrix. Attempt were also made to better understand the rate of polymerization in the presence of organic and

inorganic entities such as MB, PR and TiO₂ along with the monomer. It was observed [13, 18] that the mass and thickness of the PANI film formed on the electrode are proportional to the anodic peak current (I_{pa}) at about +0.17 V. Therefore, the rate of polymerization can be measured by the rate of increase in this peak current. Figure 3.1.9 shows typical plot of I_{pa} [therefore, the amount of polymer (or polymer/dye, polymer/TiO₂) formed on the electrode] against the number of cycles (i.e. the reaction time, t) for the polymerization of aniline in the presence of either MB, PR or TiO₂. The slope, $d(I_{pa}) / dt$, at any point of these curves, corresponds to the rate of polymerization at that particular reaction time. It is apparent in Fig. 3.1.9 that the growth of the PANI film become faster or slower depending on the system, i.e. whether it containing TiO₂ or the dyes. The result clearly demonstrates that the growth rate of PANI/TiO₂ film is faster compared to PANI, PANI/MB or PANI/PR films. The addition of specially semiconducting TiO₂, in the electrolytic media may facilitate the slow step of the polymerization, resulting in the increases in the overall rate of polymerization. However, the slower growth rate that observed with other system may result from the inhibition of nucleation species on which the polymer chain grows [12-14, 18].

3.2 Characterization of the electrode matrices

A. Infra red spectral analysis:

Almost all compounds, particularly organic substances, absorb in the IR region. Although the IR spectrum is characteristic of the entire molecule, it is true that certain groups of atoms give rise to bonds at or near the same frequency regardless of the structure of the rest of the molecule. Since we are not solely depended on IR spectra for identification, a detail analysis of the spectrum will not be required. In order to get some insight about the structure of the synthesized matrices, IR spectral analysis were performed and the results are described below:

i) PANI: Figure 3.2.1 shows the IR spectra of PANI synthesized electrochemically. It is worthwhile to mention here that the observed IR spectra are consistent with the previous studies [19-25] and discussed below according to the frequency region:

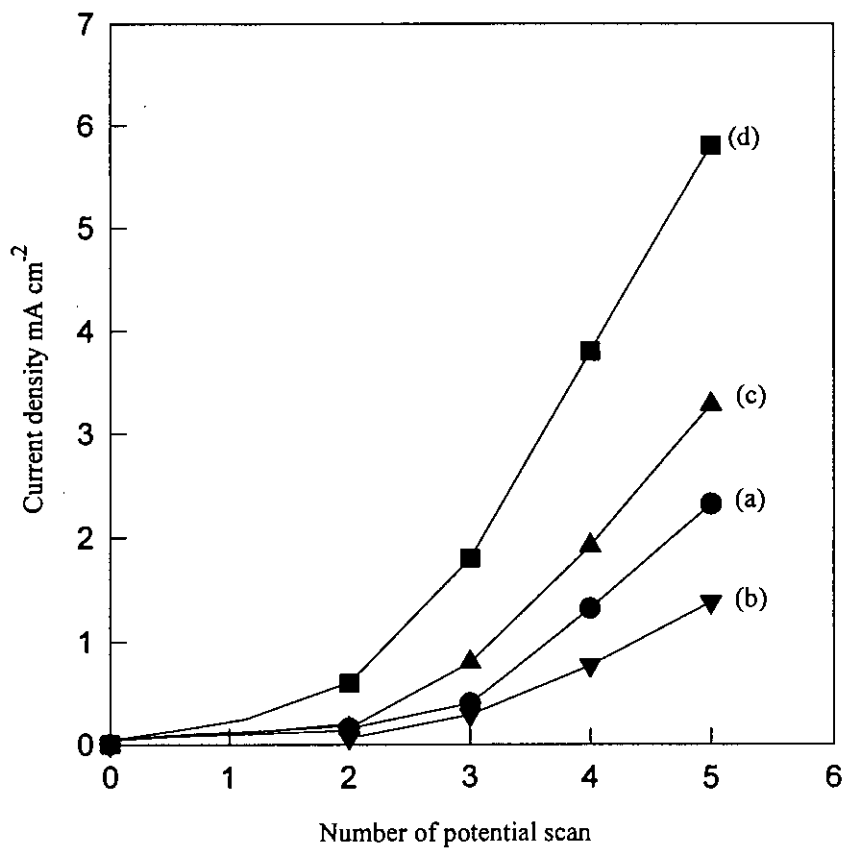


Fig. 3.1.9: Dependence of anodic peak current at *ca.* +0.17 V vs SCE on the cycle number during the electrochemical synthesis of (a) PANI (b) PANI/MB (c) PANI/PR and (d) PANI/TiO₂.

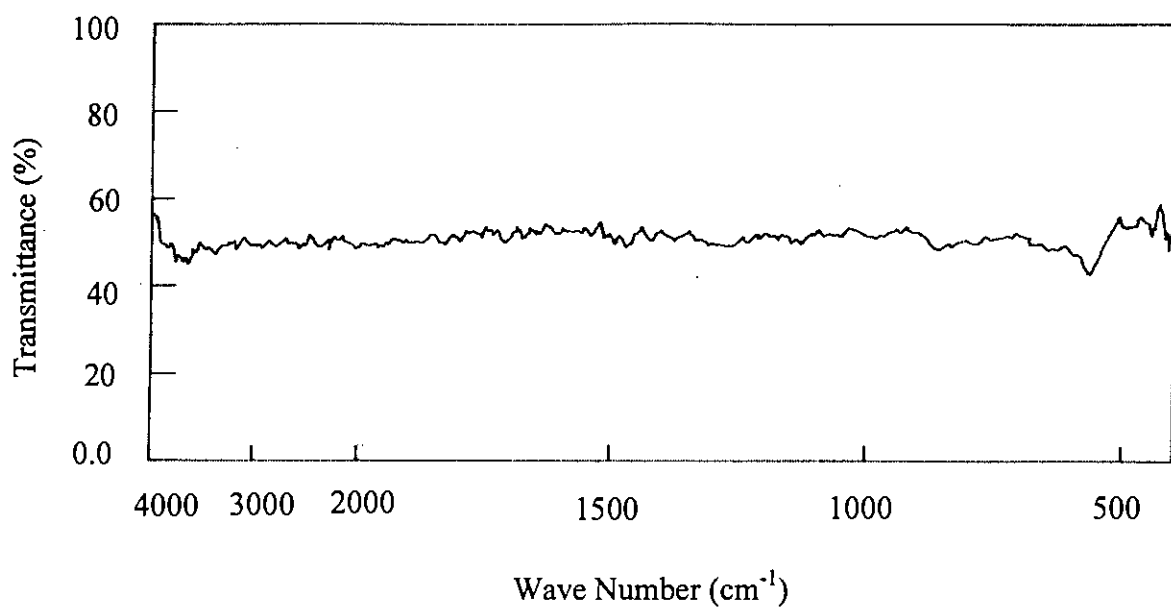


Fig. 3.2.1: IR spectrum of PANI.

(a) 3500-3100 cm^{-1}

This is the N-H stretching region. The absorption of PANI in this region is rather weak. The main absorption peaks are located at 3380 and 3310 cm^{-1} , with shoulders at 3460 and 3170 cm^{-1} .

(b) 3100- 2800 cm^{-1}

This is the C-H stretching region. The absorption of PANI in this region is even weaker, but it is observable at 3050 – 3030 and 2960 – 2850 cm^{-1} .

(c) 1600-1450 cm^{-1}

Aromatic ring breathing, N-H deformation and C=N stretching all give absorption in this region. In general, the N-H deformation band is very weak. A 1, 4- substituted benzene ring may give absorption band at 1600-1580 and 1510-1500 cm^{-1} . However, the former is very weak and even observable if the two substituents are the same and the latter is strong in the IR in this range. Therefore, it is reasonable to assign the band at 1510 cm^{-1} mainly to benzoid ring (B) stretching in PANI. Based on the following arguments, we consider the 1587 cm^{-1} band as a characteristic band of nitrogen quinone (Q).

(d) 1400-1240 cm^{-1}

This is the C-N stretching region for aromatic amines. The intrinsic PANI shows three peaks: medium absorption at 1240 cm^{-1} and weak ones at 1380 and 1240 cm^{-1} . The band at 1160 and 1140 was referred as “electronic like band” and was considered as a measure of the degree of delocalization of electrons on PANI and thus are the characteristic peaks of PANI conductivity [26, 27]. The band at 1160 and 1140 cm^{-1} be assigned separately: 1160 cm^{-1} to intrinsic structure and 1140 cm^{-1} to the doped (acid treated) structure. The 1140 cm^{-1} band is a vibrational mode of $\text{B-NH}^+=\text{Q}$ or $\text{B-NH}^+-\text{B}$ which is formed in doping reactions. This may be attributed to the existence of the positive charge and the distribution of the dihedral angle between the B and Q rings [28].

99115

(e) $1220-500\text{ cm}^{-1}$

This is the region of in-plane and out-of-plane bending of C-H bonds on aromatic rings. The main absorption bands for intrinsic PANI are located at 1160 and 830 cm^{-1} and some weak bands can be observed. It is easy to judge the substitution pattern on the benzene ring from the frequencies of these peaks. For example, 1220 , 1105 , 1010 and 830 cm^{-1} stands for 1,4- substitution, 1115 , 1060 , 960 , 895 and 850 cm^{-1} for 1, 2, 4-substitution and 740 and 690 cm^{-1} for 1,2- or mono-substitution.

Peaks at 1120 and 625 cm^{-1} are also observed in the spectra of the PANI film and correspond to the presence of SO_4^{2-} ions, which were used as an electrolytic anion in the film [29].

A summary of tentative assignments of the IR spectra of intrinsic PANI are presented in Table-2.

Table-2: Tentative assignment of the IR spectra of PANI sample

| Frequency (cm ⁻¹) | Assignment* |
|-------------------------------|---|
| 3710 | presence of H ₂ O |
| 3470 | NH ₂ asym. str. |
| 3360 | NH ₂ sym. str., NH str |
| 3175 | =NH str. |
| 1563 | str. of N=Q=N |
| 1538 | str. of N – B – N |
| 1450 | str. of benzene ring |
| 1368 | C – N str. in QB _t Q |
| 1315 | C – N str. in QB _c Q, QBB, BBQ |
| 1245 | C – N str. in BBB |
| 1160 | a mode of N=Q=N |
| 1140 | a mode of Q=NH ⁺ -B ⁺ or B-NH ⁺ -B |
| 1225 | |
| 1104 | C – H <i>ip</i> on 1,4-ring |
| 1128 | |
| 1046 | C – H <i>ip</i> on 1,2,4-ring |
| 952 | |
| 917 | |
| 875 | C – H <i>op</i> on 1,2,4-ring |
| 847 | |
| 807 | C – H <i>ip</i> on 1,4-ring |
| 759 | |
| 690 | C – H <i>ip</i> on 1,2-ring |
| 659 | |
| 534 | aromatic ring deformation |
| 494 | |

* Abbreviations: asym = asymmetric, sym = symmetric, str = stretching, *ip* = in-plane bending, *op* = out-of-plane bending, Q = quinoid unit, B = benzoid unit, B_t= *trans* benzoid unit, B_c= *cis* benzoid unit.

ii) PANI/MB: The IR spectrum of PANI/MB obtained by electrochemical oxidation of aniline is presented in Fig. 3.2.2. The main absorption peaks are observed at 3340, 3210, 3120, 3060, 1630, 1590, 1500, 1300, 1250, 1090, 825, 760, 690, and 620 cm⁻¹. These absorption peaks are the same as that observed with the PANI (Fig. 3.2.1). The main IR

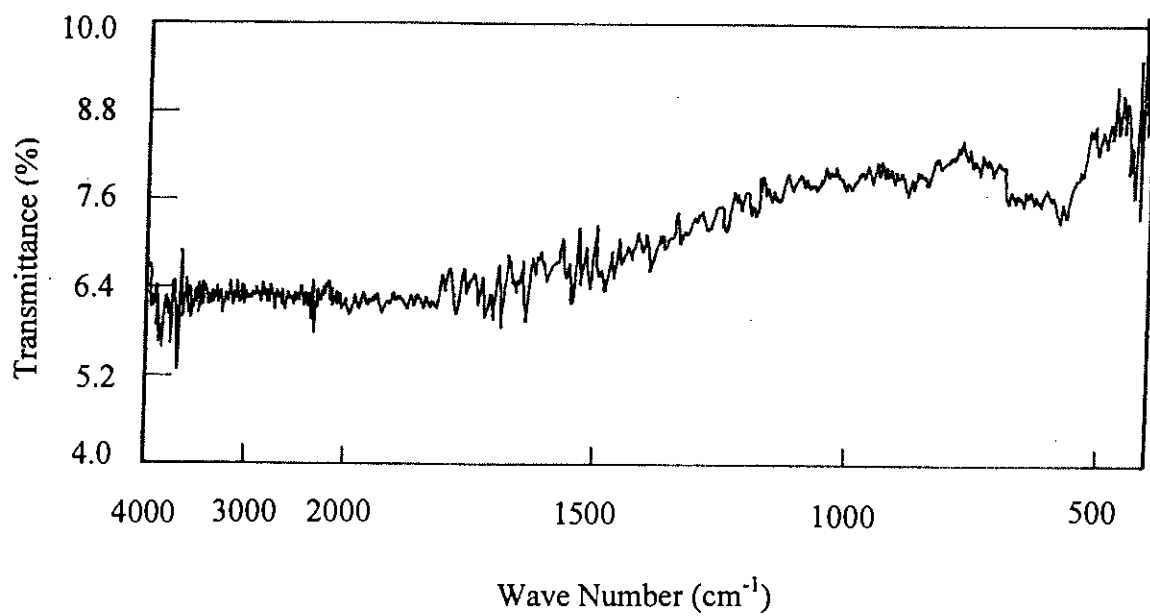


Fig. 3.2.2: IR spectrum of PANI/MB.

absorption for the MB component is presented in Fig. 3.2.3. The peaks are seen at 1596, 1487, 1392, 1354, 1251, 1219, 1180, 1151, 1060, 1034, 883, 851, 799, 662, 533, and 443. The spectrum of the PANI/MB seems to exhibit most the peak for MB component in it although the intensity of the peak differs significantly. However, the results of IR analysis for the PANI/MB and MB samples indicate that the MB component is incorporated into the PANI matrix during its electrochemical polymerization from the aqueous electrolyte containing MB solution.

iii) PANI/PR: The IR spectrum of the PANI/PR sample not only display the same basic vibrations as for the PANI film, but also shows peaks which are characteristics of the PR component. The typical IR spectra for PANI/PR and PR are shown in Fig. 3.2.4 and Fig. 3.2.5, respectively. In general the IR spectrum of PANI/PR appears to be consisted of too many absorption bands. However, careful observation reveal that it contains the main absorption corresponding to PANI entities: 3346, 3208, 3121, 3058, 1629, 1585, 1499, 1298, 1253, 1086, 827, 689, and 621 cm^{-1} and the absorption characteristics of PR component : 2365, 1735, 1720, 1605, 1560, 1500, 1392, 893, 765 and 632 cm^{-2} . Thus, the IR spectral features indicate that PR component is embedded into the PANI matrix during the course of polymerization from its electrolytic solution.

iv) PANI/TiO₂ : Figure 3.2.6 shows the IR spectrum of the PANI/TiO₂ film formed on the electrodes during anodic oxidation of aniline from an electrolytic solution containing TiO₂ suspension. The absorption peaks of the composite film at 3060, 1600–1585, 1500 and 700 cm^{-1} , are characteristics of the various mode of the C–H and C–C bonds of the aromatic nuclei. The peaks at 3400, 3250, 3200, 3120 and 3080 cm^{-1} correspond to the stretching of the N–H bonds; those at 1310 – 1300 and 1250–1245 cm^{-1} correspond to the stretching of the C–N bonds of the secondary aromatic amines, and the peaks at 1625–1620 cm^{-1} correspond to the stretching of the C=N bonds [29–31]. However, the present result essentially shows the characteristic peak for PANI as discussed earlier (Fig. 3.2.1). The IR spectrum of TiO₂ is shown in Fig. 3.2.7. The principal absorptions are: 1248, 1187, 1132 and 1095. The region 1250–1090 seems to be the characteristic peak of Ti–O bond. The IR spectrum of PANI/TiO₂ samples indeed

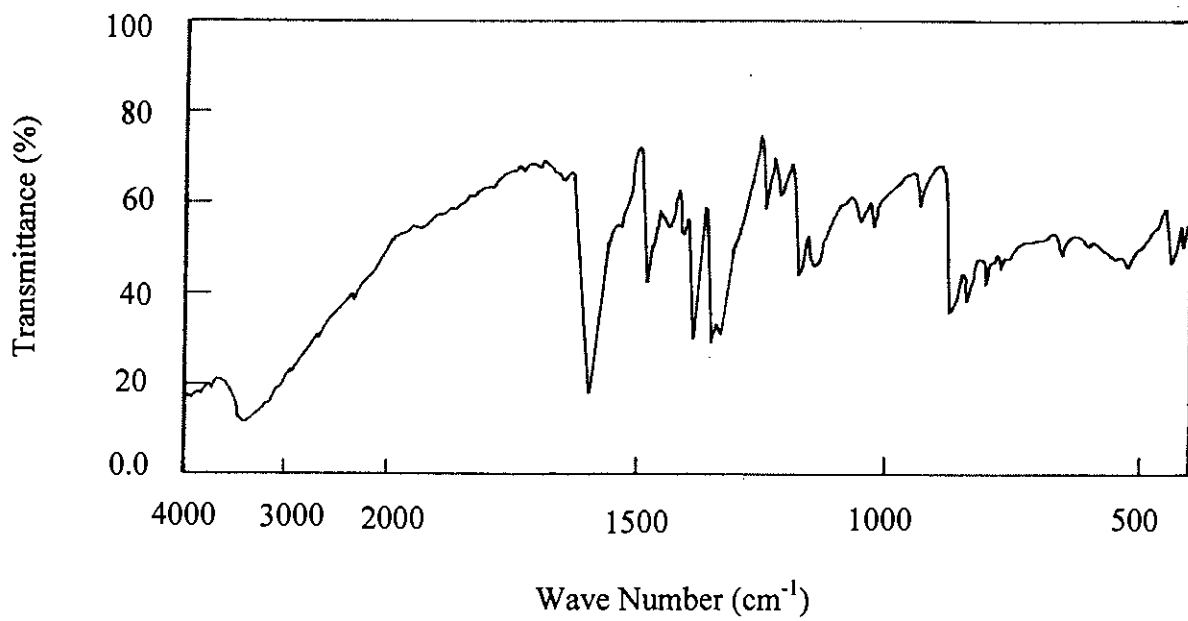


Fig. 3.2.3: IR spectrum of MB.

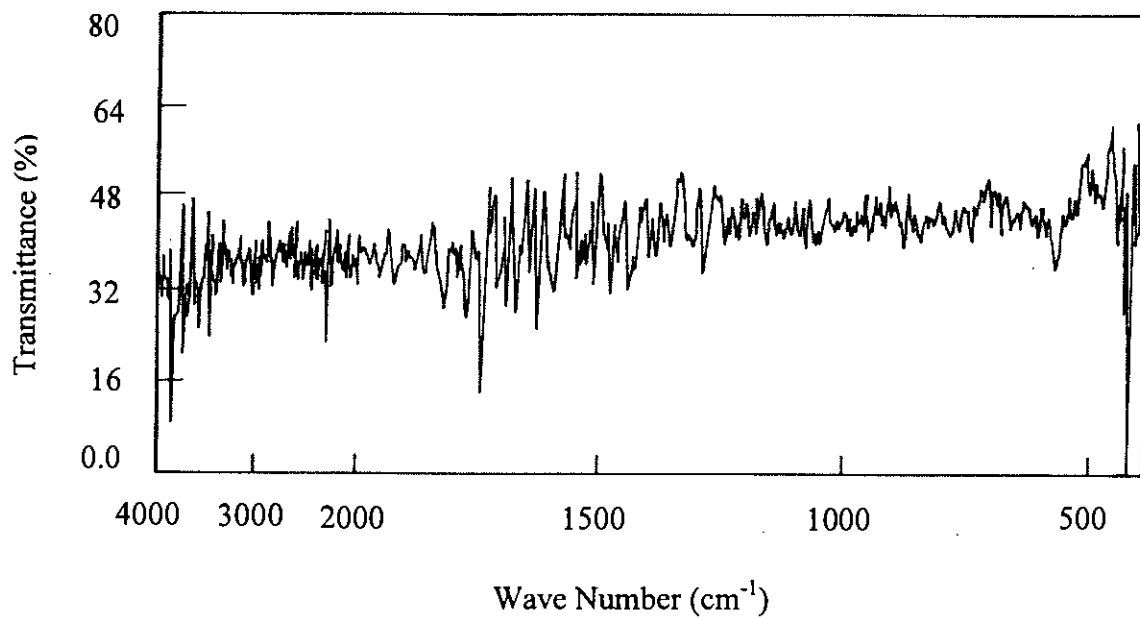


Fig. 3.2.4: IR spectrum of PANI/PR.

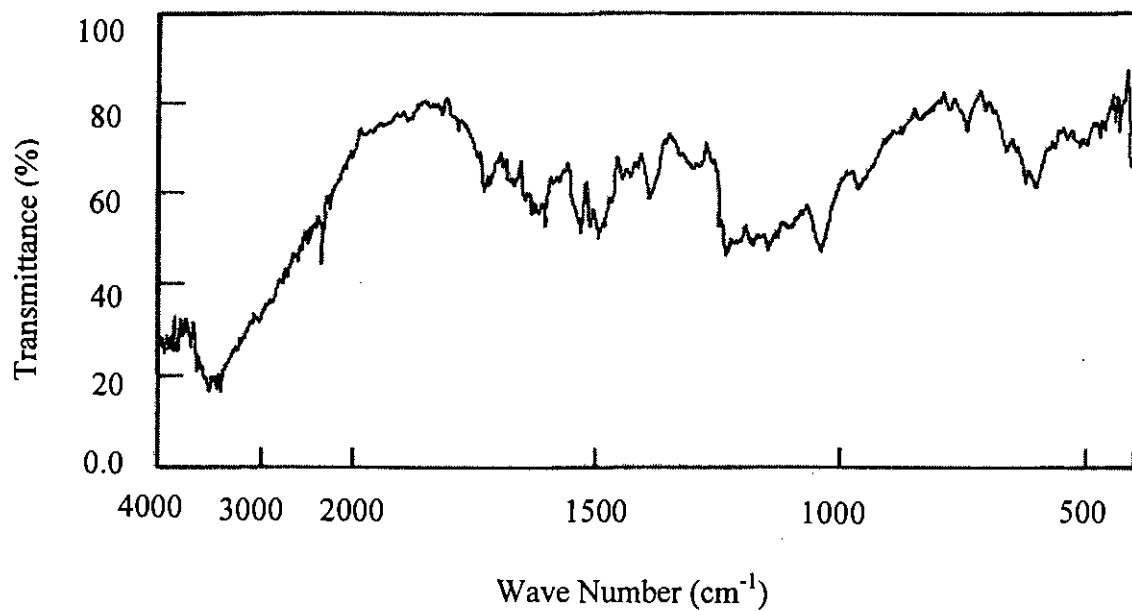


Fig. 3.2.5: IR spectrum of PR.

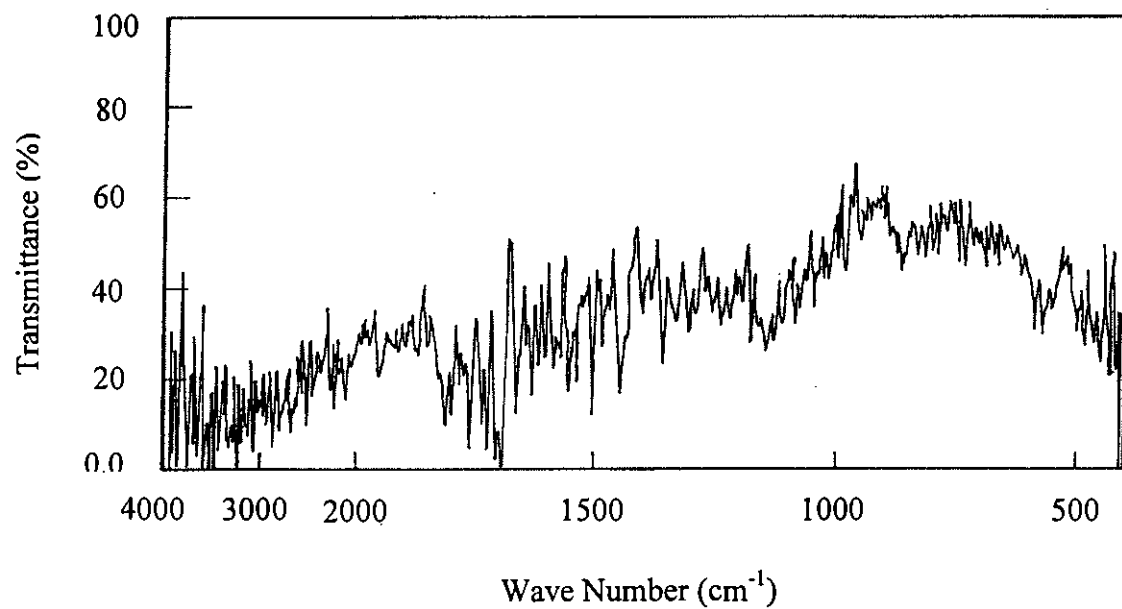


Fig. 3.2.6: IR spectrum of PANI/TiO₂.

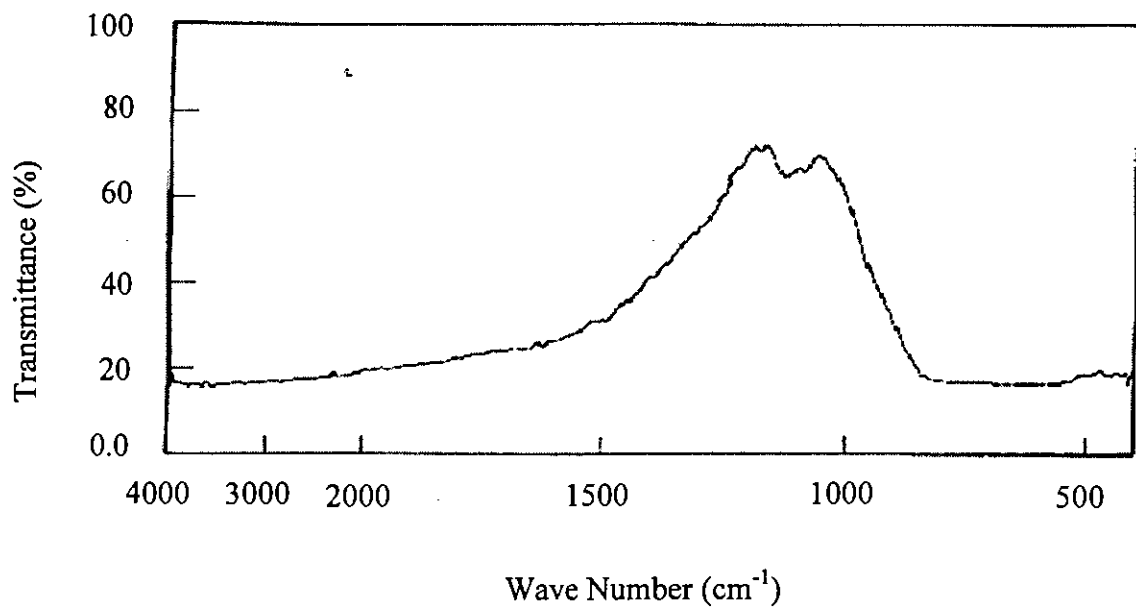


Fig. 3.2.7: IR spectrum of TiO₂.

shows several peaks in this region and may indicate the presence of TiO₂ into the PANI matrix.

B. Ultra violet- visible spectroscopy

UV- Vis spectra of doped PANI, MB and PANI/MB samples recorded in DMF solutions at room temperature are given in Fig. 3.2.8, Fig. 3.2.9 and Fig. 3.2.10 respectively.

The PANI doped (Fig. 3.2.8), samples shows peaks at 335 and 450 nm and a weak shoulder at *ca.* 660 nm. The result is similar to the studies reported by the early workers [32, 33] and suggests that the peak observed at 335 nm corresponds to the interband $\pi - \pi^*$ (valence band to conduction band) transition while the other two transitions observed in the spectra at around 450 and 660 nm may be responsible for PANI conductivity by forming polaron and bipolaron as mid-gap state. Similar phenomenon has also been observed with other conducting polymers such as PP [34, 35]. In fact, polaron state is a radical cation, *i.e.* contains one electron whereas bipolaron is a dication, *i.e.* electronless. At low doping level, polaron formation takes while at highly doped states, bipolaron formation predominates. However, because of the greater stability, a bipolaron is favored over polaron.

Figure 3.2.9 shows the UV-Vis absorption spectra of MB solution in DMF solvent. The peak at 664 nm in the spectrum represents the characteristic feature of the dye MB. The dye seems to be stable in the DMF and the acid media used in this experiment, at least for 2 hr [36]. Thus, any degradation of the MB either in DMF or H₂SO₄ may be ruled out.

Figure 3.2.10 shows optical absorption spectrum of PANI/MB in the DMF solvent. The result shows a peak at 453 nm with absorption maxima and a broad shoulder in the region 700-900 nm. Its tail indeed starts from *ca.* 600 nm. It seems that, this spectrum is at least

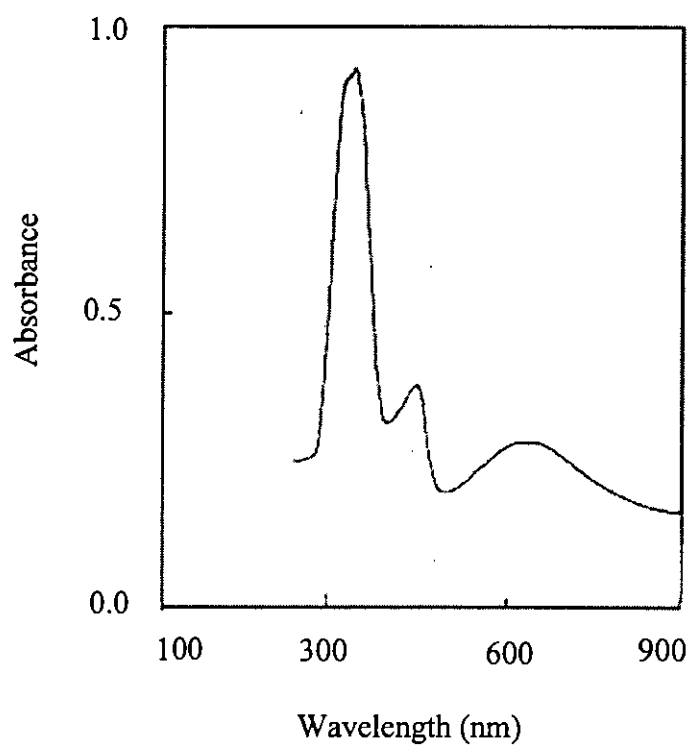


Fig. 3.2.8: UV- Visible absorption spectrum of PANI in DMF solution.

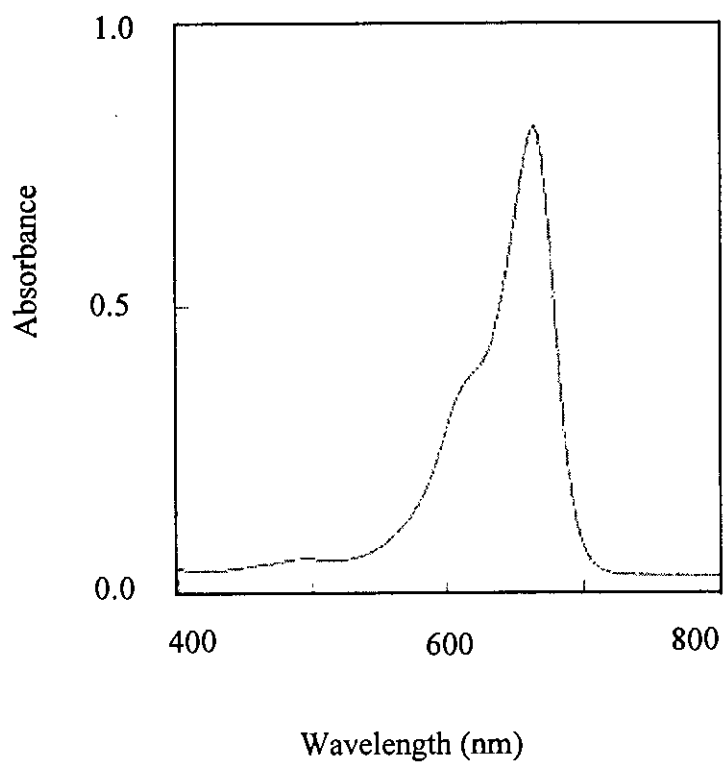


Fig. 3.2.9: UV-Visible absorption spectrum of MB in DMF solution.

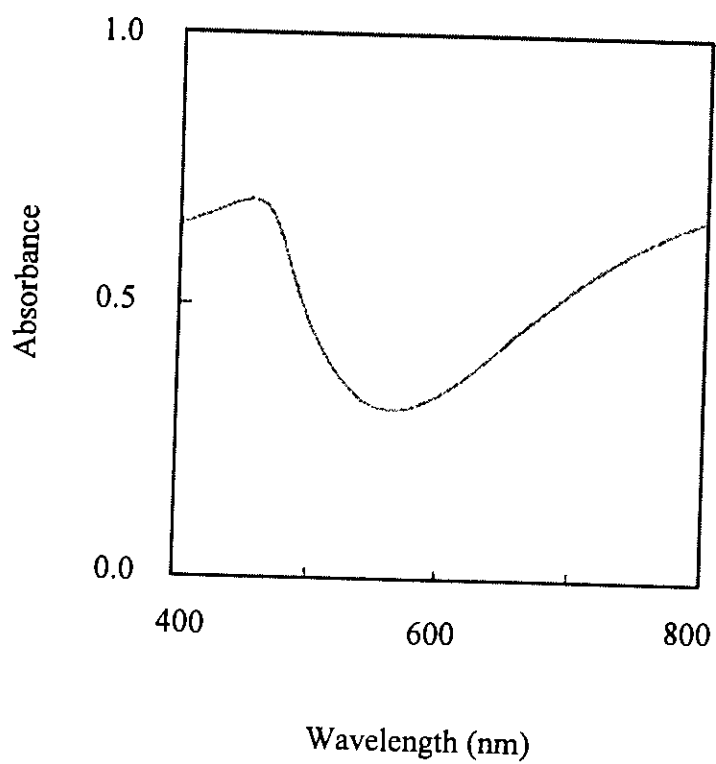


Fig. 3.2.10: UV-Visible absorption spectrum of PANI/MB in DMF solution.

qualitatively not identical to those observed for PANI and MB (Figs. 3.2.8 and 3.2.9). However, a careful observation reveals that the peak at 453 and the shoulder tails from 600 nm are indeed also observed for the PANI sample (Fig. 3.2.8). The interband transition, as observed at about 335 nm in Fig. 3.2.8, is not seen in this spectrum. The optical window for the Fig. 3.2.10 was limited between 400-800 nm for the safety of the dye degradation under UV-Vis irradiation and thus the interband transition for the PANI/MB sample could not be recorded. Hence, it is convincing that the Fig. 3.2.10 represents the optical feature of PANI considerably. The MB component should reflect a peak in the shoulder region of the spectrum in Fig. 3.2.10. Although the prominent MB peak characteristic is not observed, it is noticeable that the shoulder observed in Fig. 3.2.10 is greatly broadened compared to that in Fig. 3.2.8. Because of the low concentration of MB in the PANI/MB matrix, the characteristic peak of MB in the PANI/MB probably weak and thus merges within the shoulder region of Fig. 3.2.10. The optical characterization of the present sample provides further support that MB is embedded into the PANI matrix during its electropolymerization.

C. X-ray diffraction pattern

The X-ray technique is one of the powerful tool for structural analysis of solids. This can provide information on the intermolecular arrangement, *i.e.*, the level of crystallinity of the solids. The solid matrices, *viz.* PANI, PANI/MB, PANI/PR and PANI/TiO₂ prepared electrochemically were examined for their structural analysis in the powdered state by using wide angle X-ray diffraction. The scattering patterns as function of the Bragg angle, 2θ at $\lambda = 1.54 \text{ \AA}$ for the studied samples powders are presented in Fig. 3.2.11–3.2.14. The results show that the patterns consist of only diffuse X-ray scattering *i.e.*, the peaks appear in the pattern are responsible for the amorphous nature of the sample. The control samples, *viz.*, MB, PR and TiO₂ also exhibited amorphous pattern. These are presented in Figs. 3.2.15– 3.2.17. Most of the conducting polymers are reported to be extremely poor crystalline. During polymerization, although most of the aniline units are linked through the 1,4-position, a significant units are couple through other positions. This introduces defects in the hypothetical ideal linear chain arrangement of the polymer and also causes some cross-linking of the polymer and consequently,

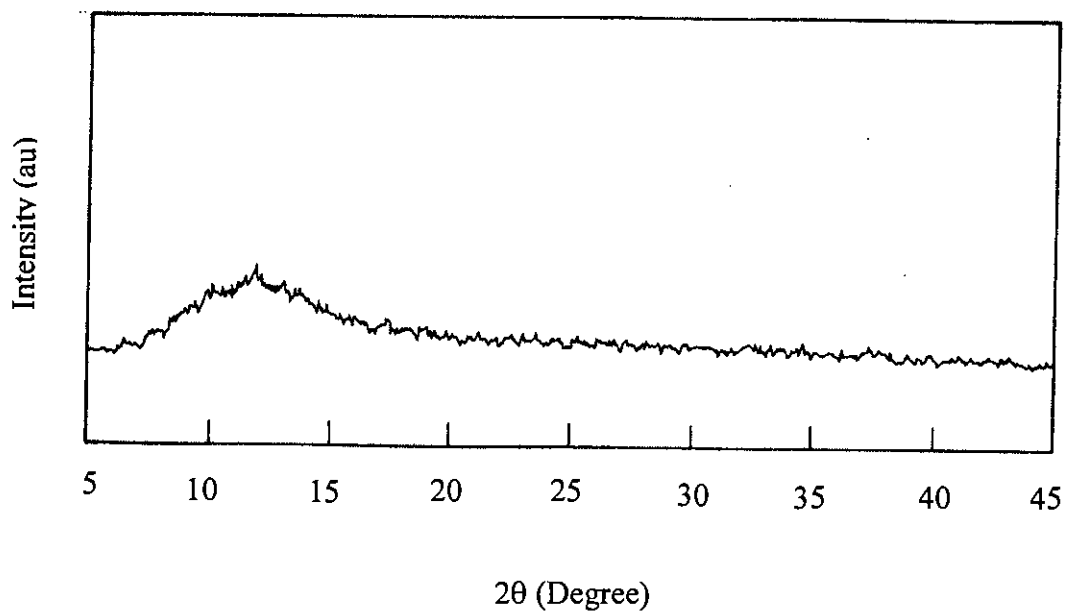


Fig. 3.2.11: XRD pattern of PANI.

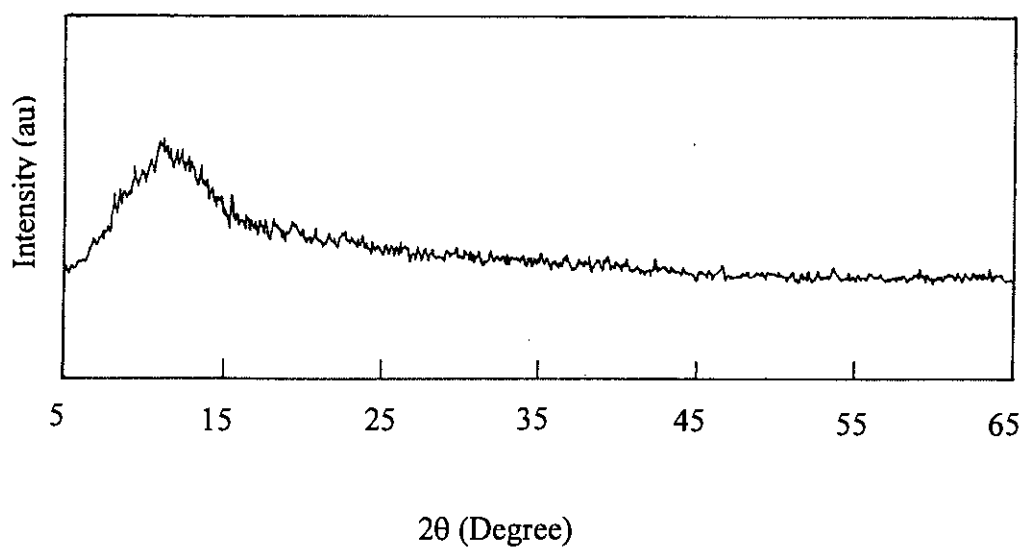


Fig. 3.2.12: XRD pattern of PANI/MB.

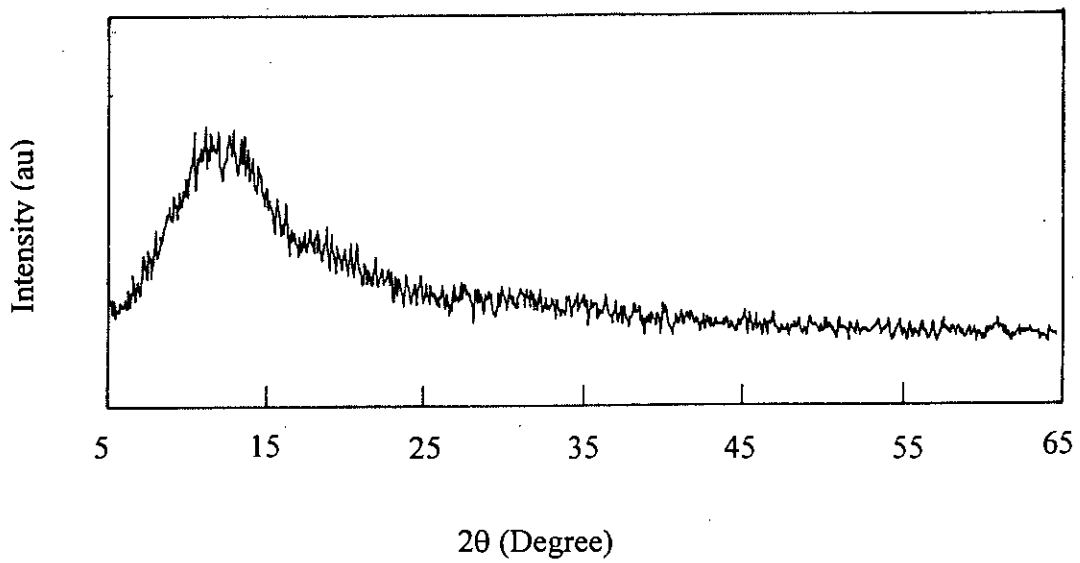


Fig. 3.2.13: XRD pattern of PANI/PR.

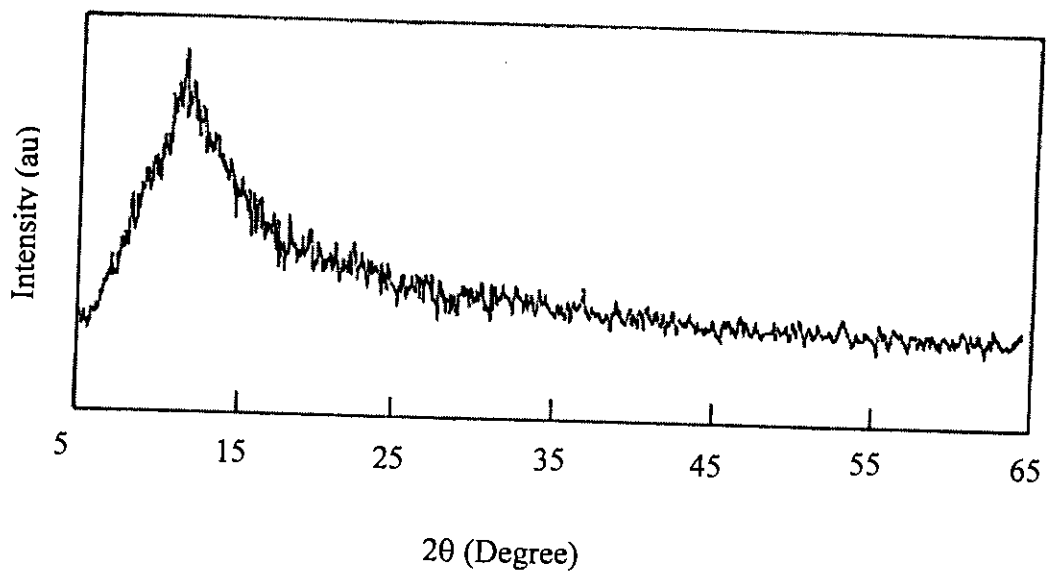


Fig. 3.2.14: XRD pattern of PANI/TiO₂.

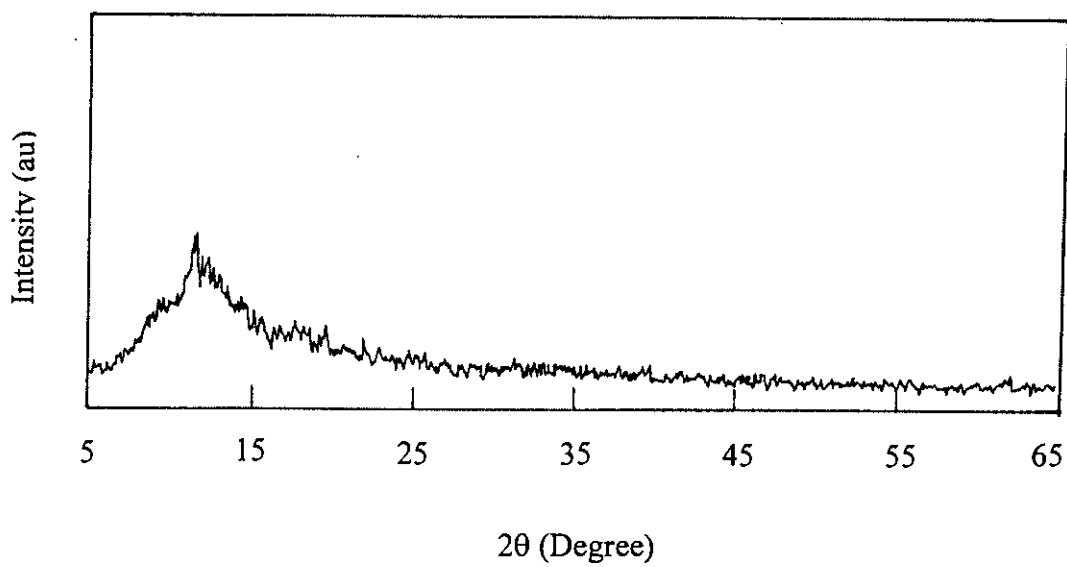


Fig. 3.2.15: XRD pattern of MB.

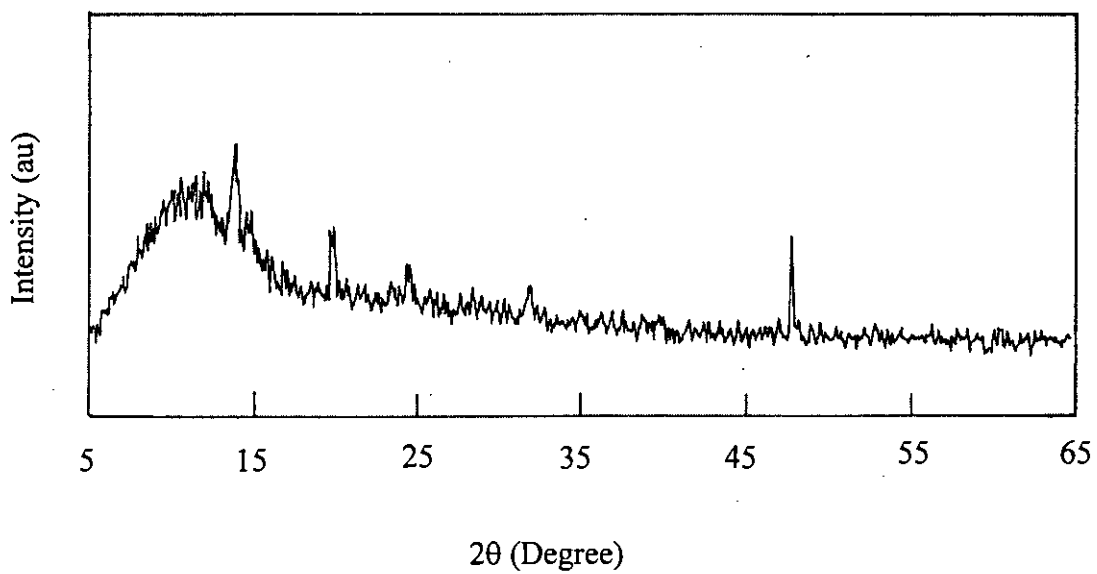


Fig. 3.2.16: XRD pattern of PR.

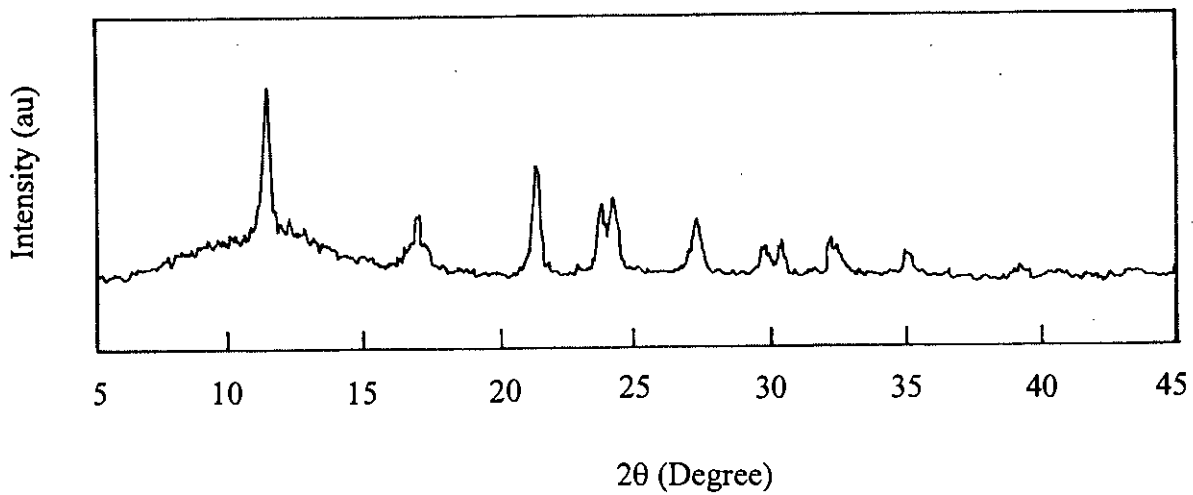


Fig. 3.2.17: XRD pattern of TiO₂.

results in a significant decrease in the crystallographic order of the chain [37, 38]. As a result, the polymer loses its crystallinity and provides diffuse diffraction pattern as exhibited in Fig. 3.2.11 –3.2.14. Other well studied conducting polymer PP, has also been reported to be amorphous in nature [39]. The importance of a better intermolecular arrangement, i.e., a level of crystallinity in the PANI samples for obtaining a higher conductivity has become a well-accepted factor all around the world and this idea is not restricted to PANI but involves most of the more prominent electronically conductive polymers. The observation that the conductivity of PANI films and fiber can be increased upon stretching is a direct evidence for the importance of a good intermolecular arrangement. Effort, we still being made for achieving the better PANI structure. Indeed, results of few studies have already been appeared and reported crystalline structure of PANI [40-42].

D. d. c. two point-probe conductivity

Electrical conductivity measurements of the samples PANI, PANI/MB, PANI/PR and PANI/TiO₂ were performed by employing conventional two point-probe method. The vacuum dried samples were compressed to a rigid mass and stored in vacuum desiccators till the conductance measurement commenced.

The results of the conductivity measurements for the samples is arranged in a bar chart as depicted in Fig. 3.2.18. The observed conductivity values of PANI, PANI/MB, PANI/PR and PANI/TiO₂ were found to be 3.11×10^{-1} , 1.6×10^{-1} , 6.19×10^{-1} and 9.63×10^{-1} S cm⁻¹, respectively. The electrical conductivity of PANI is usually in the order of 10^{-6} to 10 S cm⁻¹, depending somewhat on the polymerization and protonation conditions [43]. Thus, the observed conductivity of the present PANI sample prepared electrochemically from H₂SO₄ electrolytic media seems to be consistent with the early report. The conductivities of PANI/MB and PANI/PR matrices are less than *ca.* 2 times smaller and more than *ca.* 3 times higher, respectively, than that of PANI. The differences of the conductance values are not clearly understood at this stage, however, the ionic nature of the dyes, (*viz.*, MB is cationic and PR is anionic) may play certain role in the composite formation and thus modifying their morphological and electrical properties as reflected in the conductivity

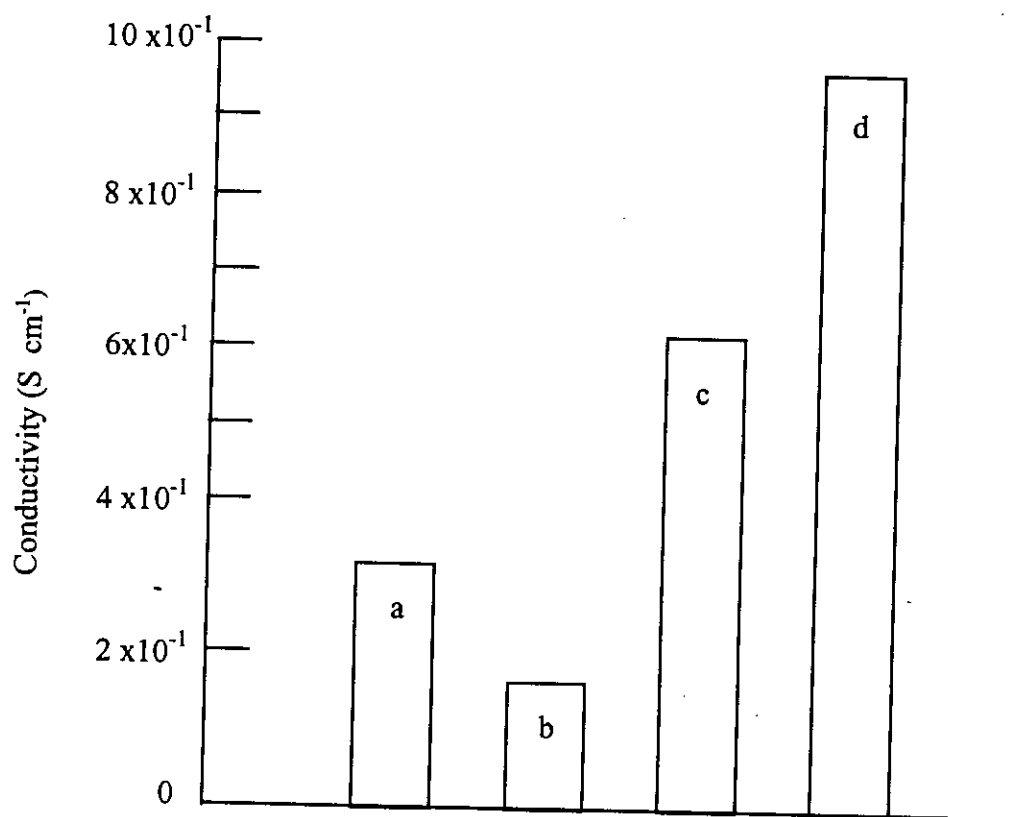


Fig. 3.2.18: Solid state d.c. conductivity of the samples (a) PANI (b) PANI/MB (c) PANI/PR and (d) PANI/TiO₂.

of the matrices. Indeed rate of composite formation, as shown in Fig. 3.1.9, found to be affected when synthesis were performed from the solutions containing MB, PR and TiO₂. The morphology of the matrices also seems to be affected considerably when MB, PR and TiO₂ are embedded into the matrices. This will be discussed in detail in the following section. The lower conductivity of the PANI/MB matrix is presumably due to the many interparticle contact resistance, present in such finely divided particles in the solid state. However, the increase conductivity of the PANI/TiO₂ matrix seems to be reasonable, if one consider the semiconducting nature of the TiO₂ particles. Thus, the presence of TiO₂ itself may contribute to the conductivity enhancement of the PANI/TiO₂ matrix. Moreover, the presence of TiO₂ colloidal particles in the synthesis may provide surface for the aniline adsorption and finally cause a massive production of PANI and thus modifying the rate of its production (Fig. 3.1.9) to yield a matrix with different morphological and electric properties. The change in conductivity is also reported by the early workers [44-46] for surfactant incorporated conducting polymers. The results depicted in Fig. 3.2.18 also indicate that the conductivity of the studied samples still fall in the range of semiconductor conductivity (10^{-6} to 10^{-1} S cm⁻¹). Since electrical behavior of the composite seems to be controlled by the polymer component, the mechanism of conduction in these composites would be similar to those of the bulk polymer. The conduction mechanism in PANI has been discussed by Li *et. al.* [47] in terms of the experimentally observed temperature dependences of the charge carrier density. The macroscopic conductivity has been interpreted as a result of anisotropic three-dimensional variable range hopping in a network of rods with metallic behavior.

E. Scanning electron microscopy

In order to examine the surface morphology, scanning electron microscopy appears to be the best choice because of its potential for precise analysis of a solid surface. Chemical composition and morphological structure of a material strongly depends on the mode of synthesis, be it chemical or electrochemical, on the synthetic conditions such as pH, concentration of reactants and products, chemical nature of oxidant, oxidation potential etc. Thus, a variety of chemical structure and morphology of a material is possible. In the present work, PANI was synthesized electrochemically and the other components, *viz.*,

MB, PR, and TiO_2 are embedded in the PANI structure to construct composite electrodes of organic/organic and organic/inorganic hybrid structure. Figure 3.2.19 shows the SEM images of (1) PANI (2) PANI/MB (3) PANI/PR and (4) PANI/ TiO_2 electrode surfaces. It can be seen that a grain-like morphology appears when PANI is prepared electrochemically from electrolytic solution containing H_2SO_4 and the surface is quite uniform covered with the PANI grain. When PANI was electropolymerized in presence of MB to prepare PANI/MB film, the surface morphology appears to be fibrillar (2). The surface uniformity seems to be reduced compared to that of PANI (1). On the other hand, when PR was embedded in PANI, the surface morphology of the resulting PANI/PR matrix seems to form agglomerates (3) and deposit as a short stack over the surface. The surface morphology in this case appears to be rather less uniform. When TiO_2 was incorporated in the PANI structure, the resulting PANI/ TiO_2 matrix shows a continuous assembly of deposit (4). The deposit in the stack is tightly packed and seems to form rigid structure and distributed non-uniformly over the substrate. The present SEM observation clearly suggests that the PANI surface is modified when MB, PR and TiO_2 are incorporated in it. Modification of the PANI surfaces is also reported by the various workers [39, 48, 49] by varying synthesis condition. From the observed dissimilar morphological features of PANI, PANI/MB, PANI/PR and PANI/ TiO_2 , it is expected that their electrode behavior for electrochemical processes could be different. The electrode behaviors of these matrices will be discussed in the following sections.

3.3 Electrochemical doping – dedoping process

A. PANI electrode:

The electrochemical behavior, i.e. doping – dedoping processes, of the PANI film electrode was examined by cyclic voltametry in aqueous 0.8 M H_2SO_4 solution. A typical CV is shown in Fig. 3.3.1. A deep blue PANI film was deposited on the Pt electrode. The film coated Pt electrode was washed several times with distilled water and then immersed in an aniline free aqueous solution of H_2SO_4 (0.8M). The CV of the PANI shows clearly one defined peak at +0.2 V in the anodic sweeping while in its cathodic scan the peak

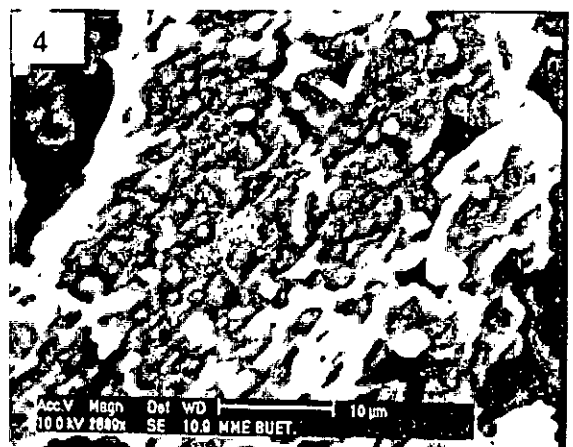
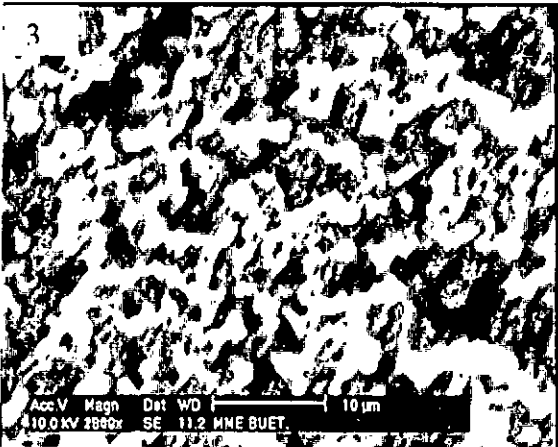
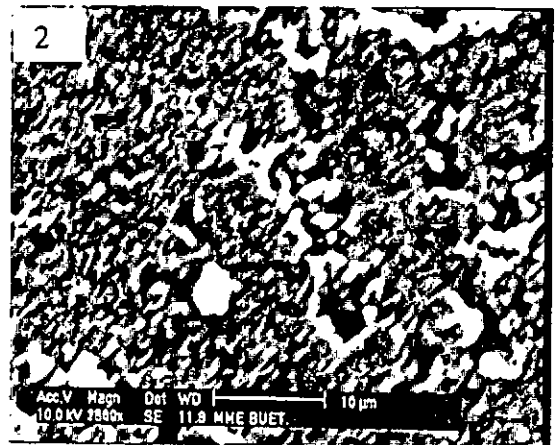
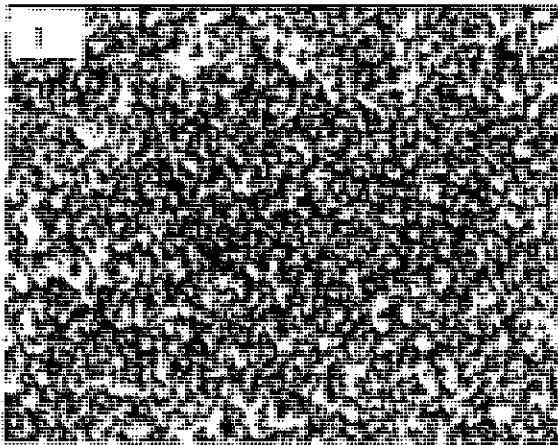


Fig. 3.2.19: SEM micrographs of (1) PANI (2) PANI/MB (3) PANI/PR and (4) PANI/TiO₂.

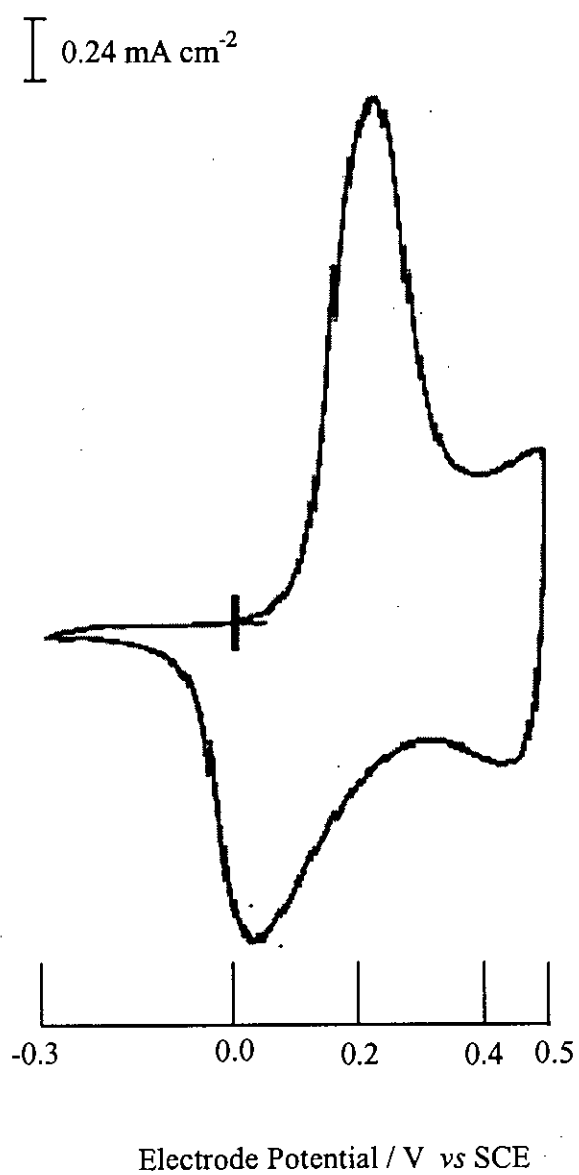
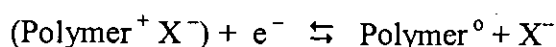


Fig.3.3.1: CV for the doping of PANI in 0.8 M H₂SO₄ solution.

appears at *ca.* +0.045 V vs SEC, suggesting the presence of electroactive regions in the film [50, 51]. On sweeping the bare Pt electrode (without PANI film) from -0.3 to +1.0 V in 0.8M H₂SO₄, no such peaks are observed (Fig. 3.3.2). The peak at +0.2 V indicates the oxidation of the PANI film at which electrolyte anion is doped into the polymer film. The PANI film reduced at +0.04 V where dedoping of the electrolyte anion occurs. The oxidation and reduction waves are not symmetrical as can be seen in the CV (Fig. 3.3.1). The shape of the two peaks and the difference in the peak potentials suggest that the electrochemical reaction is quasi-reversible and that there are differences between the reduction and oxidation kinetics [52]. The redox process of PANI in aqueous H₂SO₄ electrolytic solution may be interpreted as follows:



(Polymer⁺ X⁻) is the oxidized polymer obtained through electro-polymerization and/or doping, polymer⁰ is the reduced polymer and X⁻ is the electrolyte anion (SO₄²⁻).

The redox reaction of the PANI film is accompanied by a color changes. The film appears as a deep blue color when the electrode potential is positive by +0.2 V and turns to a transparent greenish-yellow when it is switched a negative by -0.3 V. The color changes occur evenly throughout the film with no evidence of region with different reactivity. Similar observation for color change with PANI in its redox process has also been reported previously [17, 53].

B. PANI/MB electrode:

The electrolytic solution of MB in 0.8 M H₂SO₄ was examined for its electrochemical activity on Pt electrode. This was done by sweeping the potential from -0.3 to +1.0 V using a bare Pt (0.25 cm²) electrode. The CV is presented in Fig. 3.3.3. Anodic sweeping starting from 0.0 V to 1.0 V shows no appreciable current, indicating no electrochemical reaction of MB in H₂SO₄ occurring in this range. On the other hand, a cathodic sweep beyond -0.2 V, results considerable cathodic current. The reverse process of the MB can be seen almost in the same peak position showing a well defined peak. This redox response is indeed utilized to confirm the presence of MB in the PANI/MB electrode. Figure 3.3.4 shows the CV of PANI/MB electrode coated onto Pt substrate. The

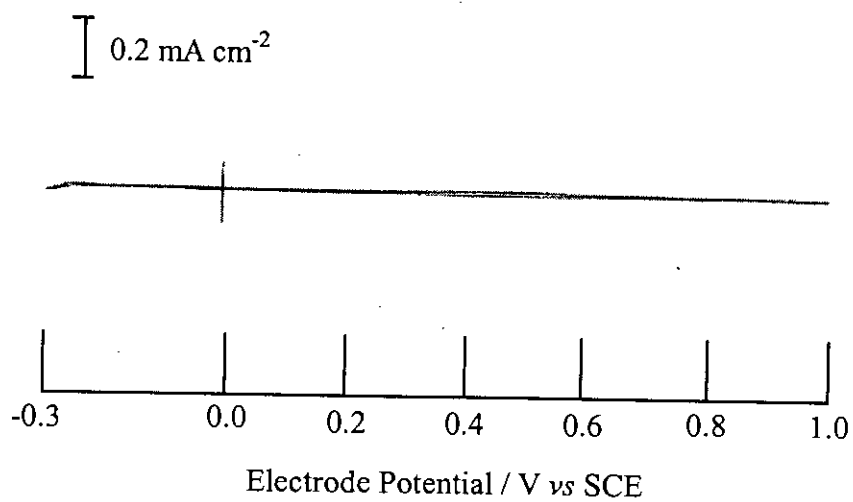


Fig.3.3.2: Background CV of bare Pt in 0.8 M H₂SO₄ solution.

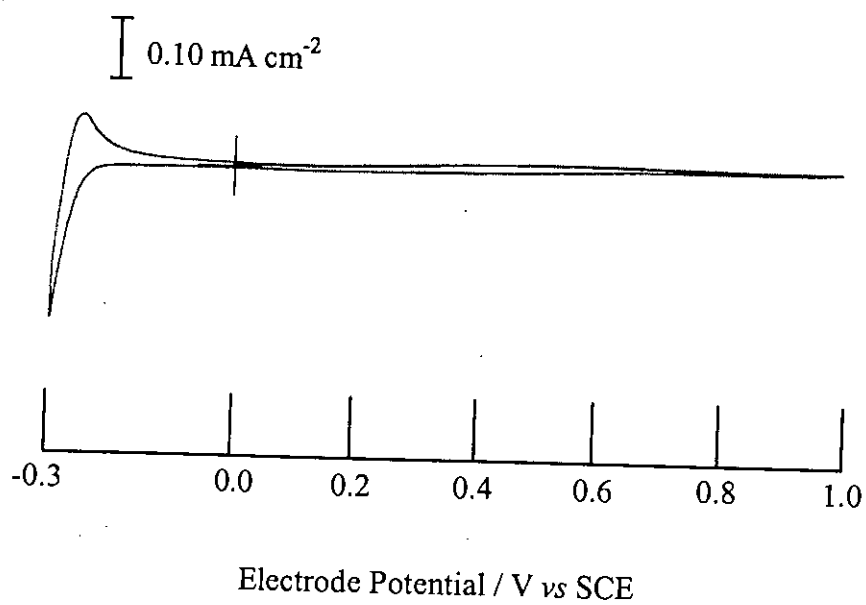


Fig.3.3.3: Background CV of bare Pt in $1.93 \times 10^{-5} \text{ M MB} + 0.8 \text{ M H}_2\text{SO}_4$ solution.

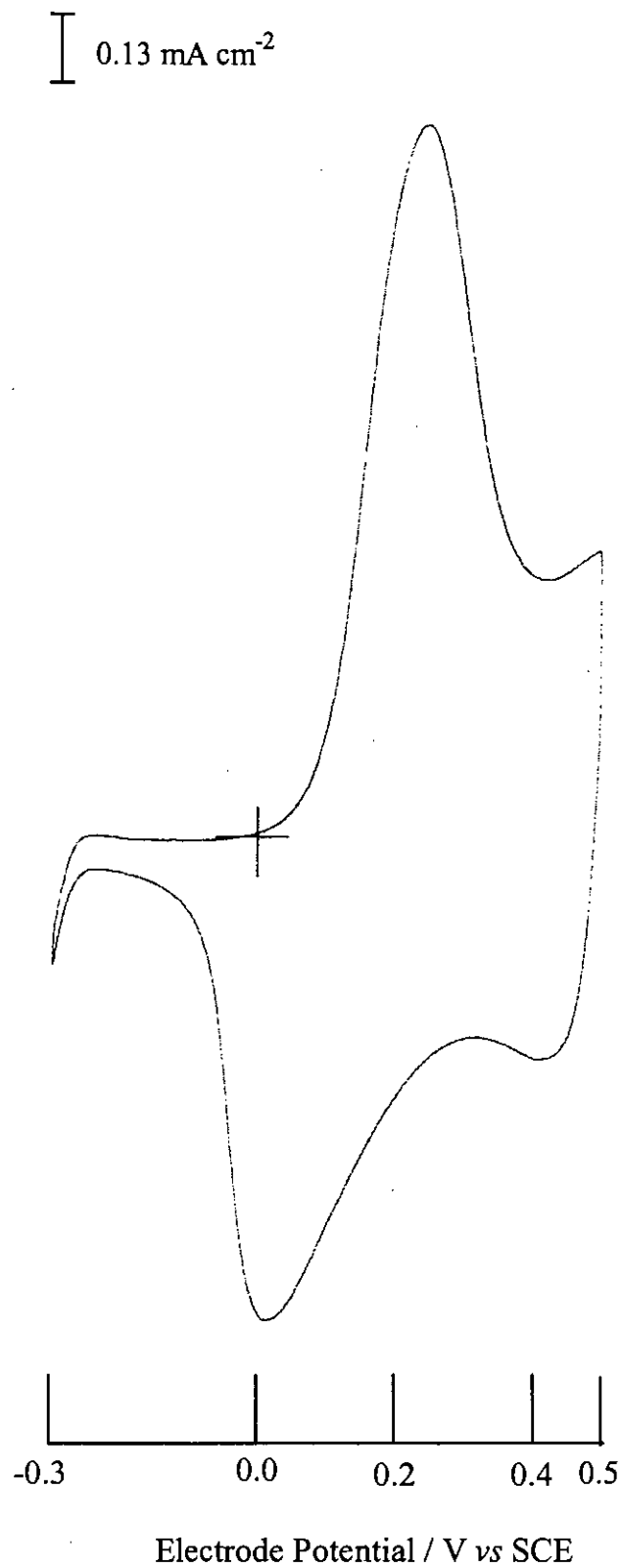


Fig.3.3.4: CV for the doping of PANI/MB in 0.8 M H₂SO₄ solution.

electrolytic H_2SO_4 solution is MB free. In general, the characteristic of the CV in the range from -0.2 to $+1.0$ V are similar to the CV of PANI (Fig. 3.3.1). That is a prominent anodic peak and its corresponding cathodic peaks are observed at about $+0.25$ V and $+0.1$ V, respectively. And this can be assigned to the oxidation of PANI/MB film deposited on the Pt electrode, corresponding to the conversion of amine units to radical cations in the polymer chain. Thus, the substrate PANI/MB also seems to be electroactive. However, the CV in the region *ca.* -0.3 V clearly shows a redox process which is exactly identical to that presented in Fig. 3.3.3. Since this process is related to the redox behavior of MB, and since the electrolytic solution is MB free, thus the response certainly made by the PANI/MB electrode. This result clearly demonstrates that MB was incorporated into the PANI matrix when it was synthesized electrochemically from an electrolytic solution containing H_2SO_4 and MB.

C. PANI/PR electrode:

The back ground current-potential response of bare Pt electrode in H_2SO_4 +PR electrolytic solution is shown in Fig. 3.3.5. The CV shows enhancement of cathodic current started beyond -0.25 V followed by a reverse process nearly in the same potential showing an anodic peak. Thus, this is the contribution of PR during the electrochemical process in H_2SO_4 that could observe onto Pt substrate. Figure 3.3.6 shows that typical behavior of PANI/PR electrode during redox process in an H_2SO_4 electrolytic solution which was PR free. A significant increase in the anodic current at about $+0.26$ V is observed. Upon reversing the sweeping, corresponding cathodic current is observed showing a peak at 0.0 V. This redox process is similar to that of PANI film indicating the oxidation and reduction of the polymer, respectively. The cathodic peak *ca.* near -0.3 V is also observed here. This could be the contribution of PR that might be embedded into the PANI film during its synthesis. Thus, this result provides clear evidence that PR entity can be incorporated into the PANI matrix electrochemically. Moreover, the present CV also demonstrates that even after incorporating PR in the polymer matrix, the PANI/PR electrode is appreciably electroactive.

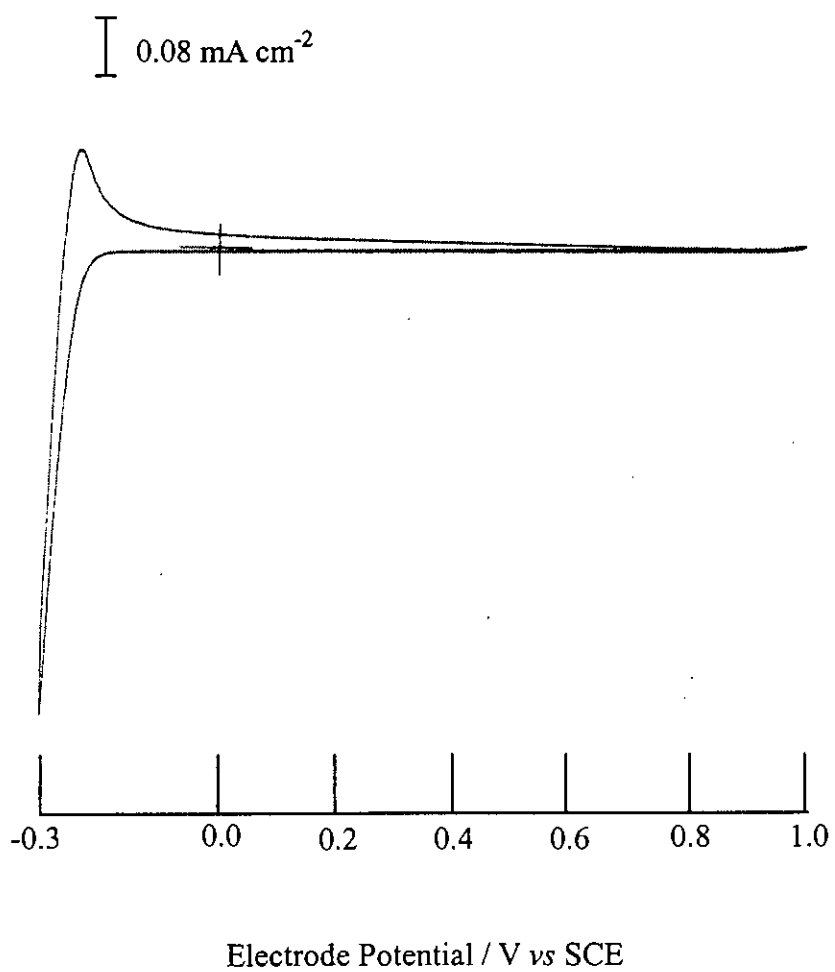


Fig.3.3.5: Background CV of bare Pt in 1.93×10^{-5} M PR + 0.8 M H_2SO_4 solution.

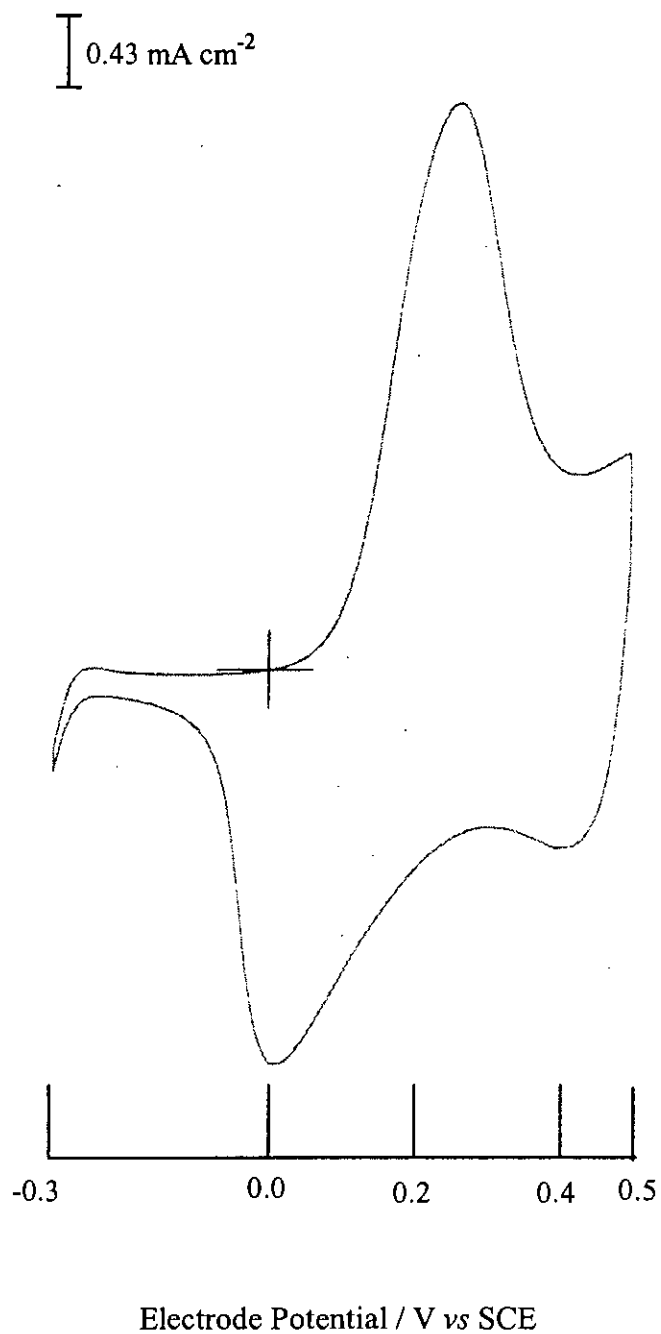


Fig.3.3.6: CV for the doping of PANI/PR in 0.8 M H₂SO₄ solution.

D. PANI/TiO₂ electrode:

Figure 3.3.7 shows the background CV of a bare Pt substrate in an aqueous H₂SO₄ solution (0.8M) containing TiO₂ as suspension. No significant current is seen within the potential window scanned from -0.2 to +1.0 V. This means that TiO₂ is electrochemically non-active within this potential range. In Fig. 3.3.8, the CV shows the electrochemical behavior of the PANI/TiO₂ electrode in H₂SO₄ solution. For this case, potential was swept between -0.2 and +1.0 V at a scan rate of 100 mV/sec. The result clearly shows that PANI/TiO₂ film can be switched between its oxidized (conductive) and reduced (insulating) states. It can be seen from the CV that, it is composed of a well-defined single redox process: anodic process at +0.3 V and the cathodic one at ca. -0.02 V, suggesting the characteristic oxidation (doping) and reduction (dedoping) of the PANI/TiO₂ film under the electrochemical conditions employed. This switching behavior indicates the presence of variable electroactive region in the PANI/TiO₂ matrix. During electrochemical oxidation (doping), the electrolytic anions (SO₄²⁻) in the solution become incorporated into the polymer to compensate the positive charges in the chain while in the reduction (dedoping) process, the incorporated anions get removed out of the polymer film [54-56]. The presence of TiO₂ in the matrix can not be evidenced from this CV, since TiO₂ is inactive in the potential window studied. However, by comparing the CV with that of PANI given in Fig. 3.3.1, it can be seen that peak potentials for the redox reaction is somewhat different to some extent. This modification of the voltammogram may arise for the incorporation of TiO₂ in the PANI matrix. A comparison of the redox reactivity of the studied electrodes, PANI, PANI/MB, PANI/PR and PANI/TiO₂ in H₂SO₄ are summarized below in the Table-3.

Table -3: Electrochemical data of the electrode matrices

| Electrode matrices | anodic peak potential, E _{pa} (V) | anodic peak current, I _{pa} (mA) | cathodic peak potential, E _{pc} (V) | cathodic peak current I _{pc} (mA) | I _{pc} / I _{pa} |
|-----------------------|--|---|--|--|-----------------------------------|
| PANI | + 0.20 | 2.35 | + 0.045 | 1.42 | 0.604 |
| PANI/MB | + 0.25 | 1.35 | + 0.01 | 0.91 | 0.674 |
| PANI/PR | + 0.26 | 3.31 | + 0.0 | 2.28 | 0.689 |
| PANI/TiO ₂ | + 0.30 | 6.88 | - 0.02 | 4.55 | 0.661 |

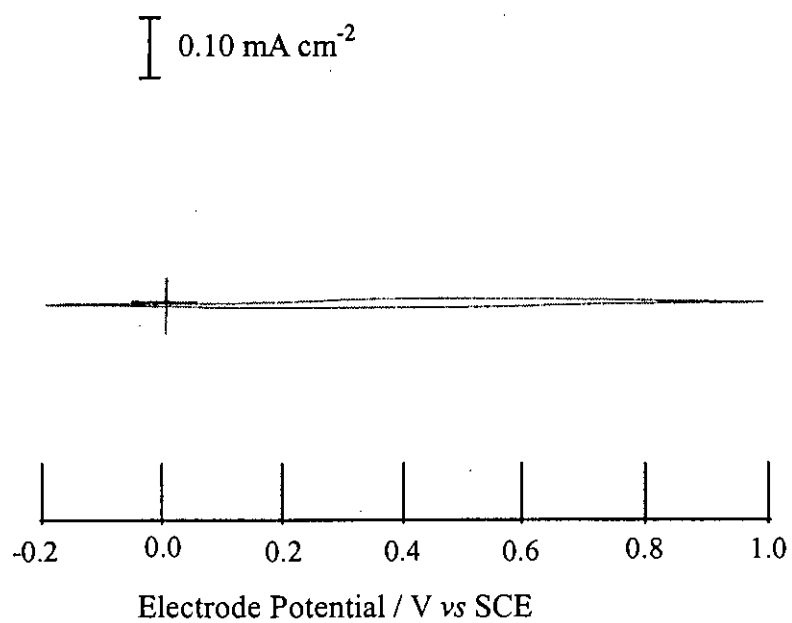


Fig.3.3.7: Background CV of bare Pt in TiO_2 + $0.8 \text{ M H}_2\text{SO}_4$ solution.

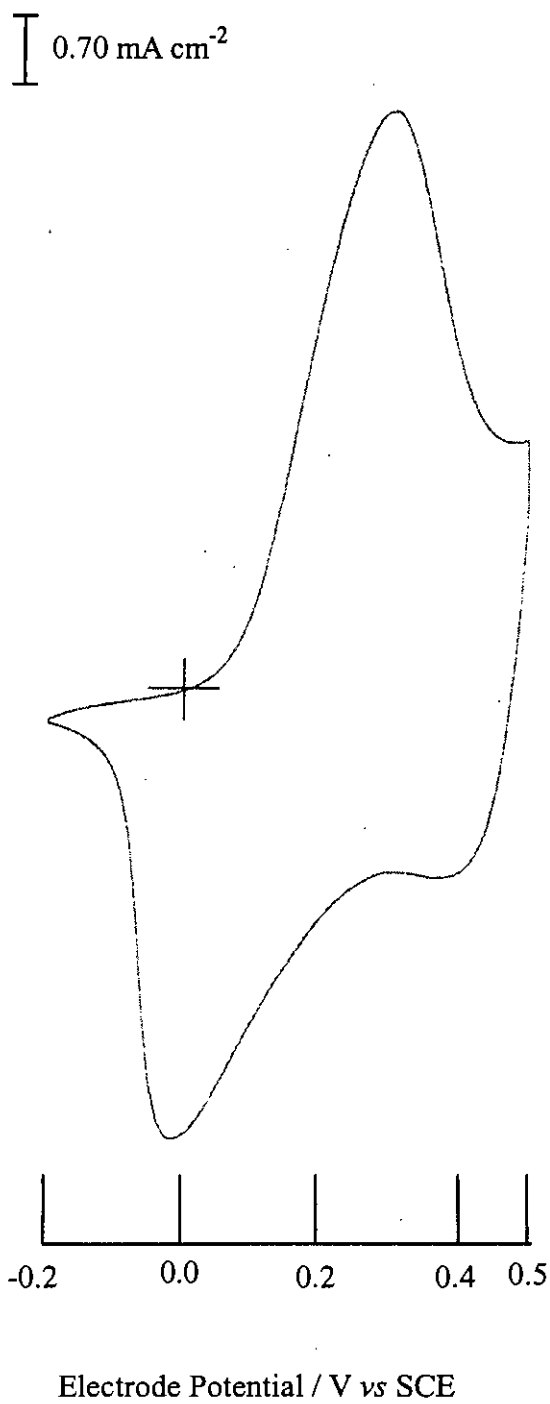
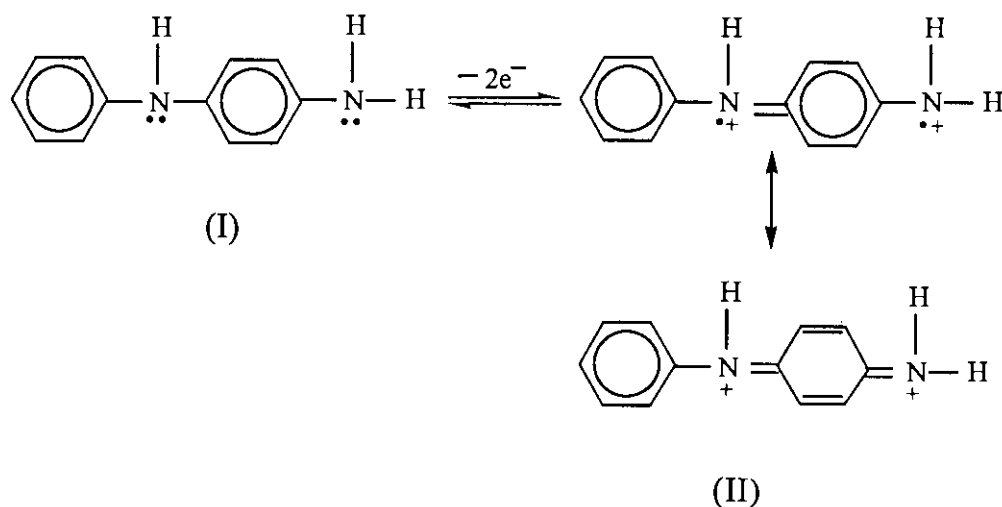


Fig.3.3.8: CV for the doping of PANI/TiO₂ in 0.8 M H₂SO₄ solution.

Mechanism of redox reaction: The electrochemical polymerization is believed to proceed via the cation radical. The anodic oxidation of aniline in the aqueous H_2SO_4 solution gives a radical cation that couples together in a head-to-tail manner to form *p*-aminodiphenyl amin (I). (I) is oxidized at *ca.* 0.02 V vs SCE:

Mechanism of redox reaction



The oxidation process is accompanied by the insertion of anion (SO_4^{2-}) to maintain the charge neutrality [57]. The above oxidation process gives rise to anodic current peak at *ca.* +0.2 V as illustrated in Fig. 3.3.1.

3.4 Electrochemical degradation

A. Oxidative degradation:

The term “oxidative degradation” is used by indicate degradation of an electrode film when a high positive potential is applied on it. Degradation of an electrode can easily be realized by recording its electrochemical processes, *i.e.* in particular, just by following the peak intensities and its position in its voltammogram.

Figure 3.3.9 shows the CV of PANI film in 0.8 M H_2SO_4 . The film gave a typically reversible redox response (curve – a) when the potential scan was reversed at a switching potential of +1.0 V vs SCE. However, when the scan was reversed at a more positive switching potential of +2.0 V (curve – b), normal redox phenomenon seems to be affected significantly. For example, the peaks observed in the curve – a, becomes broader

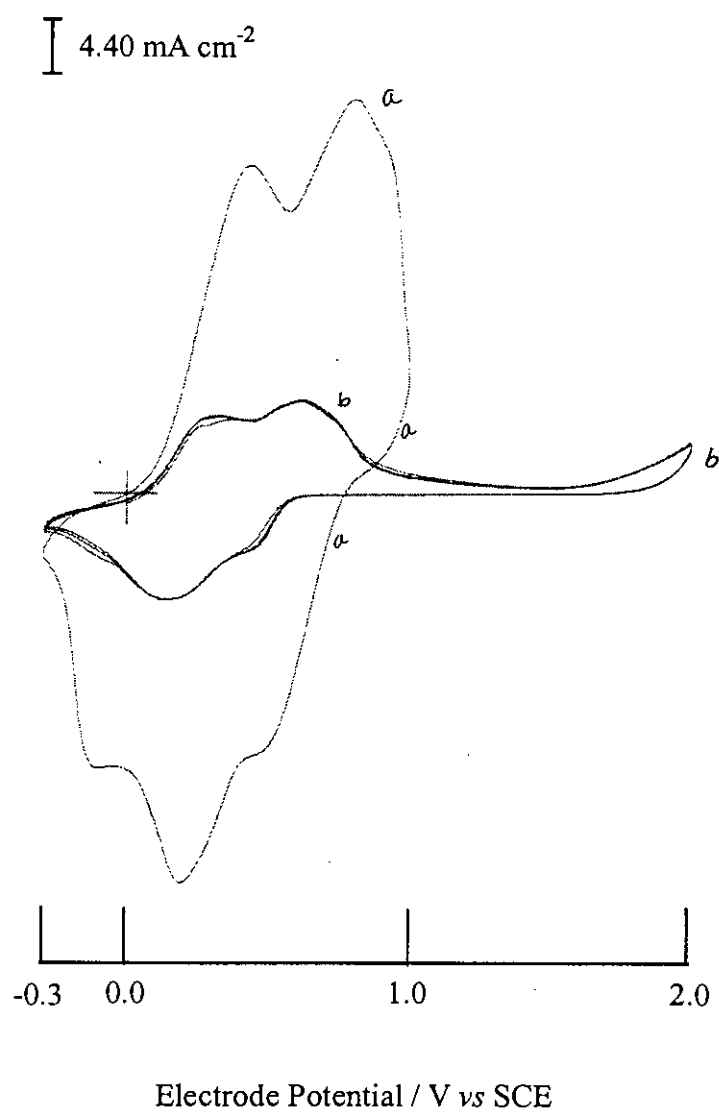


Fig.3.3.9: CV of PANI in 0.8 M H₂SO₄ solution: +1.0 V (curve-a) and +2.0 V (curve -b).

and the peak intensities are reduced insignificantly. Moreover, the peak positions are also shifted. This phenomenon is also called “overoxidative degradation” and is found in some conducting polymers [58-63].

Oxidative degradations of other electrode systems have also been examined. Figure 3.3.10 shows the CV of PANI/MB system recorded for its degradation under applied high potential. The result shows that when the potential was switched to +1.0 V, the PANI/MB system can perform the usual redox processes (curve - a) as efficiently as PANI does. When the potential was switched to +2.0 V, the PANI/MB electrode gave exactly identical response (curve -b). This result indicates that by incorporating MB into the PANI matrix, a superior stability of the electrode can be achieved. Moreover, the performance of the MB embedded PANI matrix toward electrochemical process is quite comparable to that of semiconducting PANI. Similar observation was also found when PR is embedded into the PANI matrix. Typical CV is shown in Fig. 3.3.11. The redox responses of the PANI/PR electrode under the potentials of +1.0 V (curve - a) and +2.0 V (curve - b) are almost identical. This result also provides evidence for the stability of the PANI/PR electrode than that of PANI one. Interesting result was also obtained with the PANI/TiO₂ electrode. Figure 3.3.12 show the CV representing the typical redox characteristics in 0.8M H₂SO₄ when the electrode was biased at +1.0 (curve - a) and +2.0 V (curve -b). Both curves show nearly the normal redox response as expected for PANI in the same acid media although the peak intensities and position changes slightly. However, the present study clearly demonstrate that incorporation of MB, PR and TiO₂ into a PANI film electrode produces a better stability of the electrode under applied potential of as high as +2.0 V vs SCE and the redox efficiency of these electrodes remain as superior as a metal electrode.

Overoxidative degradation may be due to the formation of di-cations of aniline moieties in the PANI film. The di-cations should be very strong electrophiles and easily undergo nucleophilic attack with successive decomposition, as shown in Scheme - 2 [64, 65].

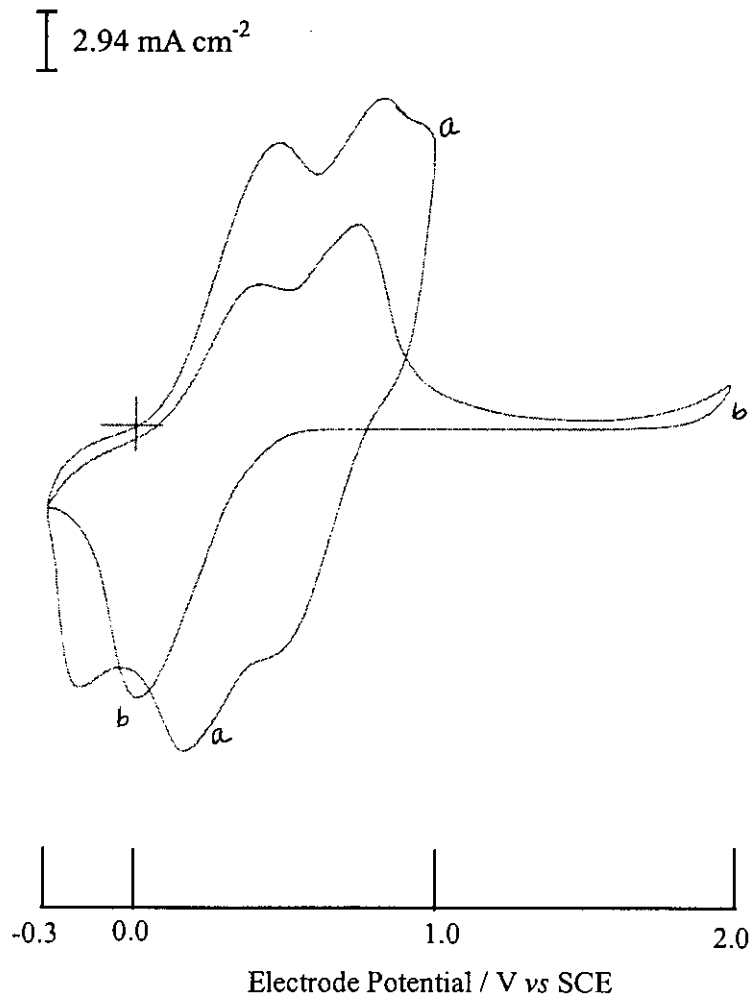


Fig.3.3.10: CV of PANI/MB in 0.8 M H₂SO₄ solution: +1.0V (curve-a) and +2.0V (curve-b).

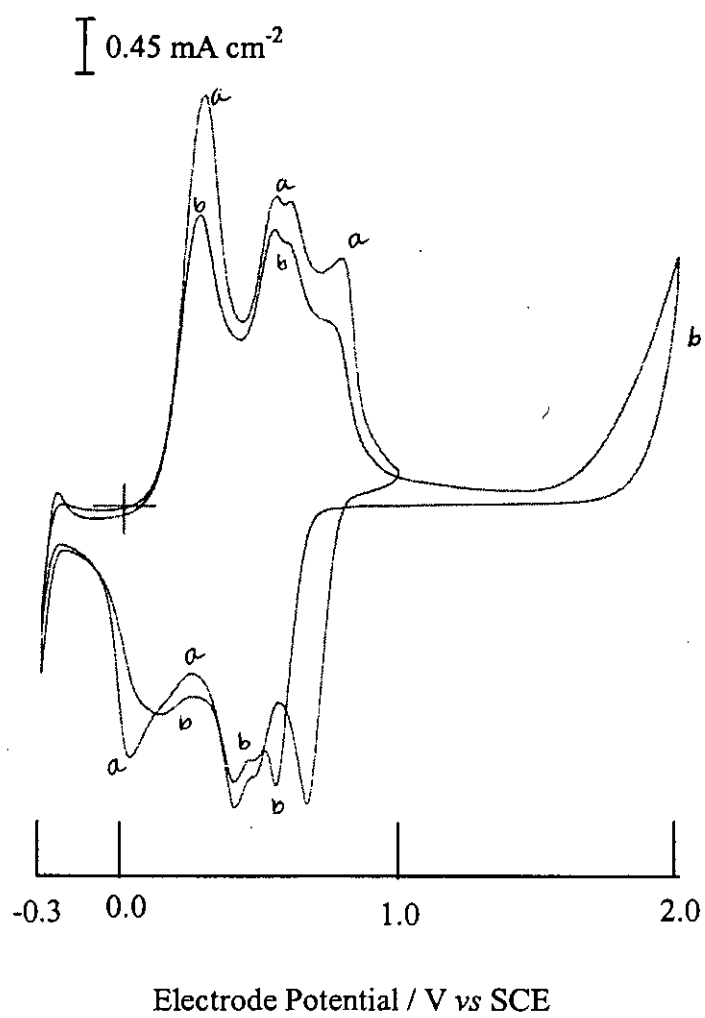


Fig.3.3.11: CV of PANI/PR in 0.8 M H₂SO₄ solution: +1.0 V (curve-a) and +2.0 V (curve-b).

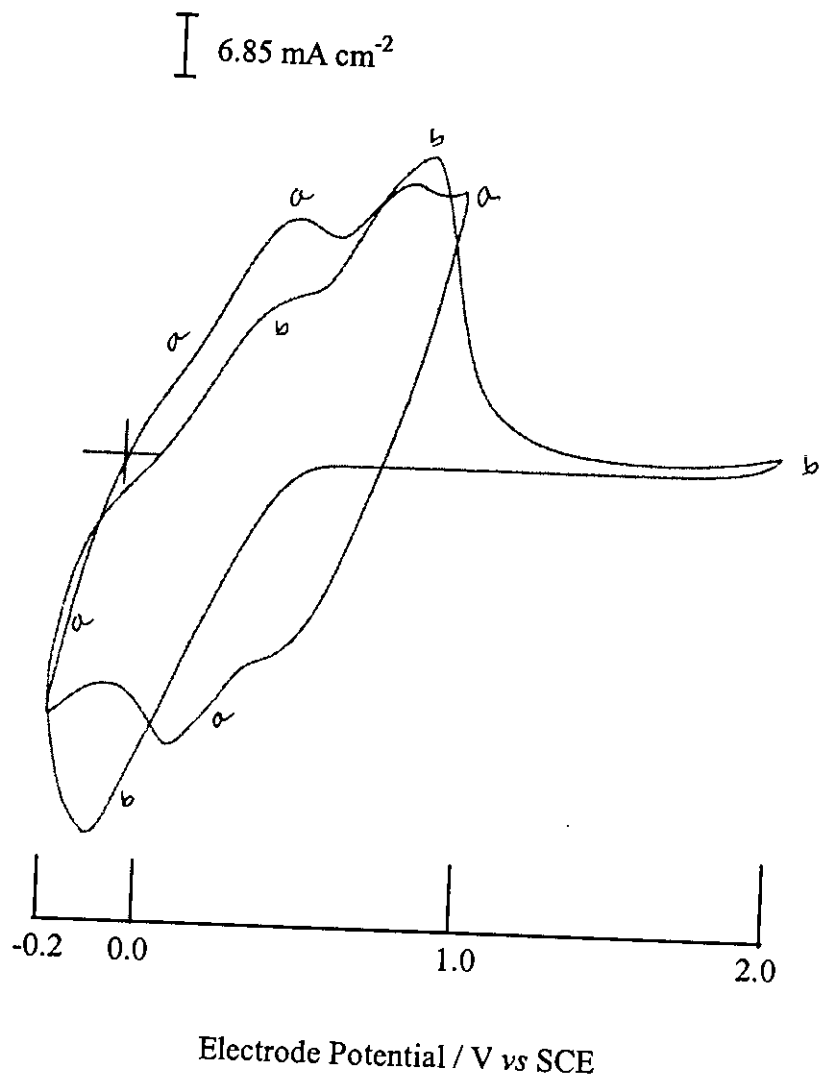
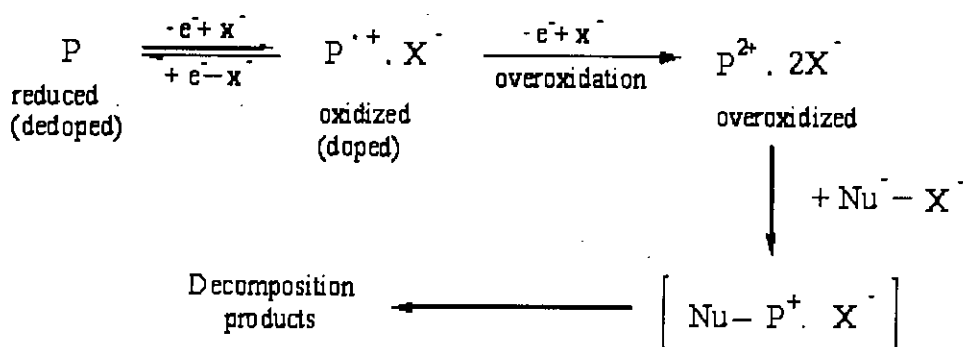


Fig.3.3.12: CV of PANI/TiO₂ in 0.8 M H₂SO₄ solution: +1.0 V (curve-a) and +2.0 V (curve-b).

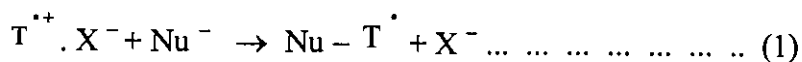
Scheme- 2: Overoxidative degradation



P : monomer unit of polymer, X^- : supporting electrolyte anion,
 Nu⁻ : nucleophile.

B. Degradation by repeating potential scan

In this work, a different type of degradation was found, such that the response current decreased gradually with no change or slightly change in the peak potential upon repeating the potential scan between -0.3 and +0.6 V vs SCE. The results for PANI, PANI/PR and PANI/TiO₂ are presented in Fig. 3.3.13, Fig. 3.3.14 and Fig. 3.3.15, respectively. In all the cases, the reversibility of the response and the color change between the reduced and oxidized states of the film were not affected by repeating the scan. The extent and mechanism of degradation in all three cases seem to be nearly similar. The response current is decreased by the presence of nucleophilic additives, solvents and supporting electrolyte anions [66, 67]. Therefore, it is suggested that the degradation can be caused by nucleophilic attack on not only the overoxidized state ($P^{2+} \cdot 2X^-$ in scheme-2) but also on the oxidized (doped) state ($P^{\cdot+} \cdot X^-$) (scheme-1 and equ. 1). Reaction 1 should be irreversible:



If the oxidative degradation is caused by the attack of nucleophiles on the oxidized (doped) state as shown in equ. (1), it seems difficult to recover the electroactivity of degraded films. On the other hand, it should be possible to protect the original films from the degradation in some way. The most natural way is to use solvents, supporting

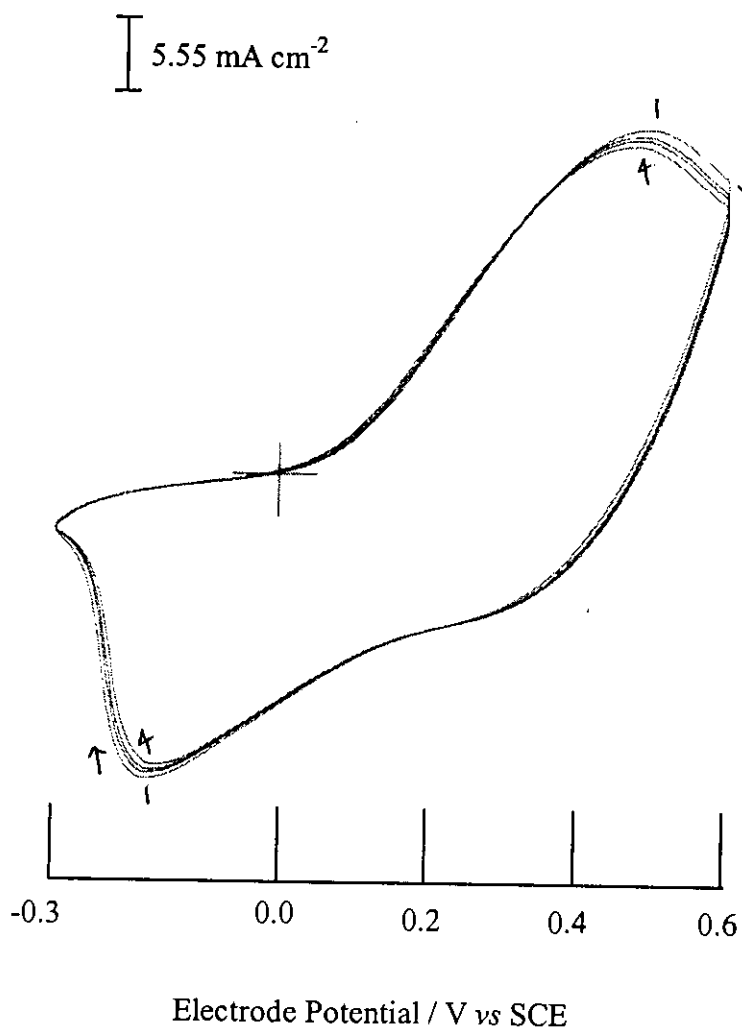


Fig.3.3.13: CV of PANI in 0.8 M H₂SO₄ solution at different no. of scan cycle: (1)1st (2) 25th (3) 50th and (4) 100th.

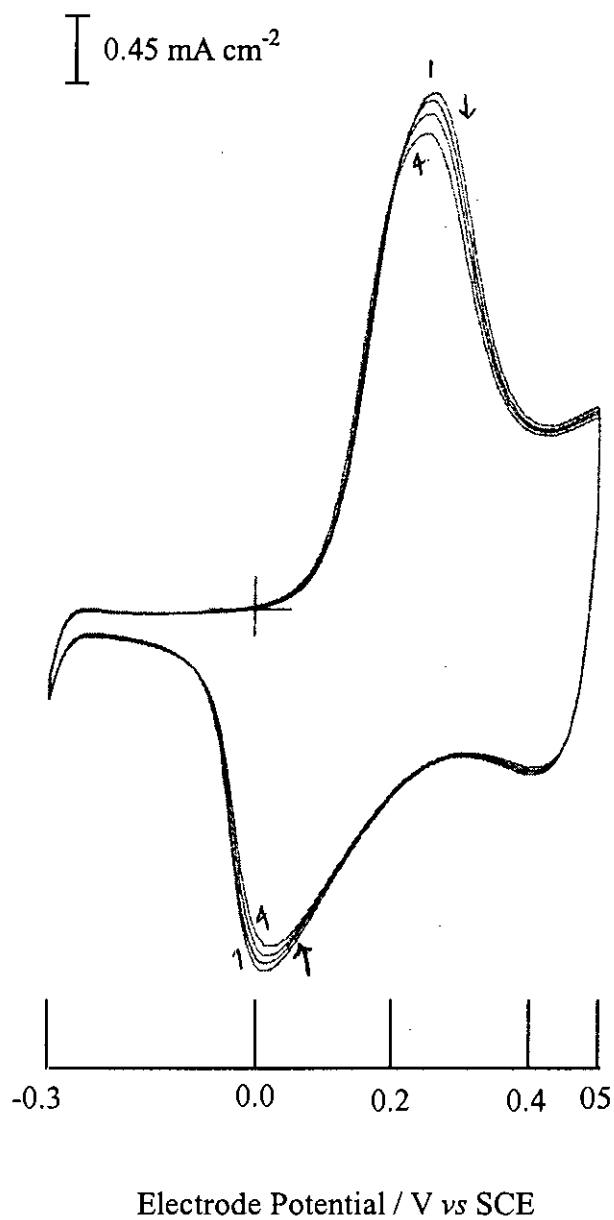


Fig.3.3.14: CV of PANI/PR in 0.8 M H₂SO₄ solution at different no. of scan cycle: (1)1st (2) 25th (3) 50th and (4) 100th.

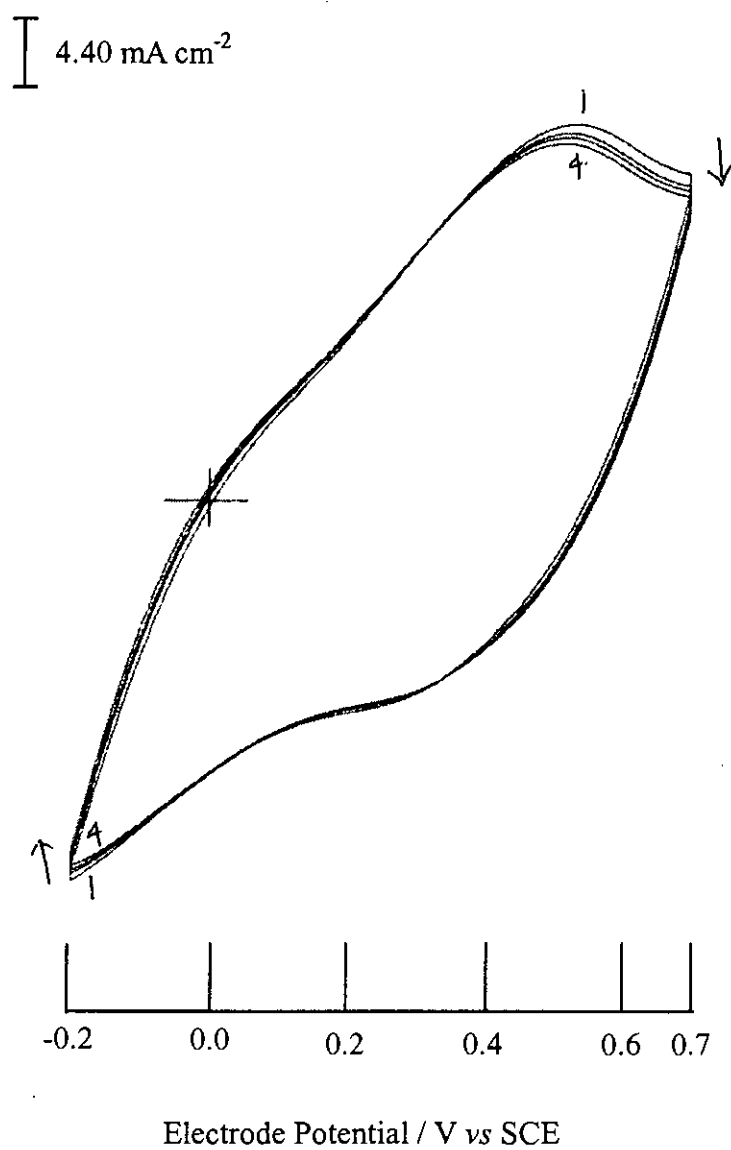


Fig.3.3.15: CV of PANI/TiO₂ in 0.8 M H₂SO₄ solution at different no. of scan cycle: (1)1st (2) 25th (3) 50th and (4) 100th.

electrolyte anions and additives without nucleophilicity. However, it not easy to keep nucleophilic contaminants such as H_2O out completely.

References

1. D. M. Mohilner, R. N. Adams and W. J. Argersinger, *J. Am. Chem. Soc.*, **84** (1962) 3618.
2. J. Bacon and R. N. Adams, *J. Am. Chem. Soc.*, **90** (1968) 6596.
3. E. M. Genies and C. Tsintavis, *J. Electroanal. Chem.*, **195** (1985) 109.
4. E. M. Genies, C. Tsintavis and A. A. Syed, *Mol. Cryst., Liq. Cryst.*, **121** (1985) 181.
5. A. Volkov, G. Tourillon, P. C. Lacaze and J. E. Dubois, *J. Electroanal. Chem.*, **115** (1980) 279.
6. E. M. Genies and C. Tsintavis, *J. Electroanal. Chem.*, **200** (1986) 127.
7. B. Wang, J. Tang and F. Wang, *Synth. Met.*, **13** (1986) 329.
8. E. W. Paul, A. J. Ricco and M. S. Wrighton, *J. Phys. Chem.*, **89** (1985) 1441.
9. A. G. MacDiarmid, J.-C. Chiang, M. Haipern, W.-S. Huang, S.-L. Mu, N. L. D. Somasiri, W. Wu, and S. I. Yaniger, *Mol. Cryst. Liq. Cryst.*, **121** (1985) 173.
10. W.-S. Huang, B. D. Humphery, and A. G. MacDiarmid, *J. Chem. Soc., Faraday Trans. 1*, **82** (1986) 2385.
11. W. W. Focke, G. E. Wnek, and Y. Wei., *J. Phys. Chem.*, **91** (1987) 5813.
12. Y. Wei, X. Tang, Y. sun, and W. W. Focke, *J. Polym. Sci., Polym. Chem. Ed.*, **27** (1989) 2385.
13. Y. Wei, Y. Sun, and X. Tang, *J. Phys. Chem.*, **93** (1989) 4878.
14. Y. Wei, Y- Sun, G.-W. Jang and X. Tang, *J. Polym. Sci. (Part-c)*, **28** (1990) 81.
15. E. M. Genise and M. Lapkowski, *J. Electroanal. Chem.*, **236** (1987) 189, 199.
16. A. G. MacDiarmid, S-L. Mu, N. L. D. Somasiri and W. Wu, *Mol. Cryst. Liq.*, **121** (1985) 187.
17. A. F. Diaz and J. A. Logan, *J. Electroanal. Chem.*, **111** (1980) 111.
18. D. E. Stilwell and S.-M. Park, *J. Electrochem. Soc.*, **135** (1988) 2254.
19. Y. Cao, S. Li, Z. Xue and D. Guo, *Synth. Met.*, **16** (1986) 305.
20. F. Wang, J. Tang, X. Jing, S. Ni and B. Wang, *Acta Polym. Sinica.*, **5** (1987) 384.
21. G. Socrates, *Infrared Characteristic Group Frequencies*, Wiley, Chichester, 1980, p-53.
22. F. R. Dollish, W. G. Fateley and F. F. Bentley, *Characteristic Raman Frequencies of Organic Compounds*, Wiley, New York, 1974.
23. L. J. Bellamy, *The Infrared Spectra of Complex Molecules*, Chapman and Hall, London, 1975, p. 82, p. 277.
24. M. Angelopoulos, A. Ray and A-G. MacDiarmid, *Synth. Met.*, **21** (1987) 21
25. S. Ni, J. Tang and F. Wang, *Preprints of Symposium on Polymers*, Chinese Chemical Society Polymer Division, Wuhan, China, 1987, p. 638.

26. W. R. Salaneck, B. Liedberg, O. Inganas, R. Erlandsson, I. Lundstrom, A. G. MacDiarmid, M. Halpern and N. L. D. Somasiri, *Mol. Cryst., Liq. Cryst.*, **121** (1985) 191.
27. J. Tang, X. Jing, B. Wang and F. Wang, *Synth. Met.*, **24** (1988) 231.
28. S. Stafstrom and B. Sjogren, *Synth. Met.*, **16** (1986) 31.
29. (a) D. Dolphine and A. Wick, *Tabulation of Infrared Spectral Data*, John Wiley & Sons, New York, London, Sydney, Toronto, 1977; (b) A. D. Cross and R. A. Jones, *An Introduction to Practical Infrared Spectroscopy*, 3rd edn., Butterworth, London, 1969.
30. Y. Ohnuki, T. Ohsaka, H. Matsuda and N. Oyama, *J. Electroanal. Chem.*, **158** (1983) 55.
31. A. Volkov, G. Tourillon, P. C. Lacaze and J. E. Dubois, *J. Electroanal. Chem.*, **115** (1980) 279.
32. F. Wudl, R. O. Angus, F. L. Lu, P. M. Allemand, D. J. Vachon, M. Nowak, Z. X. Liu and A. J. Heeger, *J. Am. Chem. Soc.*, **109** (1987) 3677.
33. M. Angelopoulos, G. E. Asturias, S. P. Ermer, A. Roy, E. M. Scherr, A. G. MacDiarmid, A. Akhter and Z. Kiss, *Mol. Liq. Cryst.*, **160** (1988) 151.
34. (a) F. Genoud, M. Guglielmi, M. Nechtschein, E. Genice and M. Salmon, *Phys. Rev. Lett.*, **55** (1985) 118; (b) E. M. Genies and J. M. Pernaut, *Synth. Met.*, **10** (1984) 117.
35. J. H. Kaufman, N. Colaneri, J. C. Scott and G. B. Street, *Phys. Rev. Lett.*, **53** (1984) 10005.
36. S. Rezina Jesmeen, *Polymeric Adsorbant for the Removal of Organic and Inorganic Pollutants from Aqueous Solution*, M. Phil Thesis, Department of Chemistry, BUET, Dhaka, September 2003.
37. Y. Roichman, G. I. Titelman, M. S. Silverstein, A. Siegman and M Narkis, *Synth. Met.*, **98** (1999) 201.
38. S-A. Chen and W-G Fang, *Macromolecules*, **24** (1991) 1242.
39. K. K. Kanazawa, A. F. Diaz, R. H. Geiss and G. B. Street, *J. Chem. Soc. Chem. Commun.*, (1979) 854.
40. J. P. Pouget, M. E. Jozefowicz, A. J. Epstein, X. Tang and A.G. MacDiarmid, *Macromolecules*, **24** (1991) 779.
41. J. P. Pouget, M. Laridjani, M. E. Jozefowicz, A. J. Epstein, E. M. Scherr and A. G. MacDiarmid, *Synth. Met.*, **51** (1992) 95.
42. J. E. Fischer, X. Tang, E. M. Scherr, V. B. Cajipe and A. G. MacDiarmid, *Synth. Met.*, **41-43** (1991) 661.
43. F. Lux, *Polymer*, **35** (1994) 2936.
44. R. B. Bjorklund and B. Liedberg, *J. Chem. Soc., Chem. Commun.*, (1986) 1293.
45. C. DeArmitt and S. P. Armes, *J. Colloidal Interface Sci.*, **150** (1992) 134.

46. C. DeArmitt and S. P. Armes, *Langmuir*, **9** (1993) 652.
47. Q. Li, L. Cruz and P. Phillips, *Phys. Rev.* **B47** (1993) 1840.
48. M. Atobe, A.-N. Chowdhury, T. Fuchigami and T. Nonaka, *Ultrason. Sonochem.*, **10** (2003) 77.
49. M. E. Jazefowiz, R. Laversanne, H. H. S. Javadi, A. J. Epstein, J. P. Pouget, X-Tang and A. G. MacDiarmid, *Phys. Rev.* **B39** (1989) 12, 958.
50. N. Mermillod, J. Tanguy, M. Hoclet and A. A. Syed, *Synth. Met.*, **18** (1986) 359.
51. J. Tanguy, N. Mermillod and M. Hoclet, *J. Electrochem. Soc.*, **134** (1987) 795.
52. T. J. Kemp (ed), *Instrumental Methods in Electrochemistry*, Ellis Horwood Limited, West Sussex, England 1985.
53. S. N. Bhadani, M. K. Gupta and S. K. S. Gupta, *J. Appl. Polym. Sci.*, **49** (1993) 397.
54. A. Kitani, J. Yano and K. Sasaki, *J. Electroanal. Chem.*, **209** (1986) 227.
55. D. Orata and D. A. Buttry, *J. Am. Chem. Soc.*, **109** (1987) 3574.
56. C. Chiang and A. G. MacDiarmid, *Synth. Met.*, **13** (1988) 193.
57. H. Daifuku, T. Kawagoe, T. Matsunaga, N. Yamamoto, T. Ohsaka and N. Oyama, *Synth. Met.*, **41** (1991) 2897.
58. D. E. Stilwell and S.-M. Park, *J. Electrochem. Soc.*, **136** (1989) 427.
59. D. E. Stilwell and S.-M. Park, *J. Electrochem. Soc.*, **136** (1989) 688.
60. B. Sun, J. J. Jones, R. P. Burford and M. Skylas-Kazacos, *J. Electrochem. Soc.*, **136** (1989) 698.
61. F. Beck, P. Braun and M. Oberst, *Ber. Bunsenges, Phys. Chem.*, **90** (1987) 967.
62. B. Krische and M. Zagorska, *Synth. Met.*, **28** (1989) C257.
63. B. Krische and M. Zagorska, *Synth. Met.*, **28** (1989) C263.
64. E. W. Tsai, S. Basak, J. P. Ruiz, J. R. Reynolds and K. Rajeshwar, *J. Electrochem. Soc.*, **136** (1989) 3683.
65. Y. Takenaka, T. Koike, T. Oka and M. Takahashi, *Synth. Met.*, **18** (1987) C207.
66. N. Sato and T. Nonaka, *J. of The Chin. I. Ch. E.*, **24(6)** (1993) 407.
67. H. Harada, T. Fuchigami and T. Nonaka, *J. Electroanal. Chem.*, **303** (1991) 139.

Conclusion

The electrochemical polymerization of aniline from an aqueous acidic electrolytic solution results a free-standing, tightly adhere film PANI coated onto a Pt substrate working electrode.

When the electrolytic solution contains either of MB or PR or TiO_2 , the polymerization leads to the formation of composite film of hybrid structure such as PANI/MB or PANI/PR or PANI/ TiO_2 . Each film coated onto the Pt electrode appears to be free-standing too and show excellent redox activity during electrochemical processes.

The PANI and the composite films, PANI/MB, PANI/PR and PANI/ TiO_2 thus electro-synthesized show good electro activity in sulphuric acid solution. The voltammetric features confirm that these film electrodes can be switched between doped (conductive) and dedoped (insulating) states with concomitant color changes suggesting their potential use as the new electrode materials. The redox reactivity, i.e., doping and dedoping of these films in the acid solution is not same and this may happen as the different entities, viz., MB, PR and TiO_2 are incorporated into the PANI film. The inclusion of these entities probably could modify the behavior of the electrode surface properties to lead different redox reactivity of the film electrodes. However, all the film electrodes show good reversibility although the extent of reversibility varies film to film.

The mass and thickness of the film formed on the electrode was proportional to the anodic peak current at +0.17 V. Therefore, the rate of polymerization can be measured by the rate of increase in this peak current. The rate of polymerization in the presence of MB, PR and TiO_2 was found to be different. The growth rate of PANI/ TiO_2 film is found to be faster compared to that of PANI, PANI/MB or PANI/PR.

The IR spectrum of PANI shows characteristics absorption for PANI components. The general pattern of the spectrum is consistent with the previous observation. The samples PANI/MB, PANI/PR and PANI/ TiO_2 and their respective controlled components, viz., MB, PR and TiO_2 were also characterized by IR. Their spectra show characteristics peaks

identifying the presence of the MB, PR and TiO₂ in the polymer matrix. The UV-Vis optical analysis was also performed in the DMF solution. The UV-Vis spectra of the samples show mainly two absorptions at 335 and 660 nm which represent interband transition and mid-gap state transition of the PANI. The characteristic optical feature is seen to be modified when MB and PR was incorporated to the PANI matrix although the peak appears to be in the same position. XRD studies of the samples indicate the amorphous nature both for PANI and the composite matrices. This result indicates that even incorporating the MB, Pr and TiO₂, the molecular arrangement of the matrices remain unchanged and exists as that of the parent PANI. However, the d. c. conductivity of the samples was found to be considerably affected when MB, PR and TiO₂ were incorporated to the PANI matrix. The conductivity of PANI/TiO₂ was found to be 3 time higher while that of PANI/MB were seen to be about 3 time lower than that of PANI does. The surface morphology of the PANI matrix also seems to be modified significantly when MB, PR and TiO₂ are embedded into the matrix. The grain like PANI morphology seen to be fibrillar when MB is embedded whereas a deposits of agglomerates appears when PR is incorporated in the PANI matrix. On the other hand, a non-uniform deposit results when TiO₂ is embedded.

The composite films, PANI/MB, PANI/PR, and PANI/TiO₂ thus prepared electrochemically in this work are found not only to show good electroactivity, they also show better durability and stability in the electrochemical processes when used as film electrodes. The electrochemical degradation either by repeated potential scan or biasing at high anodic voltage, these film electrodes show more stable voltammetric features than that of the PANI does. The stable voltammetric response is an indicator of the electrode stability in the electrochemical processes. Thus, it may be conclude that, by incorporating either of MB, PR or TiO₂ into a PANI matrix, a new class of organic/organic and organic/inorganic electroactive electrode system with better electrochemical stability can be achieved.

